On the phenotype of white-tailed deer antlerogenic progenitor cells

by

Ethan Daley

**A dissertation submitted in partial fulfillment
of the requirements for the degree of
Doctor of Philosophy
(Biomedical Engineering)
in the University of Michigan
2013**

Doctoral Committee:

**Professor Emeritus Steven A. Goldstein, chair
Research Assistant Professor Andrea I. Alford
Professor David H. Kohn
Professor Laurie K. McCauley
Assistant Professor Joshua D. Miller**

“Basic research leads to new knowledge. It provides scientific capital. It creates the fund from which the practical applications of knowledge must be drawn. New products and new processes do not appear full-grown. They are founded on new principles and new conceptions, which in turn are painstakingly developed by research in the purest realms of science.”

Science the Endless Frontier (a letter to President Truman), Vannevar Bush, July 1945

To my father, Laurence Daley and my buddy, Jacob Kaizerman (1970-2010.)

ACKNOWLEDGEMENTS

Though this list is no doubt incomplete, the author wishes to acknowledge the instrumental roles of many, many folks in shepherding this project to completion.

I would first like to thank my thesis and research advisor, Steve Goldstein. Without his tremendous and unwavering support, this project would have been impossible. From my committee, thanks go out to Andrea Alford, for her help and patience with respect to my endless nagging about laboratory techniques and data interpretation; to Laurie McCauley for her generosity and assistance in getting the murine ossicle model up to speed; to Josh Miller for his mentoring on project design and data interpretation; and to David Kohn for his advice regarding hypothesis development and project focus.

I have many people to thank from the Orthopaedic Research Lab: Charles Roehm for the fabrication and repair of equipment, for culling and tracking deer for a pilot project in godforsaken heat, for providing critical help in baiting, tracking and habituating bucks at the Edwin S. George Reserve, and for keeping us students filled with homemade food cooked on the George Foreman grill. Thanks to John Baker for getting innumerable tiny specimens paraffin-embedded and sliced up. We are endlessly grateful to Bonnie Nolan and Kathy Sweet for all their help working with creatures great and small. Our stats sabom-nim (and now engineering professor) Jacqueline Cole-Husseini helped me beat those results into submission. Dana Begun and Basma Khoury provided much-needed microCT advice and assistance. Former ORL PhD student Connie Pagedas taught me how to use the fluid shear system and left behind a Red Hot Chili Peppers tape that got me through some tedious experiments. Postdocs Jason Long and Eugene Manley leant solid career advice over many beers. Peggy Piech and

Sharon Vaaseen kept the lab running smoothly. Other folks who made life better in the ORL included: Lauren Smith, Ben Sinder, Mathieu Davis, Joey Peroskey, Erin Bigelow, Alex Brunfeldt, Rob Goulet (who kept lab hardware and software tip top), Erik Waldorff (long since graduated) and many others. A special thanks to our master electromechanical engineer, the late Dennis Kayner.

This project was enabled by many folks at the University of Michigan. First, Amy Koh-Paige, in the McCauley lab, played an important role in assisting us with the murine ossicle model. Earl Werner and Christopher Davis in the Department of Ecology and Evolutionary Biology were instrumental in providing access and assistance with the Edwin S. George Reserve.

Outside of UM, we need to express appreciation to Karl Malcolm, of Venatio Ltd, whose crack team of professionals got us three bucks in three nights. A shout out to Karl's Large Munsterlander, Luna, who tracked buck #2 in minutes when the trail got cold for us humans. At the University of Georgia, we need to thank David Osborn and Karl Miller, both of whom were a crucial source of animals for pilot project data. Corine Martineau, à la Université du Québec à Montréal, donne moi beacoup d'aide scientifique.

More thanks to my family as well as to Evan Pineda, Eric Horstick, Taber Burton, Kyle Yamada, Cedar Newlin et Corine Martineau encore.

Ethan Daley
September 2013

TABLE OF CONTENTS

LIST OF FIGURES

CHAPTER I

CHAPTER II

CHAPTER III

CHAPTER I:
Motivation, background and hypotheses

Motivation

Fracture healing is a multi-stage regenerative process that under most circumstances restores bone function without generating permanent scar tissue (Alman 2011). There are, however, a significant number of cases in the clinical world in which the bone fails to repair. Ten percent of all fractures require further intervention due to insufficient healing while 13% of tibial fractures result in delayed or non-unions (Colnot 2011, Dimitriou 2011.) Successful repair depends on the type and extent of injury and the body's bone repair program often cannot restore function after large segmental losses (Dimitriou 2011).

Repair of large bone defects (>2cm) is one of the key unmet clinical needs in musculoskeletal medicine (Guldberg 2012). Causes of such defects include disease, trauma and tumor resection (Dhillon 2011.) The high prevalence of blast injuries among U.S. soldiers serving overseas recently (79% of combat casualties) has heightened awareness of the need to improve outcomes for patients with traumatic bone damage: 54% of evacuated soldiers had injuries to the extremities, of which 26% involved fractures (Doukas 2013.)

Treatments for large bone defects include metallic implants, autologous bone transplants and allografts of cadaveric tissue. Unfortunately, these techniques are often beset by implant loosening, donor site complications, or limited osseointegration (Xie 2007 Tissue engineering, Dhillon 2011, Jacobson 2011.) Approximately 60% of allografts, for example, fail within ten years (Xie 2007.)

Advances in tissue engineering offer the potential to address these drawbacks through the delivery of osteoconductive or osteoinductive scaffolds and factors. The goals of bone tissue engineering, as defined by Hollister and Murphy, are to "(1) improve patient outcome, (2) reduce morbidity or complication . . . [and/or] (3) reduce procedural expenses" (Hollister 2011.) However, Hollister and Murphy also argue that bone tissue engineering has been largely unsuccessful in translating successes in the lab to the clinic due to a combination of technical, philosophical and business-related factors.

One overarching barrier to the realization of viable tissue engineering therapies is the poor regenerative capacity of most mammalian tissues compared to those of vertebrates such as the newt and axolotl (the Mexican Salamander, *Ambystoma mexicanum*), which can completely regrow severed appendages (Poss 2010.) A rare exception to the limits of mammalian regeneration is the deer antler, the only example of complete, repeated organ regrowth in an adult mammal (Kierdorf 2007.) Though they have largely escaped the attention of the tissue engineering field, the antlerogenic progenitor cells (APC) at the heart of antler regeneration have the potential to provide tremendous insights into potential strategies for directing adult somatic progenitor cells to achieve large scale tissue repair.

At this stage, however, basic questions about the APC phenotype remain unanswered. A better understanding of what APC are and how they differ from other cervid bone forming cells will guide future explorations of the mechanisms behind the unique behavior of these cells.

Background

Antlers are bony appendages that are annually cast, regrown and fully mineralized to a largely acellular state (Fig 1). With the important exception of reindeer, antlers are worn by the male members of deer species (Kierdorf 2007). This seasonal process is coupled to the reproductive cycle and is associated with fluctuations in levels of circulating androgens (Price 2004). Due to their size, nutritional requirements and role in "boxing" contests between rival males, antlers serve as outward indications of mate quality (Fig 2) (Price 2005, Landete-Castillejos 2007). The demands of annual regrowth require some of the fastest rates of bone growth in nature, exceeding 2cm/day in some species (Price 2004). Antlers grow so quickly that as much as 60-75% of the calcium required comes from bone resorption elsewhere in the body (Landete-Castillejos 2007.)

Antlers elongate through endochondral ossification occurring in growth centers in the tip of each antler tine (Fig 3) (Price 1994, Kierdorf 2009). Within each growth center, antlerogenic progenitor cells (APC) reside in a niche called the reserve mesenchyme, where undifferentiated APC undergo rapid proliferation as well as robust apoptosis (as many as 64% of cells there are apoptotic) (Colitti 2005, Rolf 2008). More proximally, APC undergo chondrogenic differentiation while those in perivascular niches differentiate into osteoblasts. The result is a tough matrix with a low mineral content compared to other mammalian long bones (Currey 2004).

Deer Antler Growth, Regrowth and Anatomy

The mechanisms that regulate the growth of a deer's first set of antlers and subsequent regrowth are thought to differ in critical ways. The former can be considered to be a more orthodox post-natal growth akin to the development of secondary sex characteristic (Faucheux 2004, Landete-Castillejos 2007) and the latter exploits not only mechanisms similar to wound healing and fracture repair (Li 2005), but is thought to recapitulate those of embryonic growth (Mount 2006). They are therefore described separately below.

First Antler Growth

First or “primary” antler growth is, by definition, not a regenerative event (Kierdorf 2007). First antlers are generated from pedicles, bony, vascularized masses of nerves, connective tissue and skin from which the antlers extend (Fig 4) (Price 2004). The pedicles are permanent projections of the frontal bones of the skull and are retained after the antlers are cast (Price 2004). Both the pedicles and antlers are thought to be derived from an “antlerogenic periosteum”, a term coined by Richard Goss, a pioneer in the field of deer antler research (Li 1994). Consisting of both cellular and fibrous layers, the antlerogenic periosteum is, in turn, likely derived from neural-crest tissue (Li 1994). Price cites Li and Suttie’s conjecture that the antlerogenic periosteum is a site of post-natally-retained embryonic tissue (Price 2004).

A male deer grows its first antlers during puberty (5-7 months for red deer, *Cervus elaphus*) (Price 2005). The first antlers (“spikers”) are not branched, and develop via intramembranous and then endochondral ossification extending from the distal tips (Price 2004).

Li and Suttie performed histological categorization of the stages and substages of pedicle and first antler growth in red deer (Li 1994.) Except where indicated, the following is a summary of Li and Suttie’s 1994 paper. There are two main stages of first antler growth, “internal” and “external”, during which the pedicle and first antlers are generated, respectively. Li and Suttie further divided the internal (pedicle growth) stage into three substages: intramembranous ossification (IMO), ossification pattern change (OPC) and endochondral ossification (ECO).

The IMO substage, occurring at about 4 months of age, is marked by the differentiation and proliferation of antlerogenic cells into osteoblasts (Price 2004). In the presence of the ample vascularization of the antlerogenic periosteum, the newly formed osteoblasts begin to lay down trabecular bone directly (Li 1994 and Price 2004). The bone produced at this stage is continuous with the frontal bone of the animal’s skull and is not visible from the exterior.

In OPC or “transitional” ossification, antlerogenic cells at the free ends of the trabeculae form chondrocytes (Li 1994 and 1998, Price 2004). The osseocartilaginous

tissue that forms is intriguing in that it is highly vascularized, though the sites of osteoblast differentiation seem to be distal to the furthest reaches of the capillaries. The pedicle is not palpable from the exterior during this substage.

If the capillary growth "catches up" to the antlerogenic cells at the free end of the trabeculae, the cells will again differentiate into osteoblasts and form bone intramembranously. Li and Suttie believe the OPC substage is triggered by rising levels of androgens.

The final substage of pedicle growth, endochondral ossification (ECO) occurs when the pedicle is between 2.5 and 4.0 cm long. The ECO substage is indicated by the establishment of fully vascularized cartilaginous trabeculae orientated vertically, parallel to the long axis of the pedicle. At this point, four distinct zones can be discerned within the pedicle. These are (from proximal to distal): trabecular bone (from the IMO substage), osseocartilaginous tissue (from the OPC substage), cartilaginous tissue (from the ECO substage) and a hyperplastic perichondrium The hyperplastic perichondrium, at the distal tip of the pedicle, is comprised of fibrous tissue arranged in a wave-like patterns and numerous, randomly-oriented cells engaged in rapid proliferation.

The tissue generated during first antler growth is not distinguishable histologically from that from the ECO stage of pedicle formation. In red deer, first antler growth is apparent as the pedicle/antler attains a height of approximately 4-6 cm. Also, the skin that grows on the newly formed tissue takes on the silky appearance of antler velvet.

Antler Regrowth

The annual regrowth of deer antlers is a process of appendage regeneration unique among mammals (Kierdorf 2007). Certain amphibians, the urodeles, are capable of complete regeneration of severed limbs. There is considerable debate as to how antler regrowth and the regrowth of limbs in urodeles are similar and different. This is not surprising, as this section illustrates how the process of regrowth itself is poorly understood and subject to controversy.

Antler regeneration follows a yearly cycle of shedding ("casting"), regrowth, and ossification (Fig 1). It is widely believed that this cycle is closely coupled to, but not directly regulated by, fluctuations in levels of circulating androgens (Price 2004).

Li examined the histological traits of regrowing red deer antlers and was able to distinguish five general stages of regeneration: precasting, casting, early wound healing, late wound healing/early antler regeneration and the formation of main beam and brow tine (Li 2005). His characterization of these stages was based on his study of red deer and certain details may not be applicable to all deer species.

In late winter or early spring, testosterone levels in male deer fall, possibly triggered by increasing day length (Price 2004, 2005; Bubenik 2006). Through a process not well understood, an abscission line appears, marking a transition zone between "living" and "dead," or fully mineralized antler (Li 2005). At this abscission line extremely rapid osteoclastic resorption occurs, cleaving the antler from the permanent pedicle (Kierdorf 2007, Price 2004). Price noted just how rapid casting can be, "…we noted an antler to be firmly attached to the pedicle at 08.00 only to find it was cast *30 min. later*" (Price 2004, emphasis added).

What follows antler casting is the formation of a blastema in a process resembling wound healing (Faucheux 2004, Kierdorf 2007, Li 2005, Price 2004). A thick skin layer (the "wound epithelium") begins to grow over the wound within hours. At the same time, osteoclasts selectively resorb bone from the abscission line, leading to a smoothing of the exposed bone (Li 2005, Price 2005, Kierdorf 2007). The skin grows substantially over the next 1 to 2 days, and the advancing edge of the epidermis is anchored to the bone via "tongue-like" projections that extend into a layer of rapidly growing tissue below in the center of the pedicle (Li 2005). Re-epithelialization is typically complete in 7 to 9 days (Faucheux, 2004).

The exact nature of the tissue underneath the newly grown skin is unknown. Li described it as "granulation tissue" because of its resemblance to that formed during wound healing (Li 2005). However, Price and Faucheux, citing the latter's finding of cells staining positive for PTHrP, believe this tissue to be mesenchymal (Faucheux 2004, Price 2005).

Faucheux's work suggests a recapitulation of embryonic growth processes during this stage of antler regrowth in conjunction with a more conventional wound healing response (Faucheux 2004). Recall that a blastema, rather than a scab, forms at the site of casting. It is not known why normal wound repair is not the sole response after casting, though it is thought that antler regeneration requires activation by the wound healing response (Price 2004). There is a great deal of speculation about the role, or lack thereof, of the immune system after the antlers are shed. Some suspect that the local environment around the pedicle is immunodeficient, and that there is a positive association between immunodefiency and ability to regenerate (Price 2004). Note that, despite the large area of exposed tissue after casting, bacterial infections rarely occur at these sites (Price 2004).

The blastema that develops beneath the wound epithelium is comprised of 3 broadly defined zones (Price 2004). Immediately under the skin is an area that resembles the future perichondrium. Below that are proliferating mesenchymal cells (Price 2004). Underneath the mesenchymal cells is a region of chondrogenesis (Price 2004).

So far we have covered Li's stages of pre-casting, casting and early wound healing. In red deer, as in many other species, the initiation of antler regrowth immediately follows these stages (Li 2005). In reindeer and moose, however, this is not the case (Price 2005). For these species there can be a delay of several months between casting and regrowth, possibly as a means of conserving nutrients during the winter (Price 2005). Such exceptions call into question the notion that casting necessarily triggers antler regrowth (Kierdorf 2007). In fact, the existence of "double antlers" suggests the regeneration process begins before the previous set of antlers are even cast (Kierdorf 2007).

Whenever it occurs, Li divides the stage of late wound healing/early antler regeneration into three substages (Li 2005). First is the initiation of anterior and posterior growth centers (Li 2005). Here, discrete clusters of chondrocytes are generated at the anterior and posterior edges of the pedicle (Li 2005). The tips of these cartilaginous growth centers are topped with a hyperplastic periosteum/perichondrium layer which is heavily populated by mesenchymal "antlerogenic progenitor cells" (Li

2005, Rolf 2006). The second substage involves the formation of continuous cartilaginous columns in the growth centers (Li 2005). These columns are generated by the hyperplastic periosteum/perichondrium from the first substage and lead to bone formation in a sequence that closely mirrors the ossification stages of primary antler growth: intramembranous ossification (leading to trabecular bone formation), then "transitional" growth (in which osseocartilaginous tissue forms) and, finally, endochondral ossification (Li 2005).

The third and last substage of late wound healing/early antler regeneration is a process of remodeling of the cartilaginous region formed in the previous substages (Li 2005). This final substage marks the end of an apparent wound healing response (Li 2005). In addition, the growth centers formed in the previous substage begin to "bulge out" from the pedicle (Li 2005).

Finally, the last stage of antler regeneration defined by Li is that of the formation of the main antler beam and brow tine (Li 2005). This stage ends in the fall as testosterone levels peak, triggering full mineralization of the antler and shedding of the velvet (Bubenik 2006). The "hard" antlers are now exposed (Price 2004).

The rate of regrowth of the antler occurs in an "S"-shaped growth curve (Price 2004). Regrowth during the first 4 to 6 weeks is fairly slow but accelerates rapidly in the following 60-80 days of late spring and early summer (Price 2004). The longitudinal growth rate during those 60-80 days can approach 2 centimeters per day, though this figure is closer to 6.35mm for white-tailed deer (Ozoga 1996, Price 2004). As fall approaches, the growth rate slows again and the above-mentioned process of mineralization occurs (Price 2004).

Structure of the Regenerating Antler

In her 2004 paper, Price delineates the anatomy of the regrowing antler and some candidate regulatory mechanisms (Fig 5) (Price 2004). Except where indicated, the following is drawn from her 2004 paper. The longitudinal growth of the antler is driven mainly by endochondral ossification at the tip of each antler branch. The tip can be divided into the following zones (from distal to proximal): dermis, perichondrium, periosteum, "zone of proliferation" and "transition zone".

The cellular region of the perichondrium, with its low concentration of ALP, is thought to be the “niche” that containing progenitor cells (Li 2001, Kierdorf 2007). The periosteum is continous with the perichondrium and is a site of intramembranous bone formation. Cells here have been found to express PTHrP, RANKL and the retinoic acid-synthesizing enzyme RALDH2.

The zone of proliferation has also been called the “reserve mesenchyme” or, simply, the “mesenchyme”. It is a region heavily populated with cells that are not wholly differentiated down an osteoblastic lineage, as indicated by the dearth of ALP there. These cells have of late been referred to as “antler progenitor cells” by Mount and others (Mount 2006). A low level of Type I collagen mRNA expression has been detected in the zone of proliferation and Type II collagen mRNA has not been found. This result suggests that there are few chondroprogenitor cells in this region.

The zone of proliferation is thought to be the epicenter of growth for the regenerating antler (Price 2004, Kierdorf, 2007). Cells there have a high rate of proliferation and apoptosis (64% of cells) (Colitti 2005). The role of such a high degree of apoptosis is not known, but Price opines that this could be a defense against mutation in a region that might otherwise be prone to cancerous growth.

The transition zone is where chondrogenic differentiation occurs. Cells here are aligned in vertical columns and transcribe mRNA for Types I, IIA, IIB, and X collagen. As stated above, antler cartilage is unusual in its high degree of vascularization, unlike adult growth plate cartilage. In addition, antler cartilage contains much more Type X collagen than typically found in the growth plate. Osteoblasts and osteoclast progenitor cells can be found between the columns of chondrocytes. According to Price, the rapid growth of antlers requires extensive resorption of mineralized cartilage via osteoclasts followed by the replacement of cartilage by bone by the osteoblasts supplied by the transition zone.

For reasons that remain unclear, each set of regenerated antlers is larger and more complex than that grown in the previous year. This process is termed hypermorphic regeneration (Kierdorf 2007).

Animal Studies

One of the central challenges in deer antler research is the lack of standardized animal models or cell lines. The species of deer studied have often been those convenient to the researchers. Antlers have been studies from species including:

- Fallow Deer (*Dama dama*) (Goss 1990, Kierdorf 2003)
- Spotted Deer (*Axis axis*) (Rajaram 1982)
- Red Deer (*Cervus elaphus*) (Price 1994, Faucheux 2001, etc.)
- Reindeer (*Rangifer tarandus*) (Kapanen 2002)
- Roe Deer (*Capreolus caprelous*) (Kierdorf 2003)
- Whitetail Deer (*Odocoileus virginianus*) (French 1956)

Most of these animals have been studied *ex vivo* in the form of cast-off antlers or via histological examination of antler tissue from culled deer. Much work has centered on the *in vivo* study of fluctuations in hormone levels (Bubenik 2006, Bartos 2009). As part of their examination of the regenerative role of the pedicle periosteum, Li, et al, studied roe deer *in vivo* (Li 2006). Several workers have generated antler-derived cell cultures, but the types of cells and methods used have varied widely (Price 1994, Faucheux 2001, Li 2001, Mount 2006, Rolf 2006). Importantly, though some of these studies have examined antler progenitor cells, there have so far been no attempts to culture other types of MSCs from deer. Marrow-derived MSCs would provide a powerful basis of comparison for the APC phenotype.

Complementary DNA libraries have been generated for proteins such as BMP-3b isolated from reindeer. Unfortunately, these libraries have since been lost (Väänänen, personal correspondence). In addition, cervid VEGF has been sequenced. However, the complete or even partial genome of deer species has yet to be sequenced (Kapanen 2002, Price 2004).

Mechanical properties of antler and mechanoresponsiveness

In general, antler is tougher, and more damage resistant than other types of bone, perhaps indicative of its evolutionary role as a secondary sex characteristic used

for fighting and display (Currey 2004). Compared to a human humerus, the antler cortex is “young bone” composed chiefly of primary osteons (Launey 2010.) Unlike other long bones, antler osteons lack cement lines and are instead surrounded by a hypermineralized region (Skedros 1995.)

The role of mechanical forces in regulating the growth of the antler is not well understood. Antlers are subject to frequent impacts during the rutting season but bear no weight other than their own. Moreover, the exigencies of annual regeneration generally obviate the need for extensiveness remodeling.

However, secondary osteons are found in antler compact bone, indicating that some remodeling occurs (Launey 2010.) In addition, the presence of osteocytes in antler bone suggests the retention of mechanosensitivity in this tissue (Rolf 1999.) More speculative is the possibility that mechanical pressures due to the stretching of the skin overlying the pedicle may trigger the transition from intramembrous to endochondral differentiation during early antler regrowth (Li 2000.)

Although there is circumstantial evidence that mechanical forces may exert some influence on the antler, no study has attempted to directly assess the effects of mechanical stimuli on antler cells. Characterization of the mechanoresponsiveness of these cells compared to that of other cervid bone forming cells may offer some insight into the uniqueness of their phenotype.

Cells and factors involved in antler regeneration

The following is a breakdown of selected cells and factors thought to be especially important in the regulation of the process of antler regeneration.

Antler Progenitor Cells

Antler regeneration was once thought to be akin to the limb regeneration witnessed in animals such as urodeles. In other words, a process driven by the de- and/or trans-differentiation of existing cells during the formation of a blastema prior to tissue regeneration (Kierdorf 2007). Kierdorf enumerated eight key differences between urodele limb and deer antler regeneration—the lack of de- or transdifferentiated cells in the latter being the most critical (Kierdorf 2007). The prevailing view of antler growth

and regeneration is now one driven by *de novo* mesenchymal stem cell generation (Li 2007, Rolf 2006, Kierdorf 2007).

The growth centers that arise early in the endochondral phase of antler regeneration contain undifferentiated and rapidly proliferating, highly apoptotic “antler progenitor cells” (APC) (Li 2005, Colitti 2005, Mount 2006). APC persist throught later growth in the reserve mesenchyme where, much like in the epiphyseal growth plate, they differentiate down chondro- and osteogenic pathways to supply the cellular “workforce” needed for antler growth.

It is thought that APC are generated within the pedicle and antler periostea. The notion of an “antlerogenic periosteum” has existed since the 1970s, when Hartwigg and Schrudde grafted a pedicle periosteum to a subcutaneous location in the leg of a roe deer and were able to successfully grow an ectopic antler (Li 2001). This experiment was later repeated in fallow deer (Goss 1985). Li was even able to use antler periosteum xenografts to grow pedicle on the heads of nude mice (Li 2001). More recently, Li showed that antler pedicles denuded of their periostea lost or suffered delays in their ability to regrow (Li 2007).

The above work has been bolstered by histological and *in vivo* LacZ cell labeling studies pointing to the periosteum as the tissue source from which antler growth derives (though he does not describe his techniques in much detail) (Li 2001, 2005). In a later paper, Li concluded that both the antlerogenic periosteum and overlying skin govern the initial stages of antler growth and that only the former is important once antler growth is initiated (Li, 2008).

As the importance of pedicle and antler periostea has been established, work has shifted toward characterizing the actual cells involved in antler regeneration. Several studies have hinged on the *in vitro* culturing of multiple cell types harvested from various regions within the regenerating antler tip (Price 1994, Li 1998, Faucheux 2001, Li 2001, Rolf 2006). However, only two recent studies have attempted to investigate the behavior of antler tip APC specifically (Mount 2006, Rolf 2008).

Mount extracted cells *post mortem* from the reserve mesenchyme region of 2-year-old red deer (*Cervus elaphus*) at 2, 4, and 8 weeks after antler casting as part of a study concerning the role of Wnt signaling in antler (Mount 2006). Mount maintained

sub-confluent cultures of these cells and treated them with either lithium chloride (a Wnt agonist) or epigallocatechin gallate (EGCG, a Wnt inhibitor). EGCG significantly reduced cell number, increased TUNEL-positive cells (indicating apoptosis) and increased ALP activity. LiCl had no effect on cell number or TUNEL staining, but significantly reduced ALP activity compared to controls.

Rolf, building on a 2006 paper in which he cultured cells from the regenerating tips of fallow deer (*Dama dama*), made the first attempt to isolate antler progenitor cells using several common MSC markers (Rolf 2008). Using fluorescence-activated and magnetic cell sorting, cells collected from chondrogenic growth zones and pedicle periostea were screened positively (STRO, CD271, and CD133) and negatively (CD14, CD34, CD105, and CD133). Rolf found that cells from the pedicle periosteum that were STRO-1+, CD271+, or CD133+ were also CD34-, a strong indicator that these cells were mesenchymal, rather than hematopoietic, progenitors.

In addition, Rolf investigated the differentiation potential of STRO-1+ cells. These cells were exposed to either non-differentiating media or media containing osteoblastic, adipogenic or neurogenic factors (Rolf 2008). Proliferation rates were greatest for cells in the osteoblastic medium. These cells also produced measurable osteocalcin levels, a late phenotypic marker of osteoblasts, by the 21st day of culturing. RT-PCR of STRO-1+ cells maintained in non-differentiating media showed some expression of collagen I (though not of the other osteoblastic markers, cbfa1/runx2, osteocalcin, or the chondrogenic marker chondroadherin), indicating that a degree of differentiation had already occurred in some ostensible progenitor cells in the pedicle periosteum. Intracellular lipid droplets were also reported in cells exposed adipogenic media via Oil Red O stain, though the criteria used for distinguishing lipid droplets from vesicles or even Golgi apparatus was arguably generous. The paper does not describe the results of the attempted neurogenic culture experiment.

Rolf's 2008 paper provides an important verification not only of the existence of mesenchymal antler progenitor cells, but of the feasibility of culturing and differentiating these cells. In essence, the groundwork has been laid for identifying APC as well as some basic cell phenotyping. The door is now open for a more thorough investigation of APC behavior.

Hormones and factors

The link between the initiation of first antler growth and the timing of the phases of regeneration and seasonal variations in sex steroid level has long been established (Price 2004, Bubenik, 2006). A widely circulated story in the literature is that Aristotle himself observed that castrated deer fail to grow primary antlers (Price 2005). In addition, castration during the mineralized antler stage will cause premature casting (Price 2004). The regrown antlers of castrated deer appear normal but fail to either mineralize completely or shed their velvet covering (Price 2004). Antler growth can be promoted in castrated and even female deer through the use of exogenous androgens (Price 2004).

Though hormones are critical to antler growth and regrowth, they are actually only half of the way in a pathway between the ultimate cause of these processes and the processes themselves.

This “ultimate cause” is the seasonal change in ambient light availability (Bubenik 2006). Signals from the retina are sent to the pineal gland, which Bubenik calls the “’clock’ and ‘calender’ [of antler growth]” (Bubenik 2006). The pineal gland produces melatonin in response to darkness, and this hormone suppresses secretion of prolactin from the pituitary gland (Bubenik 2006). Increased light availability in the springtime reduces melatonin production and allows prolactin levels to rise (Bubenik 2006). The increased levels of prolactin stimulate the anterior pituitary to produce luteinizing hormone (LH), which, in turn, triggers the Leydig cells in the testes to produce testosterone (Bubenik 2006). High levels of prolactin in the spring and summer suppress testosterone formation by blocking LH receptors on the Leydig cells (Bubenik 2006). This is why the effects of testosterone on antlers are not fully manifested until the late summer/early fall, when decreased light availability reduces the inhibitory effect that high levels of prolactin have on testosterone production (Bubenik 2006).

The fluctuating levels of circulating testosterone correspond to the phases of antler regeneration. Suppression of testosterone in the late winter/early spring triggers antlers casting. Reduced suppression of testosterone during the spring and summer (via the mechanisms outlined above) coincides with antler regrowth (Price 2005, Bartos

2009). Finally, peak levels of blood testosterone late in the fall are coupled to full antler mineralization and shedding of the velvet covering (Price 2005).

Though testosterone is closely *associated* with antler growth, there is some controversy as to whether it or other hormones act directly on antlerogenic tissues and cells (Suttie 1995, Bartos 2009). There is even conflicting evidence as to whether testosterone directly influences antler growth or regrowth (Suttie 1995, Li 2001, Price 2005, Bartos 2009). A potential source of such discrepancies could well be due to the wide range of protocols used to study the effects of hormones in deer.

In his *in vivo* study of red deer, Suttie found that blocking testosterone secretion during and prior to antler regrowth had no inhibitory effect on antler regrowth (Suttie 1995). In fact, antlers in the treated group were slightly larger than those for which testerone levels were unaffected. Bartos, on the other hand, saw a significant positive association between circulating testosterone concentrations and antler length in 2-year-old and adult red deer (Bartos 2009). Moreover, Li was able to use exogenous testosterone to induce pedicle and antler growth in several castrated male and female red deer (Li 2002). Li also reported that graded concentrations of testosterone, dihydrotesterone, or estradiol had no proliferative effect on cells cultured from antler periostea (Li 2001).

One school of thought implicates IGF-1 (insulin-like growth factor-1) as the "antler stimulating" factor (Suttie 1985). Secreted by osteoblasts, IGF-1 is one of the most prevalent growth factors in bone (Delany 2001). It is associated with increases in bone matrix formation and decreases in bone resorption (Delany 2001.) A large increase in serum IGF-1 occurs during the rapid phase of antler regrowth (Fig 6) and IGF-1 levels correlate positively with antler growth rate (Suttie 1989, Price 2005.) IGF-1 mRNA has been found in osteoblasts and chondrocytes in the antler tip (Price 2005, Gu 2007.) In culture, antler cells proliferate in response to IGF-1 (Price 1994, Li 2001, Sadighi 2001).

The mitogenic effect of IGF-1 on antler cells was completely abolished when the artificial glucocorticoid dexamethasone was added (Li 2001.) This result corroborates the view that IGF-1 is negatively regulated by glucocorticoids such as cortisol (Delany

2001.) It is therefore possible that glucocorticoids can regulate IGF-1 levels in the antler and perhaps alter the balance between proliferation and differentiation.

However, predicting the effects of glucocorticoids on antler cells is difficult. While dexamethasone was shown to decrease IGF-1-induced mitogenesis in antler cells, this glucocorticoid has also been demonstrated to enhance proliferation in some cell types (Bellows 1990, Jaiswal 2000, Tuan 2002.) Dexamethasone is also known to either increase (alkaline phosphatase activity) or decrease (collagen I and osteocalcin expression) markers of osteoblastogenesis in mesenchymal cells from other animals (Hoch 2012.) As dexamethasone is a component of many osteo-, chondro- and adipogenic differentiating media formulations, it remains to be seen what effects this glucocorticoid has on antler cell differentiation.

Hypotheses

Though not well characterized, the APC phenotype may yield insights that could elucidate mechanisms for enhancing bone regeneration. We therefore embarked on a wide ranging investigation of APC properties and behavior. In addition, we submit that any understanding of this uniqueness of APC is incomplete without also investigating how they differ from other cervid MSC. To help answer this question, we cultured a parallel, animal-matched population of marrow-derived MSC (hereafter referred to as "MSC") and subjected them to the same methods as with APC.

Using cells isolated from the antlers and marrow of whitetail deer (*Odocoileus virginianus)*, the work was guided by the following global hypothesis:

APC and cervid marrow-derived MSC conform to a mesenchymal stromal cell model but differ measurably from each other in terms of their intrinsic behavior and responses to stimuli.

Aim 1: To investigate APC behavior in culture

The following hypotheses will be tested:

1.1 Under static culture conditions, APC demonstrate increased colony formation, rates of proliferation and markers of adipo- chondro-, and osteogenic differentiation compared to animal-matched marrow MSC.

1.2 Under static culture conditions, APC will display increased apoptosis compared to MSC.

1.3 Under static culture conditions, APC and MSC will exhibit different responses to the artificial glucocorticoid steroid dexamethasone.

Aim 2: To investigate APC differentiation in an in vivo ectopic ossicle formation model

The following hypothesis will be tested:

> *APC in an in vivo ectopic ossicle formation model will generate more mineralized matrix compared to animal-matched marrow MSC.*

Aim 3: To determine APC response to oscillatory fluid flow (OFF)

The nucleation of antler growth centers at sites of potentially high shear stress may indicate that APC possess an altered sensitivity to mechanical stimuli compared to marrow-derived MSCs of the same species. The following hypothesis will be tested:

> *APC and MSC have different patterns of response when subjected to oscillatory fluid shear stress.*

Chapter I figures

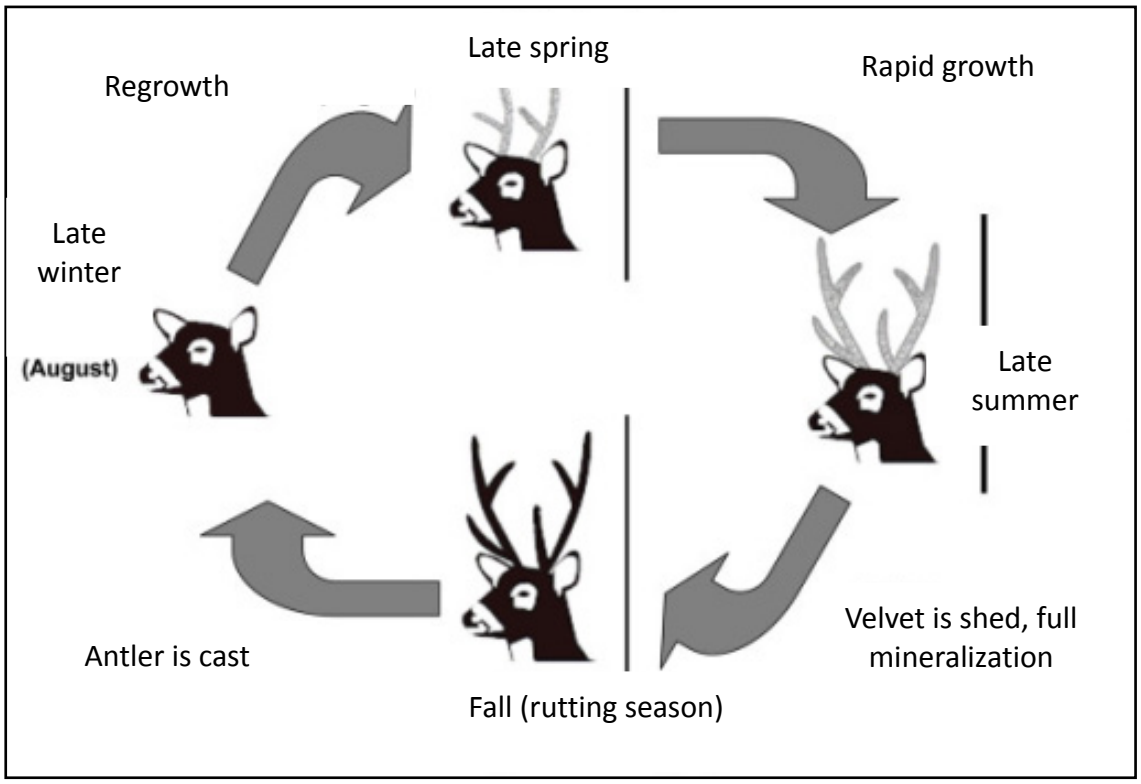

Figure 1.1: The antler cycle. Adapted from Ungerfeld 2008.

Figure 1.2: Two white-tailed bucks engaging in "boxing," or display fighting, during a spring evening west of Saline, Michigan. New antler growth is visible on the left contender. Two suitably impressed does are on the left. Image captured on a motion-activated game camera. Courtesy of Charles Roehm.

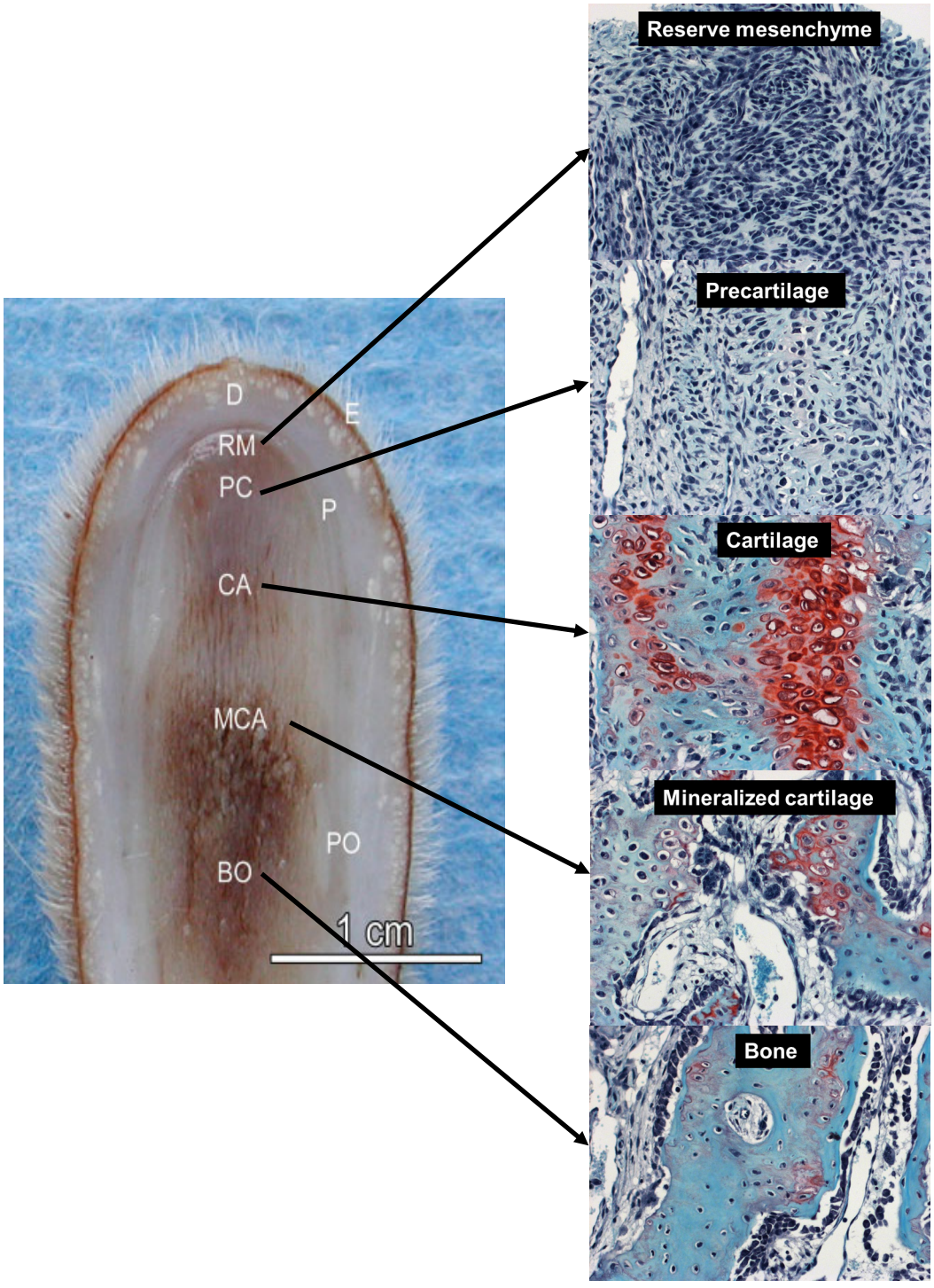

Figure 1.3: Cross section of antler tip. Image on left from Kierdorf 2007. Images on right stained with show safranin-O/Fast Green stain (200X mag.)

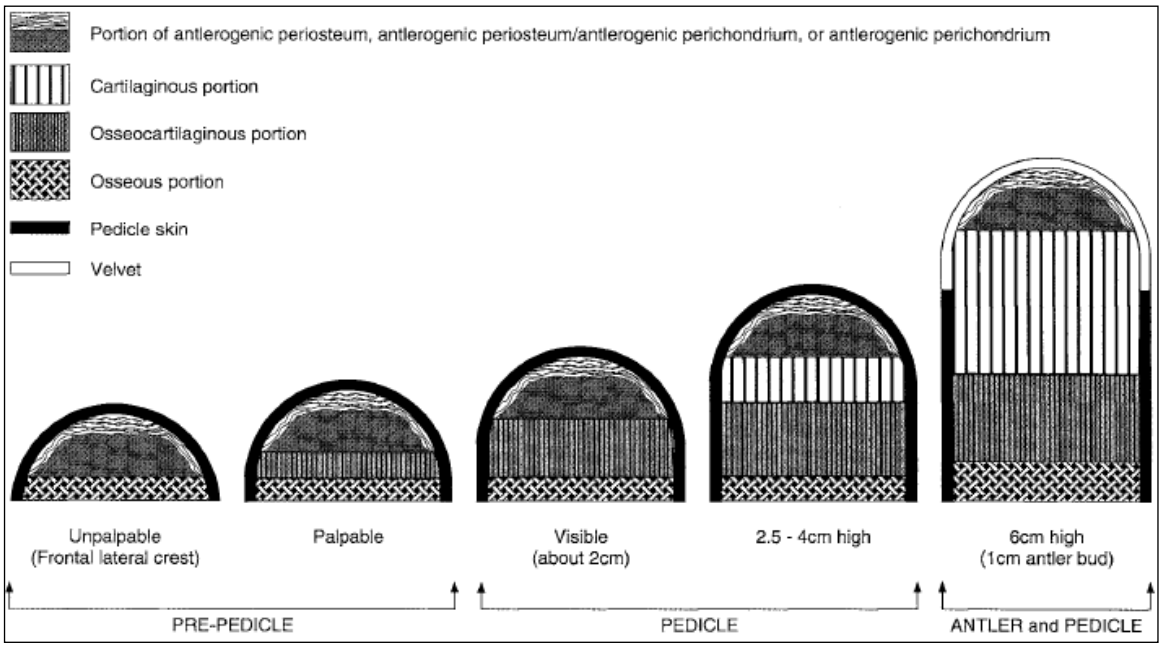

Figure 1.4: Stages of first antler growth in red deer (*Cervus elaphus*). From Li 1994.

Figure 1.5: Deer antler regrowth. Top row (left to right): Antler blastema 24hrs after casting; blastema after roughly 8 days; rapidly growing antler at about 21 days. Bottom row (left to right): fully grown antler at 100 days, still retaining velvet; fully mineralized antler at 140 days showing shedding of velvet. From Price 2004.

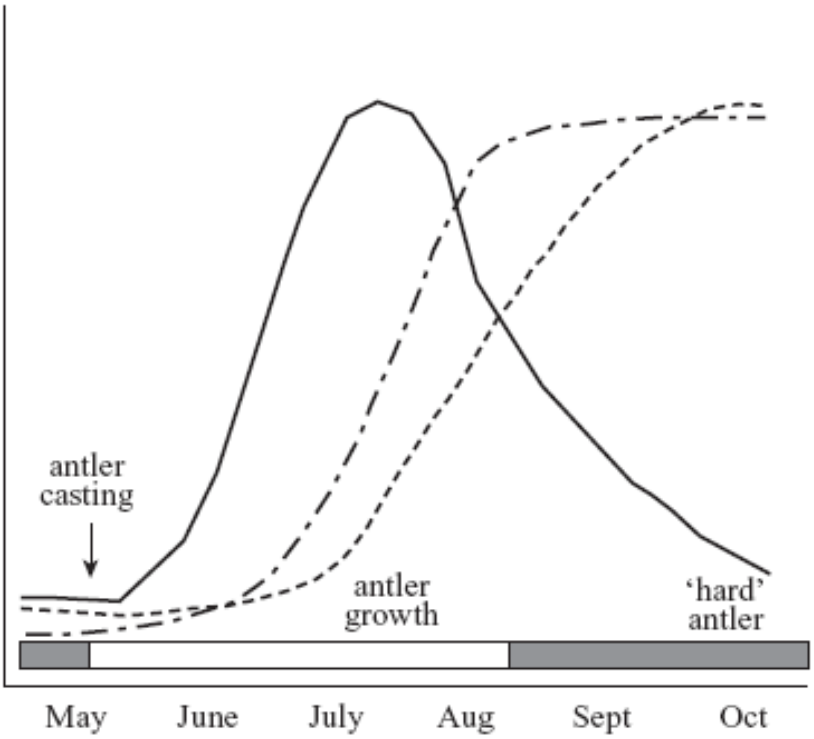

Figure 1.6: Seasonal changes in testosterone, IGF-1, antler growth. Testosterone, dashed line; IGF-1, solid line; Dot-dashed line, antler growth. From Price, 2004.

Bibliography

Alman BA, Kelley SP, Nam D. Heal thyself: using endogenous regeneration to repair bone. Tiss Engin B 2011:17(6):431-436.

Bellows CG, Heersche JNM, Aubin JE. Determination of the capacity for proliferation and differentiation of osteoprogentiro cells in the presence and adsence of dexamethasone. Dev Bio 1990;140(1):132-138.

Bartos L, Schams D, Bubenik GA. Testosterone, but not IGF-1, LH, prolactin or cortisol, may serve as antler-stimulating hormone in red deer stags (*Cervus elaphus*). Bone 2009; 44:691-698.

Bubenik GA. Seasonal regulation of deer reproduction as related to the antler cycle – a review. Veterinarski Arhiv (Suppl.) 2006; 76:S275-S285.

Clark DE, Lord EA, Suttie JM. Expression of VEGF and pleiotrophin in deer antler. The Anat Rec Part A 2006; 288A:1281-1293.

Clark DE, Li C, Wang W, Martin SK, Suttie JM. Vascular localization and proliferation in the growing top of the deer antler. The Anat Rec Part A 2006; 288A-973-981.

Colitti M, Allen SP, Price JS. Programmed cell death in the regenerating deer antler. J Anat 2005; 207:339-351.

Colnot C. Cell sources for bone tissue engineering : insights from basic science. Tiss Engin B 2011 ; 17(6):449-457.

Currey JD, Brear K, Zioupos P. Notch sensitivity of mammalian mineralized tissues in impact. Proc R Soc Lond B 2004; 271:517-522.

Delany AM, Durant D, Canalis E. Glucocorticoid suppression of IGF I transcription in osteoblasts. Mol Endochrin 2001;15(10):1781-1789.

Dhillon RS, Schwarz EM. Teriparatide therapy as an adjuvant for tissue engineering and integration of biomaterials. Materials 2011;4:1117-1131.

Dimitriou R, Jones E, McGonagle D, Giannoudis PV. Bone regeneration: current concepts and future directions. BMC Med 2011;9:66.

Donahue TLH, Haut TR, Yellowley CE, Donahue HJ, Jacobs CR. Mechanosensitivity of bone cells to oscillating fluid flow induced shear stress may be modulated by chemotransport. J Biomechanics 2003; 36:1363-1371.

Doukas 2013 WC, Hayda RA, Frisch M, Andersen RC, Mazurek MT, Ficke JR, Keeling JJ, Pasquina PF, Wain HJ, carlini AR, Mackenzie EJ. The military extremity trauma amputation/limb salvage (METALS) study. J Bone Joint Surg Am 2013;95:138-145.

Faucheux C, Nesbitt SA, Horton MA, Price JS. Cells in regenerating deer antler cartilage provide a microenvironment that supports osteoclast differentiation. J Exp Biology 2001; 204:443-455.

Faucheux C, Nicholls BM, Allen S, Danks JA, Horton MA, Price JS. Recapitulation of the parathyroid hormone-related peptide-Indian Hedgehog pathway in the regenerating deer antler. Dev Dynamics 2004: 231:88-97.

French CE, McEwen LC, Magruder ND, Ingram RH, Swift RW. Nutrient requirements for growth and antler development in the white-tailed deer. Jour Wildlife Man 1956;20(3):221-232.

Goss RJ. Tumor-like growth of antlers in castrated fallow deer: an electron microscopic study. Scanning Microsc 1990;4(3)715-720.

Gu L, MO E, Yang Z, Zhu X, Fang Z, Sun B, Wang C, Bao J, Sung C. Expression and localization of insulin-like growth factor-I in four parts of the red deer antler. Growth Factors 2007;25(4):264-279.

Guillot PV, Gotherstrom C, Chan J, Kurata H, Fisk NM. Human first-trimester fetal MSC express pluripotency markers and grow faster and have longer telomeres than adult MSC. Stem Cells 2007;25:646-654.

Guldberg, RE. “Limb regeneration: effects of local biomechanical and biologic factors.” International Bone & Mineral Society Workshop: Musculoskeletal Biology. Sun Valley, Idaho. 6 Aug. 2012.

Harper’s Illustrated Biochemistry, 27th edition. Murray RK, Granner DK, Rodwell VW, editors. New York: Lange/McGraw-Hill, 2006; pg 543.

Hoch AI, Binder BY, Genetos D, Leach JK. Differentiation-dependent secretion of proangiogenic factors by mesenchymal stem cells. PLoS ONE 2012;7(4):e35579.

Hollister SJ, Murphy WL. Scaffold translation: barriers between concept and clinic. Tiss Engin B 2011;17(6):459-474.

Jacobs CR, Yellowley CE, Davis BR, Zhou Z, Cimbala JM, Donahue HJ. Differential effect of steady versus oscillating flow on bone cells. J Biomechanics 1998; 31:969-976.

Jacobson JA, Yanoso-Scholl L, Reynolds DG, Dadli T, Bradica G, Bukata S, Puzas EJ, Zuscik MJ, Rosier R, O'Keefe RJ, Schwarz EM, Awad HA. Teriparatide therapy and beta-tricalcium phosphate enhance scaffold reconstruction of mouse femoral defects. Tiss Engin A 2011; 17(3,4):389-398.

Jaiswal RK, Jaiswal Neelam, Bruder SP, Mbalaviele G, Marshak DR, Pittenger MF. Adult human mesenchymal stem cell differentiation to the osteogenic or adipogenic lineage is regulated by mitogen-activated protein kinase. J Bio Chem 2000; 275:9645-9652.

Kapanen A, Ryhänen, Birr E, Väänänen K, Tuukkanen J. Bone morphogenetic protein 3b expressing reindeer antler. J Biomed Mater red 2002;59(1):78-83.

Kierdorf U, Stoffels E, Stoffels D, Kierdorf H, Szuwart T, Clemen G. Histological studies of bone formation during pedicle restoration and early antler regeneration in roe deer and fallow deer. The Anat Rec Part A 2003; 273A:741-751.

Kierdorf U, Kierdorf H, Szuwart T. Deer antler regeneration: cells, concepts, and controversies. J Morphology 2007; 268:726-738.

Kierdorf U, Li C, Price JS. Improbable appendages: deer antler renewal as a unique case of mammalian regeneration. *Seminars Cell Dev Bio* 2009; 20(5):535-542.

Lai AKW, Hou WL, Verdon DJ, Nicholson LFB, Barling PM. The distribution of the growth factors FGF-2 and VEGF and their receptors, in growing red deer antler. Tissue and Cell 2007; 39:35-46.

Landete-Castillejos T, Estevez JA, Martinez A, Ceacero F, Garcia A, Gallego L. Does chemical composition of antler bone reflect the physiological effort made to grow it [sic]? Bone 2007:1095-1102.

Launey ME, Chen PY, McKittrick J, Ritchie RO. Mechanistic aspects of the fracture toughness of elk antler bone. Acta Biomaterialia 2010;6:1505-1514.

Li C, Suttie JM. Light microscopic studies of pedicle and early first antler development in red deer (*Cervus elaphus*). The Anat Rec 1994; 239:198-215.

Li C, Suttie JM. Histological studies of pedicle skin formation and its transformation to antler velvet in red deer (*Cervus elaphus*). The Anat Rec 2000;260:62-71.

Li C, Suttie JM. Deer antlerogenic periosteum: a piece of postnatally retained embryonic tissue? Anat Embryol 2001; 204:375-388.

Li C, Littlejohn RP, Corson ID, Suttie JM. Effects of testosterone on pedicle formation and its transformation to antler in castrated male, freemartin and normal female red deer (*Cervus elaphus*). Gen and Comparative Endochrinology 2003; 131:21-31.

Li C, Wang W, Manley T, Suttie JM. No direct mitogenic effects of sex hormones on antlerogenic cells detected *in vitro*. Gen and Comparative Endochrinology 2001; 142:75-81.

Li C, Mackintosh CG, Martin SK. Identification of key tissue type for antler regeneration through pedicle periosteum deletion. Cell Tissue Res 2007; 328:65-75.

Li C, Suttie JM, Clark DE. Histological examination of antler regeneration in red deer (*Cervus elaphus*). The Anat Rec Part A 2005; 282A:163-174.

Li C, Yang F, Xing X, Gao X, Deng X, Mackintosh C, Suttie JM. Role of heterotypic tissue interactions in deer pedicle and first antler formation—revealed via a membrane insertion approach. J Exp Zoology (Mol Dev Evol) 2008; 310B:267-277.

Mount JG, Muzylak M, Allen S, Althnaian T, McGonnell IM, Price JS. Evidence that the canonical Wnt signaling pathway regulated deer antler regeneration. Dev Dynamics 2006; 235:1390-1399.

Ozoga John J, Whitetail Spring: Season of the Whitetail. 1996 Willow Creek Press: Minocqua, WI, pg 82.

Poss KD. Advances in understanding tissue regenerative capacity and mechanisms in animals. Nat Rev Gen 2010;11:710-722.

Price JS, Oyajobi BO, Oreffo ROC, Russel RGG. Cells cultured from the growing tip of red deer antler express alkaline phosphatase and proliferate in response to insulin-like growth factor-I. J of Endochrinology 1994; 143:R9-R16.

Price JS, Allen S. Exploring the mechanisms regulating regeneration of deer antlers. Phil Tran Roy Soc London B 2004; 359:809-822.

Price JS, Allen S, Faucheux C, Althnaian T, Mount JG. Deer antlers: a zoological curiosity or the key to understanding organ regeneration in mammals? J Anat 2005; 207(5):603-618.

Rajaram A, Ramanathan N. Tensile properties of antler bone. Calcif Tissue Int 1982; 34:301-305.

Riddle RC, Khatri R, Schipani E, Clemens TL. Role of hypoxia-inducible factor-1α in angiogenic-osteogenic coupling. J Mol Med 2009; 87:583-590.

Rolf HJ, Enderle A. Hard fallow deer antler: a living bone till antler casting? The Anat Rec 1999;255:69-77.

Rolf HJ, Wiese KG, Siggelkow H, Schliephake H, Bubenik GA. In vitro-studies with antler bone cells: structure forming capacity, osteocalcin production and influence of sex steroids. Osteology 2006; 15:245-257.

Rolf HJ, Kierdorf U, Kierdorf H, Schulz J, Seymour N, Schliephake H, Napp J, Niebert S, Wolfel H, Wiese KG. Localization and characterization of STRO-1+ cells in the deer pedicle and regenerating antler. PLoS ONE 2008; 3(4):e2064.

Ruether T, Rohmann D, Scheer M, Kübler AC. Osteoblast viability and differentiation with Me_2SO as cryoprotectant [sic] compared to osteoblasts from fresh human iliac cancellous bone. Cryobiology 2005; 51:311-321.

Sadighi M, Li C, Littlejohn RP, Suttie JM. Effects of testosterone either alone or with IGF-I on growth of cells derived from the proliferation zone of regenerating antlers *in vitro*. Growth Hor & IGF Res 2001;11:240-246.

Schipani E, Ryan HE, Didrickson S, Kobayashi T, Knight M, Johnson RS. Hypoxia in cartilage: HIF-1α is essential for chondrocyte growth arrest and survival. Genes & Dev 2001;15:2865-2876.

Skedros JG, Durand P, Bloebaum RD. Hypermineralized peripheral lamellae in primary osteons of deer antler: potential functional analogues of cement lines in mammalian secondary bone. J Bone Miner Res 1995;10:S441.

Suttie JM, Gluckman PD, Butler JH, Fennessy PF, Corson ID, Laas FJ. Insulin-like growth factor 1 (IGF-1) antler-stimulating hormone [sic.] Endochrinol 1985;116(2):846-848.

Suttie JM, Fennessy PF, Corson ID, Laas FJ, Crosbie SF, Butler JH, Gluckman PD. Pulsatile growth hormone, insulin-like growth factors and antler development in red deer (*Cervus elaphus scoticus*) stags. J. Endochrinol 1989;121:351-360.

Suttie JM, Fennessy PF, Lapwood KR, Corson ID. The role of steroids in antler growth of red deer stags. J Exp Zoology 1995; 271:120-130.

Tropel P, Noel D, Platet N, Legrand P, Benabid AL, Berger F. Isolation and characterisation of mesenchymal stem cells from adult mouse bone marrow. Exp Cell Res 2004; 295:395-406.

Tuan RS, Boland G, Tuli R. Adult mesenchymal stem cells and cell-based tissue engineering. Arthr Res Ther 2002; 5:32-45.

Ungerfeld R, Gonzalez-Pensado S, Bielli A, Villagran M, Olazagal D, Perez W. Reproductive biology of the pampas deer (*Ozotoceros bezoarticus*): a review. Acta Veterinaria Scandinavica 2008; 50(16).

Xie C, Reynolds D, Awad H, Rubery PT, Pelled G, Gazit D, Guldberg RE,Schwarz EM, O'Keefe RJ, Zhang X. Structural bone allograft combined with genetically engineered mesenchymal stems cells as a novel platform for bone tissue engineering. Tiss Engin 2007;13(3):435-445.

CHAPTER II:
AIM 1

Introduction

Antler regeneration is thought to be driven by the de novo generation of progenitor cells in the cranium or pedicle (Kierdorf 2007). If this hypothesis is correct, it differs from the superficially analogous appendage regeneration processes in the urodele, which rely on trans- or dedifferentiation of existing lineage-committed cells (Kierdorf 2007).

As their name and thus their putative role implies, antlerogenic progenitor cells are connective tissue progenitor cells. APC are capable of regenerating at least the non-endodermal and non-ectodermal tissues in the antler (i.e. the bone and cartilage but likely not the velvet and vascular supply.) Using LacZ labeling and X-gal staining, Li reported that all connective tissues in the antler could ultimately be traced to cells from the pedicle periosteum (Li 2001a.) Li's methods were never fully explained and the citation in his 2001 paper referred to unpublished data, but this result supports the central role of APC in regrowing the antler.

We believe that antler chondrocytes and osteoblasts are most likely not directly derived from pedicle progenitors. Instead, due to the paradigm of endochondral ossification and the overwhelming histological evidence we argue that these cells descend from an intermediate population of antlerogenic progenitor cells in the reserve mesenchyme, a zone of undifferentiated and rapidly proliferating cells at the antler tip (Price 2005). If this assumption is valid, it likely reflects the simple expedient of maintaining a supply of progenitor cells as close as possible to the site of new tissue generation. After all, the antler grows from the tip and as the appendage lengthens, the growth zone will be displaced a substantial distance from the initial pedicle. While it is

possible that progenitors migrate through the vasculature from the pedicle to the antler tip, the fact remains that a large population of such cells are maintained at that distal location and from which chondrocytes and osteoblasts differentiate.

Little is known of the cells at the heart of antler regeneration. Most antler studies have been histological in nature; several have identified the expression of factors such as β-catenin (through which the canonical Wnt pathway acts), BMP-2 and -4, PTHrP and receptors for retinoic acid in the various tissue compartments (Feng 1995, Feng 1997, Barling 2004, Mount 2006).

It will obviously be difficult to make mechanistic assumptions behind antler regeneration until we better understand the APC phenotype through direct, experimental methods. Unfortunately, few investigations have involved the culturing of antler-derived cells. Of these, several have sought to identify an "antler stimulating factor" that may enhance APC proliferation and thus help explain the rapid regrowth of which antlers are capable. Candidate mitogenic factors include IGF-1 and steroids such as estradiol and testosterone, though debate continues as to which has the most robust effect *in vivo* (Kuzmova 2011.)

As progenitor cells, it would follow that APC have some capacity for self-renewal and multipotency (Bianco 2008.) However, APC self-renewal has not been investigated. Moreover, though APC-derived cells generate bone and cartilage, we are aware of few peer reviewed studies that have attempted to differentiate antler cells down at least one cell lineage (Faucheux 2001, Berg 2007, Rolf 2008). Rolf, for example, reported that STRO-1+ cells harvested from antler reserve mesenchyme have *in vitro* osteoblastic and adipocytic differentiation capacity (Rolf 2008).

Here, we investigated how white-tailed deer APC conform to basic criteria defining mesenchymal stromal cells (MSC), particularly in terms of self-renewal and multipotency. Drawing from the work of Bianco and Dominici, our definition will be as follows (Dominici 2006, Bianco 2008):

1. Adherence on cell culture plastic
2. Self-renewal as defined by colony formation

3. Capacity for differentiating into at least two mesenchymal lineages

Working *in vitro* as a first step, we explored colony formation, cell enumeration over time, and mesenchymal lineage differentiation (adipo-, chondro- and osteogenic) in antler tip reserve mesenchyme APC. Bianco might argue that such an investigation would ideally involve clonally-derived cells in order to verify that the same cells that possess the capacity for self-renewal are also capable of differentiation. However, due to the technical challenges of selecting and expanding candidate clonal populations, we elected to explore mesenchymal stromal cell criteria in heterogeneous cell cultures. We would counter a hypothetical "Bianco-esque" line of reasoning by arguing that the lack of literature on the APC phenotype in culture and appropriate protocols justifies a more conservative experimental approach.

In addition to investigations of APC in terms of MSC criteria, we also explored the effects of glucocorticoids on APC. Glucocorticoids regulate bone cell proliferation and differentiation directly and through interactions with hormones such as IGF-1 (Delany 1994). As the glucocorticoid dexamethasone is commonly used in differentiating medium, we investigated how it affected APC and MSC differentiation.

Another unusual feature of the antler tip is robust apoptosis in the reserve mesenchyme, the region where undifferentiated APC undergo rapid proliferation (Colitti 2005). Colitti found that as many as 64% of cells in this tissue zone were apoptotic, an extremely high proportion for an adult tissue. In this study, we explored apoptosis in APC and MSC chondrogenic cultures as well as whether it is differentially affected by dexamethasone.

Finally, an important question when looking at APC is "to what degree are the properties of these cells shared by other cells derived from the same animal?" We argue that any understanding of this uniqueness of APC is incomplete without also investigating how they differ from other cervid MSC. To help answer this question, we cultured a parallel, animal-matched population of marrow-derived MSC (hereafter referred to as "MSC") and subjected them to the same methods as with APC.

In this chapter, we will report the results of testing the following hypotheses:

1.1 Under static culture conditions, APC demonstrate increased colony formation, rates of proliferation and markers of adipo- chondro-, and osteogenic differentiation compared to animal-matched marrow MSC.

1.2 Under static culture conditions, APC will display increased apoptosis compared to MSC.

1.3 Under static culture conditions, APC and MSC will exhibit different responses to the artificial glucocorticoid steroid dexamethasone.

Here, we compared colony formation, cell expansion rates and differentiation capacities of reserve mesenchyme APC to animal-matched, phalangeal marrow-derived MSC. We also examined the effects of the glucocorticoid dexamethasone on osteogenesis *in vitro*. In chondrogenic cultures, we explored the effects of dexamethasone on cell number, apoptosis and matrix production.

Material and methods

Specimen acquisition

Cells were obtained from three wild, mature white-tailed bucks (*Odocoileus virginianus*.) Specimen acquisition took place on a University-owned nature preserve and conformed to institutional animal care and use standards and state wildlife policies. Following a three week program of baiting and game camera surveillance during July 2011, professional sharpshooters were employed to harvest the bucks on consecutive nights during the first week of August.

Disarticulated heads and front limbs (separated through the metatarsels) were placed on ice and transported immediately to the laboratory for dissection. Following recovery, specimens remained on ice for between one and three hours before dissection.

Specimen dissection and cell harvest

Disarticulated distal limbs were washed in tap water to remove dirt, blood and debris and then rinsed a chlorhexidine scrub followed by a saline or lactose Ringer's solution. The limb was degloved and the hooves and dew claws removed using a #10 scalpel. The phalanges were removed, washed again in tap water to remove any remaining dirt or hair and the soft tissue overlying the bones dissected away. Each phalanx was soaked for 2 minutes in a 50ml conical tube filled with a solution of 500 units/ml penicillin, 500µg/ml streptomyocin and 1 µg/ml amphotericin B in phosphate buffered saline (Gibco, Life Technologies, Grand Island, NY.)

Phalanges were stored for up to 10hours at 4C in complete medium: Dulbecco Modified Eagle Medium containing 110mg/L sodium pyruvate and 4mM L-glutamine (Gibco), 10% characterized FBS (Gibco), 100units/ml penicillin/100µg/ml streptomyocin/0.25 µg/ml amphotericin B (Gibco.) Fetal bovine serum for all remaining culture was obtained from a single batch that had been previously shown to give rise to robust mitogenesis in murine marrow-derived mesenchymal stromal cells (HyClone, Thermo Scientific, Waltham, MA, USA).

Antler tips were dissected as follows. After being washed as described above, a #22 scalpel blade was used to amputate the antler tip. A #10 scalpel was then used to make longitudinal cuts along the proximal-distal axis of each antler tips. Forceps were employed to peel the velvet off, with care taken not to remove the underlying soft tissue at the distal-most point. Decorticated antler tips were washed, disinfected in antibiotic-antimycotic, and stored in complete medium at 4C as above.

To obtain MSC, the proximal ends of the phalanges were removed with an oscillating, cast-cutting saw (Stryker, Kalamazoo, MI.) Fatty marrow was removed and complete medium used to flush red marrow into a 10cm cell culture dish, where it was homogenized by passing it through 18 and 26 gauge syringes. Non-adherent cells were removed 24 hours after the initial plating by aspirating and replacing the culture medium.

Antler tip APC were harvested from the reserve mesenchyme, which was dissected, minced, and plated in complete medium. As was the case for MSC, non-adherent cells were removed 24 hours after the initial plating.

As cellular antler tissue is only available on a seasonable basis, comparisons were made using both fresh and frozen cells. To freeze, cells were first detached using 0.25% Trypsin-EDTA (Gibco), resuspended in freezing medium (90% FBS, 10% DMSO.) After 24 hours at -80C in a Mr Frosty cell freezing container (Nalge Nunc International, Rochester, NY), cells were transferred to liquid nitrogen. Thawed passage 1 cells were cultured in complete medium supplemented with 6 mM L-glutamine (Gibco) and without amphotericin B.

Cell enumeration over time

First passage cells were seeded on 96-well plates (1000 cells/well or 3200 cells/cm^2). Between 1 and 8 days, relative cell number was estimated by measuring the fluorescent intensity of a nuclear binding dye (CyQUANT, Life Technologies) at 485nm excitation/530nm emission on a GENios plate reader (Tecan Schweiz AG, Männedorf, Switzerland.) Results were corrected using CyQUANT-only control wells.

Colony formation

First passage cells were plated at 6-well plates (160 cells/well or 17cells/cm^2.) After 14 days culture in complete medium, the cells were stained with crystal violet. Wells were rinsed twice with PBS and fixed in 1% glutaraldehyde in PBS for 15 minutes. Next, cells were stained with 0.1% crystal violet in distilled water for 30 minutes and rinsed 4 times with dH20. Colonies visible to the naked eye were counted manually.

Osteoblast induction

First passage fresh or thawed cells were plated at 5000cells/cm^2 in At 70-80% confluence, medium was supplemented with 0.1µm dexamethasone, 0.05mM L-Ascorbic acid 2-phosphate (Sigma-Aldrich Co LLC, St. Louis, MO), and 10mM β-

glycerophosphate (Sigma) (Jaiswal 1997). In a subset of thawed cells, dexamethasone was omitted. Unless stated otherwise, osteogenic medium contained dex.

To detect mineralized nodules, osteogenic cultures were stained in 1% alizarin red-S in 0.01%NH4OH, fixed in ice cold 70% ethanol and solubilized in 0.5N HCl + 5% SDS. Next, solubilized stain was transferred to a 24-well (fresh cells only) or a 96-well plate (3 replicates per cell type per time point.) Optical density (OD) was then read at a wavelength of 415nm and normalized to that of 0.5N HCL + 5% SDS.

To correct for cell number, parallel wells were stained with crystal violet. Crystal violet was solubilized in a 1:1 mixture of ethanol and 1% Triton X-100 for 30min. OD was read at 562nm. Alizarin Red ODs were normalized to the mean crystal violet OD for the cell type and time point.

Alkaline phosphatase activity was detected using Moreau's modification of Lowry's method in which the enzyme is permitted to hydrolyze a colorless p-nitrophenyl phosphate (pNPP) substrate into yellow p-nitrophenol (pNP) (Lajeunesse 1990, Moreau 1997)

Cells were lysed in buffer (200mM glycine, 2mM MgCl2*6H20, 2% Triton X-100) and homogenized by repeated pipetting. Lysates were transferred to 96-well plates, with three replicate wells per cell type. Next, 12.5mM pNPP in ALPase buffer was added to each well containing lysate as well as to three negative control wells holding buffer only. The reaction was conducted at 37C, after which it was stopped by adding 1N NaOH.

The pNP content in each well was quantified by measuring light absorbance at 405nm and corrected using optical density values from the buffer-only negative control wells. A standard curve was generated by way of linear regression of the optical densities of duplicate wells containing 0-60 nmol pNP. Enzyme activity was expressed as pmol of pNP divided by incubation time and lysate protein content, the latter measured by BCA assays performed as per the manufacturer's instructions (Pierce/Thermo Fisher Scientific, Rockford, IL, USA.)

Adipocyte induction

Janderova's adipogenesis protocol for human MSC was adapted to induce adipocyte formation in APC and cervid MSC (Janderova 2003.) First passage fresh or thawed cells were plated at 5000/cm^2. At 95-100% confluence (designated day 0), complete medium was replaced with adipogenesis induction medium (AIM): high glucose (4.5g/L) DMEM (Gibco), 10% FBS, 1% Pen-Strep, 1μM dexamethasone (Sigma), 0.2mM indomethacin (Sigma), 1.7μM recombinant human insulin (Sigma), and 0.5mM 1-Methyl-3-isobutylxanthine (Sigma.) On day 3, the AIM was replaced with adipogenesis maintenance medium (AMM) for one day: high glucose (4.5g/L) DMEM, 10% FBS, 1% Pen-Strep and 1.7μM recombinant human insulin.

For the first 12 days of culture, cells were exposed to a total of 3 3-day AIM treatments separated by 1-day AMM treatments. AMM was then used exclusively between days 13 and 21 and replaced every 3-4 days.

Staining to detect lipid droplet was done in triplicate wells after 21 days culture in adipogenic medium. Fifty percent of medium was aspirated from each well and an equal volume of 10% neutral buffered formalin added and allowed to incubate for 5 minutes. Wells were then completely aspirated, 10% NBF added and the cells fixed at 4C. Cells were then incubated in 60% isopropanol for 5 minutes. The isopropanol was aspirated and the wells dried completely. Oil red-O working solution (6 parts 0.5% Oil Red-O in isopropanol with 4 parts dH20) was added and the cells stained for 10 minutes under gentle shaking.

Chondrocyte induction

Chondrogenic differentiation was performed in micromass cultures (Mackay 1998). 250,000 cells were pelleted in 15mL conical tubes and cultured in chondrogenic medium: high glucose DMEM, 1% Pen-Strep, 10ng/ml, recombinant human TGFβ3 (Sigma), 0.1μM dexamethasone, 50μg/ml L-Ascorbic acid 2-phosphate, 40μg/ml L-proline (Sigma), and 1% ITS+ (BD Biosciences, Sparks, MD, USA.) Ovoid masses formed within 24 hours of culture in chondrogenic medium.

After 14 days, hypertrophic induction medium was used: high glucose DMEM, 1% Pen-Strep, 50ng/ml thyroxine (Sigma), 1nM dexamethasone, 20mM β-glycerophosphate, 50µg/ml L-Ascorbic acid 2-phosphate, 40µg/ml L-proline, and 1% ITS+. In a subset of thawed cells, dexamethasone was omitted from both chondrogenic and hypertrophic media.

At 28 days, micromasses were fixed for one hour in 10% NBF and then dehydrated and paraffin-infiltrated in an automated tissue processor for 7 hours (Shandon Hypercenter XP, Thermo Fisher.) Due to the small size of the micromasses they were processed inside custom Delrin retaining rings placed inside mesh cassettes. The retaining rings prevented the micromasses from migrating through the cassettes' vent holes during processing.

Next, micromasses were paraffin-embedded using a Leica EG1160 paraffin embedding center (Leica Microsystems Inc, Buffalo Grove, IL, USA.) Micromasses were removed from molten paraffin, placed in a groove cut into a small piece of solid wax, and the solid wax then inverted and placed inside a plastic mold. The solid wax kept the micromass affixed to the bottom of the mold, preventing movement when liquid wax was poured in. This protocol was intended to ensure reliable location of the micromass during sectioning. Six µm-thick sections were could then be cut on a Leica Microtome (Leica Microsystems) and mounted on glass slides.

Collagen content was evaluated using Van Gieson's Picric Acid Fuchsin stain (5% Acid Fuchsin in picric acid with Weigert's Hematoxylin as a counterstain). Proteoglycans were visualized with 0.1% Safranin-O with 0.02% Fast Green and Weigert's Hematoxylin as counterstains.

As Safranin-O does not have high sensitivity (Camplejohn 1987), proteoglycan content was verified using 1% Alcian Blue in acetic acid (pH 2.5) on separate sections. Alizarin red staining (1 minute in 2% alizarin red-S in an aqueous solution of ammonium hydroxide, pH 4.2) was also performed on micromasses in the dexamethasone denial study.

To measure micromass apoptosis and cell number, slides were dual-labeled using a TUNEL- Hoechst kit (Click-iT TUNEL assay, Molecular Probes/Life

Technologies, Eugene, OR). TUNEL staining was visualized through the conjugation of an Alexa Fluor 594 fluorphore. Three images were taken per section in the same field of view using a Zeiss Axiovert 200M (Carl Zeiss Microscopy, LLC, Thornwood, NY.) First, an auto-exposed brightfield image, used to estimate tissue area, was captured slightly above the plane of the slide to enhance contrast. Next, the microscope's multiple image acquisition software sequentially captured a Hoeschst-stained and TUNEL image using exposure times of 40ms and 500ms, respectively.

Analysis was carried out using ImageJ software (National Institutes of Health, Bethesda, MD) on background corrected images. TUNEL intensity was evaluated as follow: image background grayscale levels were removed using the Subtract Background function. Grayscales levels were then measured in a region of interest drawn around the micromass section.

Cells per matrix area were calculated from Hoechst-labeled and brightfield images. Matrix area was calculated using the latter. Image backgrounds were normalized using ImageJ's Subtract Background algorithm after which the Enhance Contrast function was applied. A software-generated threshold was applied and an areal measurement obtained.

Cell number was determined from the Hoechst-stained images. Background normalization was carried out as with the TUNEL images. After the application of a software-generated threshold, ImageJ's Particle Counter was used to count putative nuclei. Only particles with an area greater than 175 pixels^2 were counted, approximately equivalent to the area occupied by a 5um diameter object at 200x magnification. Particle counter parameters were determined using images with "known good" nuclei, which yielded an estimated low end nuclear diameter of 5 um (equal to 189 pixels^2 for uncompressed images taken at 200x magnification.) The lower 175 pixels^2 figure attempted to account for small variations in nuclear size.

Statistics

As each experiment involved a small sample size (2 to 3 biological replicates), multiple experimental replicates (3 to 12) were performed for each assay. Generalized linear mixed models, which take into account nested data structures and repeated measures, were therefore used for comparisons (SPSS, IBM Corp, Armonk, NY.) For fresh and thawed cell models, "celltype" was used as a fixed effect and "animal" as a random effect.

For the dexamethasone study, "dex treatment", "celltype" and a "dex*celltype" interaction were used as fixed effects with "animal" again as a random effect.

Results

Cell enumeration over time

Rapid antler growth rates *in vivo* prompted us to compare APC and MSC expansion in culture. While MSC numbers increased before reaching a plateau at 6 days, APC numbers declined between 1 and 4 days then increased between 5 and 8 days (Fig.1A.) Contrary to expectations, APC did not exhibit greater *in vitro* proliferative capacity compared to MSC.

Colony forming units

The formation of colonies is a measure of cellular self-renewal, a key progenitor cell trait (Bianco 2008). The mean numbers of visible colonies generated by APC and MSC were similar, but APC demonstrated more inter-animal variability (Fig.1B.)

Adipogenic differentiation

The capacity to differentiate into adipocytes, osteoblasts and chondrocytes is another characteristic of mesenchymal stromal cells (Dominici 2006.) After 21 days exposure to adipogenic media, both fresh and thawed MSC displayed widespread intracellular oil red-O-positive lipid droplets. Few, if any, lipid droplets were apparent for either fresh or thawed APC at the same time point (Fig. 2).

Osteogenic differentiation

We performed osteogenic differentiation of APC and MSC in culture using both fresh and thawed cells. In a separate experiment, we measured the effects of the glucocorticoid dexamethasone on osteogenic differentiation in thawed cells. Time points were varied slightly between these three sets of experiments to match apparent degrees of differentiation in the cultures.

APC and MSC displayed different patterns of alkaline phosphatase activity over time. In both fresh and thawed cells, APC activity was greater at earlier time points while MSC activity was greater by day 14 in thawed cells (Fig.3.) In fresh cells, APC activity was greater than MSC at day 16 (Fig 3A.) However, MSC activity increased over time in the same step wise fashion seen in thawed cells.

Dexamethasone affected APC and MSC alkaline phosphatase activity differently (Fig 3C.) Dex decreased APC activity at day 7, but had no significant effect at days 10 or 14. In MSC, however, dex consistently led to decreased alkaline phosphatase activity. Significant dex*celltype interactions at days 7 and 14 further suggested a differential response to dex at those time points.

APC and MSC in osteogenic culture underwent different patterns of mineralization as well. In thawed cells cultured with dex, by days 21/22 MSC had greater cell number-corrected mineralization, while no significant difference was seen by days 28/30 (Fig.4E,F.) On the other hand, MSC maintained greater mineralization at day 30 in fresh cells (Fig.4D.) APC consistently had fewer cells in fresh and thawed cultures compared to MSC (Fig.4A, B, C.)

Dexamethasone influenced APC and MSC mineralization in different ways (Fig.4F.) At day 21, dex reduced mineralization in both APC and MSC. By day 28, dex led to increased mineralization in APC (APC+Dex: 0.232±0.08, APC-Dex: 0.142±0.06, $p=0.02$) but did not significantly alter alizarin red content in MSC at this time point ($p=0.23$) (Fig.4F.) The dex*interaction was also significant for AR at day 28, indicating dex treatment had differential effects on APC and MSC mineralization at this time point.

Dexamethasone significantly lowered cell number in MSC at day 28, but the absolute difference was small (Fig.4C.) Dex also lowered APC cell number at day 28, but the difference was a statistical trend (p=0.09.)

In culture, APC and MSC osteogenesis differ in terms of timing and mineralized matrix production. APC alkaline phosphatase activity responded more rapidly than that of MSC, yet mineralization per cell was initially more robust in the latter cell type. APC and MSC also differed in their responses to dexamethasone. Dex reduced MSC APA at all time points observed, but only delayed peak APC APA. Dex consistently reduced mineralization in MSC in osteogenic cultures, but led to a temporary reduction in APC mineralization before increasing it above the values seen when dex was denied.

Chondrogenic differentiation

We used a micromass model to induce chondrogenic differentiation in thawed APC and MSC. As the high cell density of micromasses initially resembles conditions in the antler's reserve mesenchyme, we also explored whether the robust apoptosis seen in the reserve mesenchyme could be recapitulated in culture and if there is a relationship between apoptosis and cellular differentiation state. In a separate experiment, chondrogenic differentiation and apoptosis was investigated in thawed APC and MSC with and without dexamethasone.

Putative hypertrophic chondrocytes and proteoglycans, evidence of a chondrogenic phenotype, were found in both APC and MSC micromasses (Fig 5.) However, matrix composition and the effect of dexamethasone depended on cell type.

Safranin-O staining showed a widespread distribution in MSC micromasses, but staining was faint in APC micromasses (data not shown). Alcian blue staining verified the presence of proteoglycans in the latter (Fig.5, middle panel). Dex qualitatively increased the intensity and distribution of alcian blue and safranin-O (data not shown) in MSC micromasses, while having the opposite effect in APC micromasses. Van Gieson's staining confirmed collagen production throughout APC and MSC micromasses and was not affected by dexamethasone.

Alizarin red-S staining was performed to investigate matrix mineralization during chondrocytic differentiation (Fig. 5, right panels.) Again, dex affected APC and MSC in seemingly opposite ways. MSC alizarin red staining was qualitatively more robust with dex, while the reverse was apparent in APC.

Cellularity of APC and MSC micromasses also differed. In thawed cell micromasses, APC displayed significantly more cells per matrix area than MSC (Fig. 6A,B). Dex did not affect the number of APC cells per area ($p=0.58$) but increased cellularity in MSC (MSC+Dex 11.4±0.39, vs 7.1±0.35 in untreated MSC, $p<0.001$.)

Compared to MSC, APC micromasses were more apoptotic. In TUNEL-stained images, APC micromasses had greater mean grayscale intensities and proportion of nonzero grayscale pixels compared to MSC (Fig. 6C-F). In APC micromasses, dex increased both measures of apoptosis, while reducing or having no effect on MSC.

MSC micromass cultured with dex had increased cellularity, lower apoptosis and greater matrix production than without, indicating that dex helped drive proliferation and chondrogenic differentiation in these cells. For APC micromasses, however, dex reduced matrix production and increased apoptosis while having little effect on cellularity. The above suggests that, while MSC chondrogenesis is enhanced by dexamethasone, APC undergo more robust chondrogenic differentiation when cultured in the absence of this glucocorticoid.

Discussion

Both APC and MSC demonstrated clonogenicity, or the ability to generate colonies in a density-independent manner in culture (Bianco 2008.) The lack of difference in mean APC and MSC colony numbers suggests that overall self-renewal capacity is conserved across different connective tissue progenitors in a regionally restricted whitetail population. On the other hand, the greater APC standard deviation indicates a greater variation in self-renewal of antlerogenic cells from deer to deer compared to marrow-derived MSC.

It should be stated that APC and MSC colony formation cannot be attributed to the presence of cells strictly defined as CFU-Fs (colony forming units-fibroblastic) (Bianco 2008.) This is due to the fact that we used passage 1, rather than fresh primary cells, for the colony formation assay. Still, the goal of this assay was to confirm the existence of colony forming cells derived from the antler and marrow in culture, not estimate their numbers *in vivo*. Our results make a compelling argument for the existence of a population of cells capable of self-renewal in the antler reserve mesenchyme and marrow compartments, as it seems unlikely that an *in vitro* culture could induce colony formation in cells not otherwise predisposed to it.

White-tailed deer antlers regrow rapidly, about 0.25 inches (6.35mm) per day (Ozuga 1996). *In vitro*, however, antler progenitor cells from these deer expanded less rapidly than MSC overall. Interestingly, after 5 days of decline in a monolayer culture APC numbers began to recover.

Cells were cultured from late summer antlers when growth has slowed. However, proliferation of red deer (*Cervus elaphus*) APC *in vitro* is independent of the stage of antler regrowth during which the cells were harvested (Kuzmova 2011). It is conceivable that the situation is similar in the white-tailed deer as well.

Slower APC proliferation in a monolayer culture may instead be due to one or more disadvantageous components of the culture system—initial plating density, oxygen tension, the lack of APC-specific mitogenic factors in the medium, etc.

Though it is risky to over interpret a negative result, another potential explanation for the relatively poor proliferation for APC is an increased stemness compared to MSC. One key feature of adult stem cells is a resilient quiescence, especially *in vitro* or ex vivo (Winer 2009.) In case of hematopoietic stem cells, the only stem cells that have been definitively characterized, the promotion of proliferation can lead to stem cell "exhaustion," or a decline in function (Orford 2008.)

Interestingly, APC in a micromass culture consistently exhibited a greater cell number per area compared to MSC in the same conditions, both with and without dexamethasone. Although greater cellularity does not necessarily reflect the cell proliferation rate, these data raise the possibility that APC mitogenesis may be more sensitive to milieu compared to MSC (i.e. monolayer versus three dimensional micromass.) A time course study in which APC and MSC micromasses are cultured in complete, rather than chondrogenic, medium would be necessary to confirm whether the greater cellularity of APC micromasses is due to more rapid proliferation or, more likely, an altered balance between proliferation and differentiation.

An alternative explanation for the seeming paradox of lower APC proliferation relative to MSC could be that rapid antler growth is instead due to robust matrix production per cell rather than rapid mitogenesis. Unfortunately, the results from our APC differentiation assays do not support such a hypothesis. We found that, at best, APC were able to match MSC matrix production per cell.

Interestingly, no qualitative relationship was apparent between the colony forming ability and relative proliferative capacity of APC and the size of the antlers of the individual animal from which they were cultured. In fact, though buck R2 exhibited the largest rack out of the three animals used for this study, the cells culture from its antlers were the slowest to proliferate. Without further investigation it remains to be seen if this observation reflects an actual *in vivo* discrepancy or is the product of the individual animal's maturity, specimen collection procedure and/or culture protocols.

In terms of cell potency, our results suggest that, compared to MSC, antler tip APC are more lineage restricted osteo/chondrogenic progenitors, with little adipogenic capacity. This result may reflect that adipose tissue is not a primary antler constituent

while it is present in the phalangeal marrow space. In the case of true stem cells, for example, differentiation is generally limited to the lineages present in the tissue of origin (Orford 2008.) However, as heterogeneous cell cultures were used here, further investigation will be needed to determine whether differences in APC and MSC adipogenesis were exaggerated by the presence of committed adipocytic precursors in the latter culture.

These findings contrast with those of Rolf, who reported positive oil red-O staining in fallow deer (*Dama dama*) STRO-1+ APC exposed to a commercial adipogenic medium (Rolf 2008). Possible sources of discrepancy between his work and this study include the use of cells from different deer species and of commercial differentiating media as well as differences in subjective standards of what constitutes a "lipid droplet" rather than, say, intracellular vesicles.

Under osteogenic conditions, APC alkaline phosphatase activity was higher than that of MSC for the first ten days in culture. This suggests more rapid lineage commitment in APC in response to osteogenic factors, perhaps due to a greater degree of intrinsic osteo/chondrogenic commitment compared to MSC. Despite higher initial alkaline phosphatase activity, APC mineralization was delayed until later time points or reduced relative to MSC, perhaps reminiscent of the delay in complete mineralization that occurs in the antler after full regrowth is achieved.

Dex consistently inhibited mineralization in MSC cultures, but its effects on APC mineralization were time dependent. This suggests that dex affects APC-derived osteoblasts in a manner dependent on differentiation stage, consistent with studies of glucocorticoid action on osteoblasts (Delany 1994.). In contrast, dex consistently reduced markers of early and late osteoblast differentiation in cervid MSC cultures.

In addition to influencing matrix production in APC and MSC micromass, dex treatment led to differences in cellularity and apoptosis. For APC, dex fostered more robust apoptosis but had no significant impact on cellularity. In MSC micromass, dex led to greater matrix production, increased cellularity and reduced apoptosis over untreated micromasses. This suggests that, in MSC undergoing chondrogenesis, dex

enhances both proliferation and differentiation, though these effects are likely dependent on the stage of cell lineage progression.

Antler regrowth is associated with hormone levels changing throughout the mating cycle. However, it has been difficult to determine which factors directly regulate APC proliferation and differentiation. Factors such as testosterone, whose fluctuations are closely associated with the antler cycle (Suttie 1995), failed to promote mitogenesis in antler cell cultures (Li 1999.) On the other hand, it is unclear whether IGF-1, which stimulates antler cell proliferation *in vitro* (Li 1999, 2001b) is the key stimulatory factor in antler growth (Kuzmova 2011.

Dexamethasone can promote or suppress bone cell proliferation and differentiation directly and through interactions with steroids such as IGF-1 (Delany 1994, Delany 2001, Tuan 2002, Hoch 2012.) Dex can also reduce antler cell proliferation *in vitro* (Li 2001b.) In APC cultures, we found that dex reduced markers of chondrogenic differentiation while promoting apoptosis. High levels of apoptosis have been reported in the reserve mesenchyme, adjacent to regions of active chondrogenesis (Colitti 1005.) This suggests that factors such as glucocorticoids might contribute to the shifting balance between progenitor proliferation and differentiation in the antler as it undergoes regeneration. Additionally, an inverse relationship between apoptosis and chondrogenesis raises the possibility that apoptosis may help maintain a population of non-differentiating APC within the reserve mesenchyme. Compensatory proliferation, in which caspases released from apoptotic bodies act as mitogenic factors, is one means by which apoptosis can contribute to tissue homeostasis (Fan 2008.)

The observed pattern of time, factor, and milieu dependence of APC proliferation and differentiation may reflect a system of regulation required to confine antler growth to a specific anatomical and temporal range. Antler regrowth does not proceed “automatically” in response to antler casting, it is initiated by seasonally determined signaling (Kierdorf 2007.) Complete mineralization of the antler is delayed until circulating androgens peak during the fall rutting season, after it is fully regrown (Price 2004.) Moreover, antler regrowth occurs concurrently with bone resorption elsewhere in

body, indicating a differential responsiveness to circulating factors in the antler compared to other bone tissue (Landete-Castillejos 2007.)

We have demonstrated that APC and cervid-marrow-derived MSC differ in terms of proliferative capacity, differentiation, apoptotic potential and hormone responsiveness. Contrary to expectations, APC did not exhibit greater *in vitro* proliferative capacity compared to MSC. Mean numbers of visible colonies generated by APC and MSC were similar, but APC demonstrated more inter-animal variability.

APC and MSC exhibited different patterns of differentiation. Unlike MSC, no evidence of adipogenesis was seen in APC. Under osteogenic conditions, APC displayed greater alkaline phosphatase activity at earlier time points yet generally less mineralization. While dexamethasone reduced mineralization in MSC, this glucocorticoid had time dependent effects on APC. In chondrogenic micromass culture, APC were more cellular than MSC, yet were also more apoptotic. Dexamethasone had opposing effects on APC and MSC chondrogenesis, increasing markers of differentiation in latter cells with reducing them in the former. Dexamethasone also increased apoptosis in APC but not MSC.

As knowledge of the APC phenotype improves, a compelling avenue of future research would be the elucidation of the mechanisms behind the properties and behavior of these cells. A thorough understanding of the antler's unique process of regeneration would be of great value in guiding the development of novel skeletal regenerative therapies.

Chapter II figures

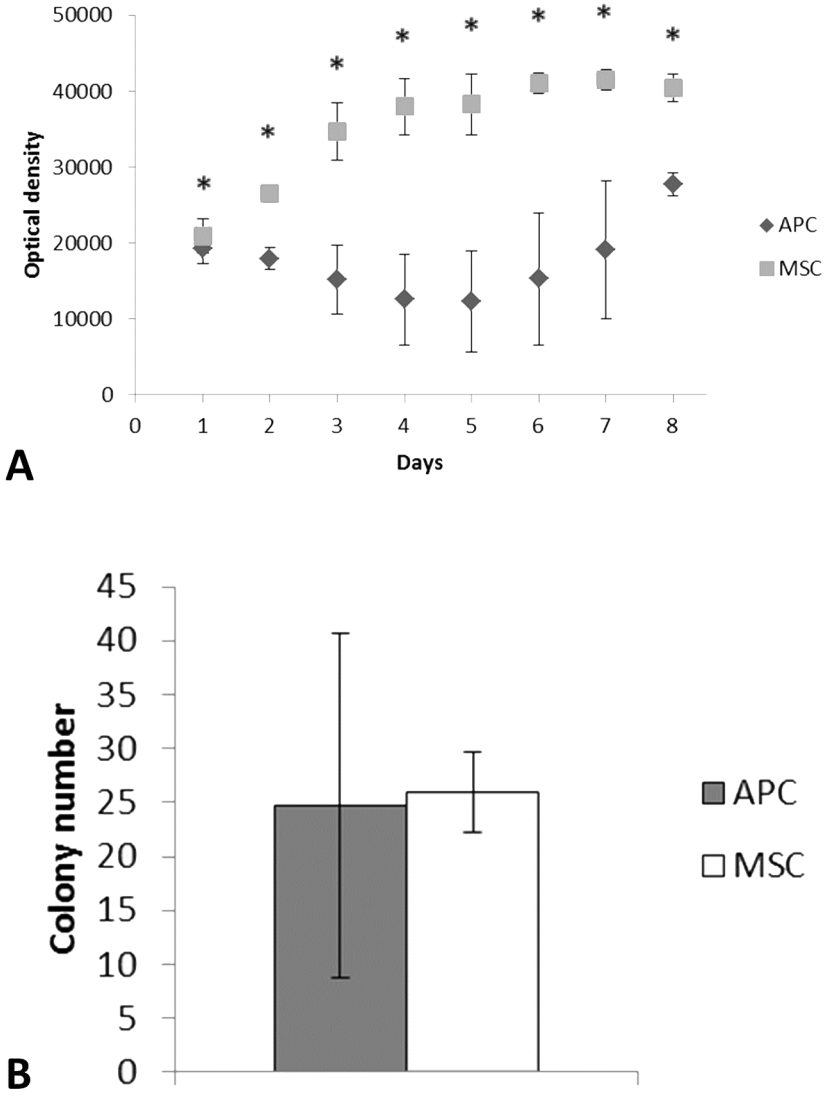

FIG. 2.1: Comparison of APC and MSC cell number and colony formation. (A) Relative cell number over time as measured by optical density. $P \leq 0.05$ APC vs MSC at each time point. 8-16 wells per group per time point, n=3 bucks. (B) Colony formation at day 14 (n=3, p=0.89)

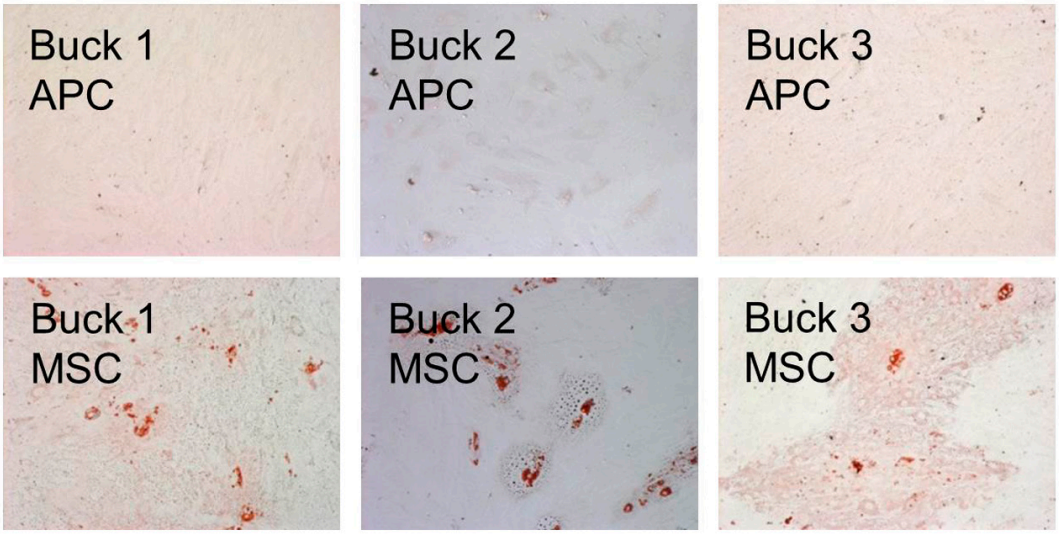

FIG. 2.2: Adipogenic differentiation of thawed cells. MSC exhibit more Oil Red-O positive lipid droplets than APC from all three bucks.

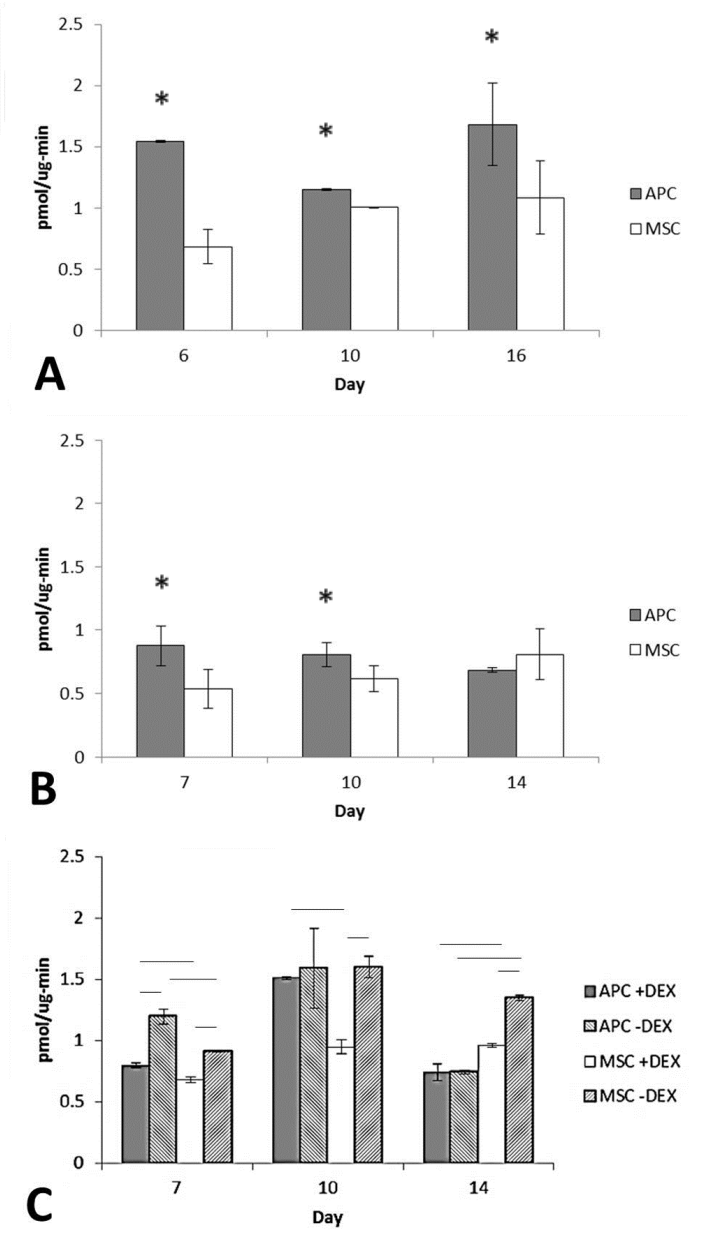

FIG. 2.3: Alkaline phosphatase activity in fresh and thawed cells. (A) Fresh cell alkaline phosphatase activity (n=2 bucks) (B) Thawed cell activity (n=3) (C) Alkaline phosphatase activity in thawed cells cultured with or without dexamethasone (n=2). * or line: $p \leq 0.05$, #:$p \leq 0.1$.

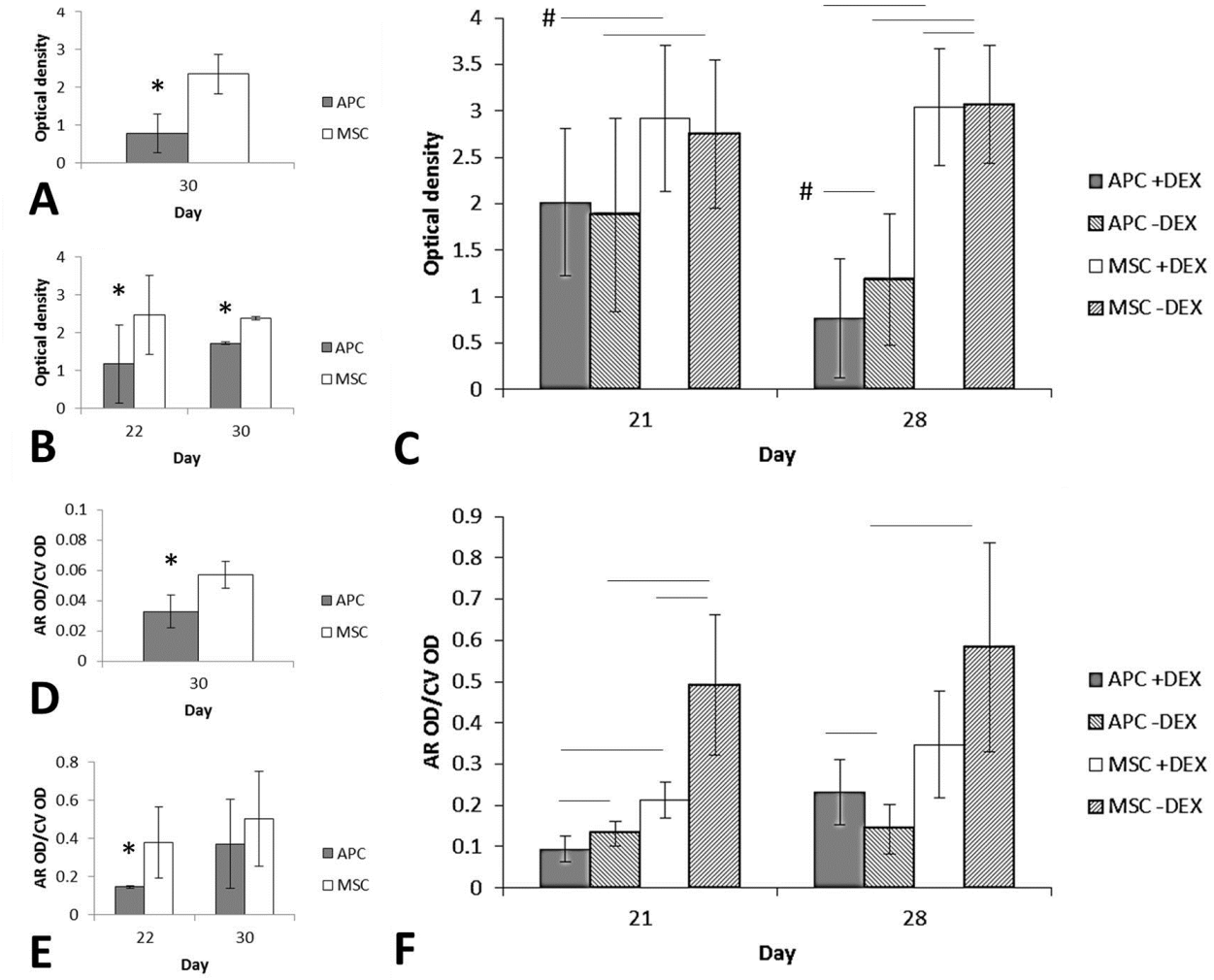

FIG. 2.4: Relative cell number and mineralization during osteogenic differentiation (A) Fresh cell number (crystal violet optical density, n=2 bucks) (B) Thawed cell numbers (n=3) (C) Thawed cell numbers with and without dexamethasone (n=2) (D) Fresh cell mineral, normalized by cell number (24-well plate.) (E) Thawed cell mineral (96-well plate.) (F) Thawed cell mineral, with and without dexamethasone (96-well plate). * or line: $p \leq 0.05$. Line+ #:$p<0.1$)

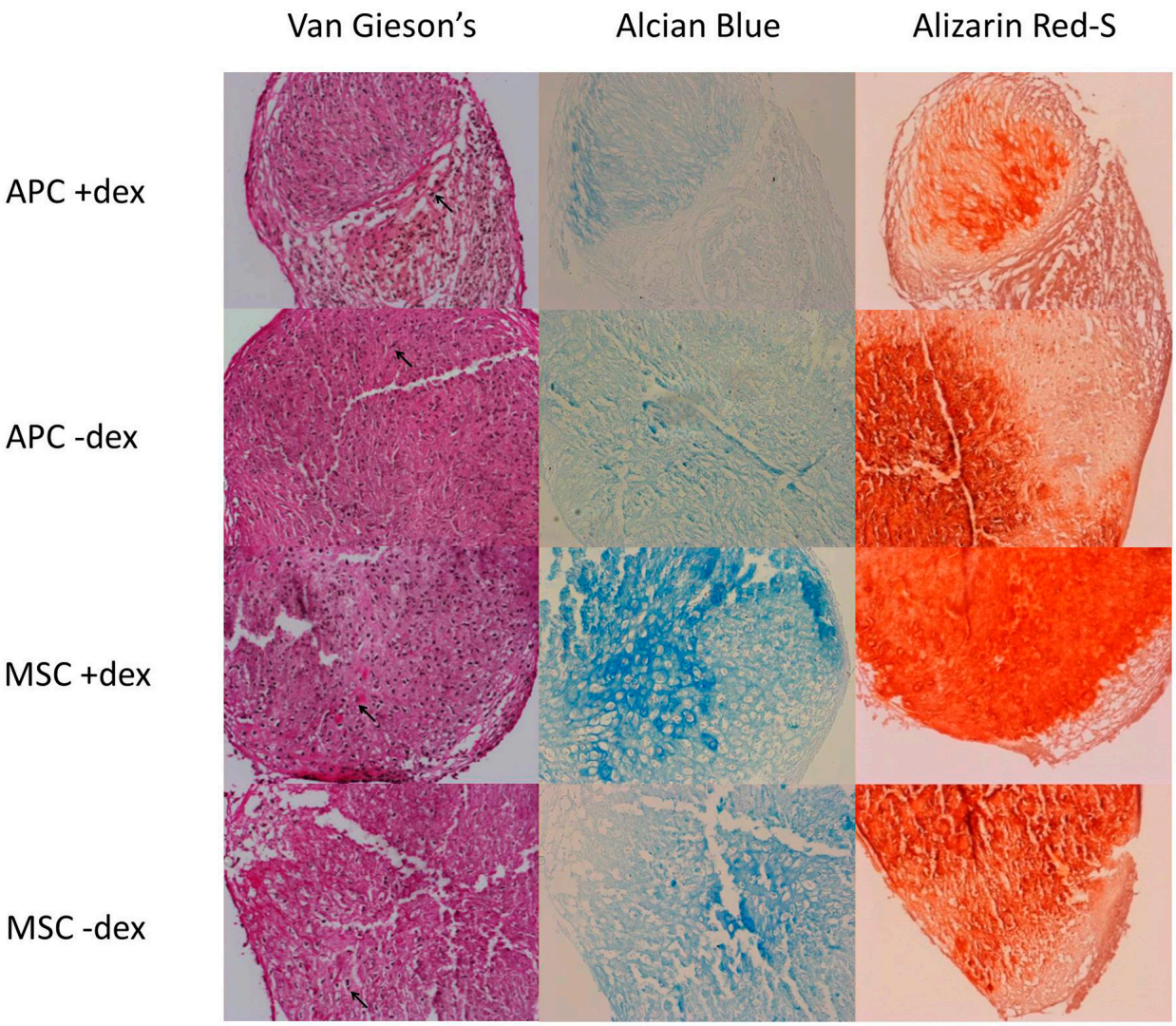

FIG. 2.5: Chondrogenic micromass histology (buck 1 cells, 200X mag.) Arrow heads indicate examples of putative hypertrophic chondrocytes.

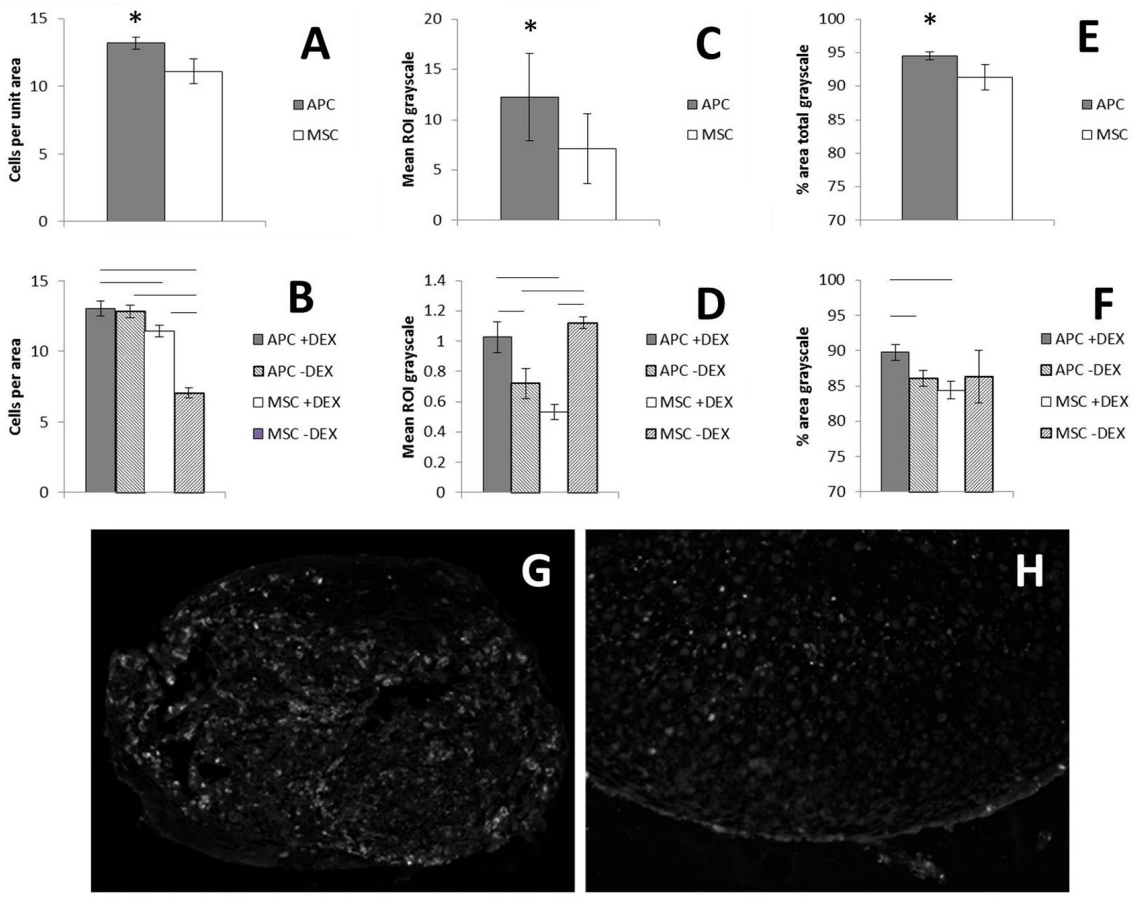

FIG. 2.6: Chondrogenic micromass cellularity and apoptosis. (A,B) Cells per area for thawed cells (n=3 bucks) and thawed cells with or without dexamethasone (n=2) (C,D) TUNEL grayscale intensity normalized by cells per area for thawed cell and thawed cells with or without dexamethasone. Different scales due to lower permeabilization of tissue in latter study. (E,F) Another measured of apoptosis: percent of pixels with nonzero grayscale, thawed cell and thawed cells with or without dexamethasone (G,H) Images of TUNEL stain, buck 1 APC and MSC, 200X mag. 6 sections per mass. * or line: $p \leq 0.05$.

Bibliography

Barling PM, Liu H, Matich J, Mount J, Lai KWA, Ma L, Frances L, Nicholson B. Expression of PTRrP and the PTH/PTHrP receptor in growing red deer antler. Cell Bio Int 2004;28(10):661-673.

Bartos L, Schams D, Bubenik GA. Testosterone, but not IGF-1, LH, prolactin or cortisol, may serve as antler-stimulating hormone in red deer stags (*Cervus elaphus*). Bone 2009; 44:691-698.

Berg DK, Li C, Asher G, Wells DN, Oback B. Red deer cloned from antler stem cells and their differentiated progeny. Biol Reprod 2007;77(3):384-294.

Bianco P, Robey PG, Simmons PJ. Mesenchymal stem cells: revisiting history, concepts, and assays. Cell Stem Cell 2008; 2(4): 313-319.

Camplejohn KL, Allard SA. Limitation of safranin 'O' staining in proteoglycan-depleted cartilage demonstrated with monoclonal antibodies. Histochemistry 1988; 89:185-188.

Colitti M, Allen SP, Price JS. Programmed cell death in the regenerating deer antler. *J Anat* 207(4):339-351, 2005.

Currey JD, Brear K, Zioupos P. Notch sensitivity of mammalian mineralized tissues in impact. Proc R Soc Lond B 2004; 271:517-522.

Delany AM, Dong Y, Canalis E. Mechanisms of glucocorticoid action in bone cells. J Cell Biochem 1994;56: 295-302.

Delany AM, Durant D, Canalis E. Glucocorticoid suppression of IGF 1 transcription in osteoblasts. Mol Endochrin 2001;15(10): 1781-1789.

Dominici M, Le Blanc K, Mueller I, Slaper-Cortenbach I, Marini F, Krause D, Deans R, Keating A, Prockop DJ, Horwitz E. Minimal criteria for defining multipotent mesenchymal stromal cells. The International Society for Cellular Therapy position statement. Cytotherapy 2006;8(4):315-317.

Fan Y, Bergmann A. Apoptosis-induced compensatory proliferation. The cell is dead. Long live the Cell! Trends Cell Biology 18(4):467-473, 2008.

Faucheux C, Nesbitt SA, Horton MA, Price JS. Cells in regenerating antler cartilage provide a microenvironment that supports osteoclast differentiation. J Exp Bio 2001; 204(Pt 3): 443-455.

Feng JQ, Chen D, Esparza J, Harris MA, Mundy GR, Harris SE. Deer antler tissue contains two types of bone morphogenetic protein 4 mRNA transcripts. Biochim Biophys Acta. 1995;1263:163–168.

Feng JQ, Chen D, Ghosh-Choudhury N, Esparza J, Mundy GR, Harris SE. Bone morphogenetic protein 2 transcripts in rapidly developing deer antler tissue contain an extended 5′ non-coding region arising from a distal promoter. Biochim Biophys Acta. 1997;1350:47–52.

Hoch AI, Binder BY, Genetos D, Leach JK. Differentiation-dependent secretion of proangiogenic factors by mesenchymal stem cells. PLoS ONE 2012;7: e35579.

Jaiswal N, Haynesworth SE, Caplan AI, Bruder SP. Osteogenic differentiation of purified, culture-expanded human mesenchymal stem cells *in vitro*. J Cell Biochem 1997; 64(2): 295-312.

Janderova L, McNeil M, Murrell AN, Mynatt RL, Smith SR. Human mesechymal stem cells as an *in vitro* model for human adipogenesis. Obesity Res 2003; 11(1): 65-74.

Kierdorf U, Kierdorf H, Szuwart T. Deer antler regeneration: cells, concepts, and controversies. J Morphology 2007; 268(8),726-738.

Kuzmova E, Bartos L, Kotrba R, Bubenik GA. Effects of different factors on proliferation of antler cells, culture *in vitro*. PloS ONE 2011; 6(3): e18053.

Lajeunesse D, Frondoza C, Schoffield B, Sacktor B. Osteocalcin secretion by the human osteosarcoma cell line MG-63. J Bone Min Res 1990;5(9):915-922.

Landete-Castillejos T, Garcia A, Gallego L. Body weight, early growth and antler size influence antler mineral composition of Iberian red Deer (*Cervus elaphus hispanicus*). Bone 2007;40(1):230-235.

Li C, Littlejohn RP, Suttie JM. Effects of insulin-like growth factor 1 and testosterone on the proliferation of antlerogenic cells *in vitro*. J Exp Zoo 1999;284(1): 82-90.

Li C, Suttie JM. Deer antlerogenic periosteum: a piece of postnatally retained embryonic tissue? Anat Embryol 2001; 204:375-388.

Li C, Wang W, Manley T, Suttie JM. No direct mitogenic effects of sex hormones on antlerogenic cells detected *in vitro*. Gen and Comparative Endochrinology 2001; 142:75-81.

Mackay AM, Beck SC, Murphy JM, Barry FP, Chichester CO, Pittenger MF. Chondrogenic differentiation of cultured human mesenchymal stems cells from marrow. Tissue Eng 1998; 4: 415.

Moreau R, Aubin R, Lapointe JY, Lajeunsse D. Pharmacological and biochemical evidence for the regulation of osteocalcin secretion by potassium channels in human osteoblast-like MG-63 cells. J Bone Min Res 1997;12(12):1984-1992.

Ozoga John J, Whitetail Spring: Season of the Whitetail, 1996 Willow Creek Press: Minocqua, WI, pg 82

Mount JG, Muzylak M, Allen S, Althnaian T, McGonnell IM, Price JS. Evidence that the canonical Wnt signaling pathway regulated deer antler regeneration. Dev Dynamics 2006; 235:1390-1399.

Orford KW, Scadden DT. Deconstructing stem cell self-renewal: genetic insights into cell-cycle regulation. Nat Rev Gen 2008;9:115-128.

Price JS, Allen S. Exploring the mechanisms regulating regeneration of deer antlers. Phil Tran Roy Soc London B 2004; 359(1445): 809-822.

Price JS, Allen S, Faucheux C, Althnaian T, Mount JG. Deer antlers: a zoological curiosity or the key to understanding organ regeneration in mammals? J Anat 2005; 207(5):603-618.

Rolf HJ, Kierdorf U, Kierdorf H, Schulz J, Seymour N, Schliephake H, Napp J, Niebert S, Wolfel H, Wiese KG. Localization and characterization of STRO-1+ cells in the deer pedicle and regenerating antler. PLoS ONE 2008; 3: e2064.

Suttie JM, Fennessy PF, Lapwood KR, Corson ID. Role of steroids in antler growth of red deer stags. J Exp Zoo 1995; 271(2): 120-130.

Tuan RS, Boland G, Tuli R. Adult mesenchymal stem cells and cell-based tissue engineering. Arthr Res Ther 2002; 5:32-45.

Winer JP, Janmey PA, McCormick ME, Funaki M. Bone marrow-derived human mesenchymal stem cells become quiescent on soft substrates but remain responsive to chemical or mechanical stimuli. Tissue Eng 2009;15(1):147-154.

CHAPTER III:
AIM 2

Introduction

At the beginning of the annual regrowth cycle, a seasonally dormant population of cells in the pedicle periosteum is activated. The direct mechanism for this seasonal activation is unknown, but it is ultimately linked to changes in day length that are mediated by the animal's pineal gland (Snyder 1983). Interestingly, initiation of regrowth is not a direct result of antler casting—there can be a substantial delay between casting and regrowth and bucks whose antlers fail to cast can occasionally grow a second set of antler (Kierdorf 2007).

Soon after the onset of regeneration, a second population of progenitor cells is generated in a growth center known as the reserve mesenchyme at the tip of each antler (Price 2005). This contrasts to the process of appendage regeneration in amphibians, in which an injury induces the de- or –transdifferentiation of "committed" cells pursuant to the formation of a blastema (Kierdorf 2007).

Based on their location in a mesenchymal niche, it is reasonable to assume that antlerogenic progenitor cells (APC) have characteristics in common with mesenchymal stromal cells. We would therefore predict that APC have the following characteristics (Dominici 2006, Bianco 2008):

1. Adherence on cell culture plastic
2. Self-renewal as defined by colony formation
3. Capacity for differentiating into at least two mesenchymal lineages

In Aim 1 (Chapter II) we demonstrated that APC and MSC both share a similar capacity for self-renewal, as estimated by colony formation. On the other hand, we saw large differences in APC and MSC differentiation down adipogenic, osteogenic and chondrogenic lineages in vitro. While we provided evidence that cervid marrow-derived MSC were amenable to induction down all three lineages, APC were reluctant to produce the Oil Red-O lipid droplets that would have indicated adipogenesis, at least in culture. This suggests that APC are more lineage committed osteo/chondropregenitors.

We also saw large differences in osteogenic and chondrogenic capacity between the two cell types. For example, compared to MSC, APC in a monolayer culture had a lower degree of cell number-corrected mineralization at early time points and were only able to match MSC mineralization at Day 28 when cultured in the presence of dexamethasone. Markers of chondrogenesis were also qualitatively lower in APC micromasses.

These results may suggest that the low mineralization capacity of the antler is manifested at a cellular level and can be recapitulated in vitro. After all antlers have a relatively poor degree of mineralization compared to other long bones, which contributes to a tough, damage-resistant matrix (Currey 2004). It is conceivable that, whether due to a need for material toughness or as a concession to yearly growth and casting, selective pressure has not guided antler osteoblasts toward a high per-cell matrix production. One could also speculate that APC have greater “stemness” than MSC and, as a result, are more prone to quiescence in culture (Winer 2009.)

An alternative explanation to the apparent disparity in the degree of osteo- and chondrogenesis between APC and MSC implicates the cell culturing milieu. The protocols used for inducing differentiation had been adapted from those developed for human marrow derived MSC (Jaiswal 1997, Mackay 1998, Janderova 2003.) Consequently, these methods may have favored cervid cells from the marrow, rather than antler, compartment.

There is also the larger issue—the degree to which an in vitro culture environment is even representative of conditions that cells would encounter in their native niches. Bianco cites reports of marrow derived cells being differentiated into

muscle or endothelial cells in vitro. He suggests that without in vivo verification of differentiation it is difficult to conclude whether these results reflect the actual differentiation capacity of these cells or is an artificial result of the non-physiologic conditions in the culture dish (Bianco 2008.) In other words, behaviors that can be coaxed out of a population of cells in vitro may not reflect the phenotype of these cells in vivo.

Drawing from the well-defined characterization of hematopoietic stem cells, researchers such as Bianco advocate for the demonstration of mesenchymal stromal cell differentiation in vivo, as opposed to in vitro: ". . . the widespread use of 'in vitro' assays in lieu of the defining in vivo asays is one of the most important sources of confusion, or at least controversy and disagreement, as to the nature, identity, and potency of 'MSCs'" (Bianco 2010.)

A convenient means for testing osteogenic differentiation in vivo is through the use of an ectopic ossicle formation model, in which culture- expanded cells are seeded onto scaffolds and implanted in an immunocompromised animal. Heterotopic ossification using diffusion chambers has been used to demonstrate marrow stromal cell differentiation for decades (Ashton 1980.) However, the model pioneered by Krebsbach and refined by McCauley seeds cells onto a porous scaffold (Krebsbach 1997, Pettway 2005, Pettway 2008.) This allows gives rise to ossicles derived from cells of both donor (undergoing differentiation) and host (usually hematopoietic) origin.

Here, we will test the following hypothesis:

APC in an in vivo ectopic ossicle formation model will generate more mineralized matrix compared to animal-matched marrow MSC.

Materials and methods

Positive control murine cell culture for use with fresh, late passage deer cells

In the first set of ossicle studies, mouse cells were cultured in a manner assumed to be analogous with that of the deer cells.

Thirteen to 14 days before implantation, 4 week-old, male C57BL/6 mice (Charles River Breeding Labs, Wilmington, MA) were anesthetized using isoflurane inhalation and killed via cervical dislocation. For each round of implantations, approximately 14 million mouse MSC were required. Between 6 and 8 BL/6 mice were sacrificed for each round.

Femora, tibiae, and humeri were dissected and placed in a 50ml conical tube containing ice cold PBS plus 200units/ml penicillin, 200µg/ml streptomycin and 0.5µg/ml amphotericin B (Gibco, Life Technologies, Grand Island, NY) until all needed bones from two mice were collected. Bones were placed in a 100cm dish in a cell culture hood and the distal and proximal ends removed with sterile scissors. Marrow was flushed into another dish using a syringe fitted with a 26-gauge needle and filled with the following medium: Dulbecco Modified Eagle Medium containing 110mg/L sodium pyruvate and 4mM L-glutamine (Gibco), 10% characterized FBS (Gibco), 100units/ml penicillin/100µg/ml streptomyocin/0.25 µg/ml amphotericin B (Gibco.)

The flushed marrow was broken up with a 3ml syringe and 21-gauge needle. The resulting cell suspension was seeded onto a single T-75 flask and 15ml of complete medium added. Four flasks of cells were generated from each two BL/6 harvests. Cells were cultured for 7 days, after which 50% of the medium was changed. After 24 hours, medium was aspirated to remove non adherent cells, the flasks washed twice in sterile PBS, and 15ml complete medium added. The BL/6 cultures were not passaged before seeding onto the implants.

Positive control murine cell culture: thawed cells

For Experiment 2, mouse cell culture strictly adhered to the McCauley lab protocol, including the preconditioning factor dexamethasone in the medium.

Fifteen to 16 days before implantation, 4 week-old, male C57BL/6 mice (Charles River Breeding Labs, Wilmington, MA) were anesthetized using isoflurane inhalation and killed via cervical dislocation. Marrow was flushed into another dish using a syringe fitted with a 26-gauge needle and filled with the following medium: α-MEM, 20% FBS, 10^{-8} M dexamethasone, 2mM L-glutamine and 100units/ml penicillin/100µg/ml streptomycin. This mouse cell growth medium (MCGM) was used only for BL/6 cell culture.

The flushed marrow was broken up first with a 5ml serological pipette then with a 3ml syringe and 18-gauge needle. The resulting cell suspension (~7ml gathered from 2 mice) was seeded onto a single T-75 flask and 13ml of MCGM added, for a total of 20ml. Cells were cultured for 7 days, after which 50% of the medium was changed. Two to three passages were performed before implantation to generate the required numbers.

Host animal care

Scaffolds were implanted in four week-old, male, immunodeficient mice (Athymic Nude, Charles River.) Mice were received at three weeks of age and acclimated for one week in the vivarium before surgery. Mice were group housed except when recovering from surgery and in the case of fighting between animals. Water and food were provided ad libitum. Animal care and use conformed to institutional regulations.

Deer cell culture: fresh, late passage cells

Fresh APC and phalangeal marrow-derived cervid MSC from three bucks were used for Experiment 1. These cells had been cultured continuously since harvest (see Chapter II) in order to generate the numbers needed for several experiments. By the day of surgery, cells had been passed multiple times: passage 3 or 7 APC and passage 4, 7 or 8 MSC were used.

Deer cell freezing, thawing and culturing: thawed cells

As cellular antler tissue was only available on a seasonable basis, Experiment 2 were performed using previously frozen passage 1 cells.

To freeze, cells were washed twice in Ca2+ and Mg2+ free phosphate buffered saline and detached by incubating in 0.25% Trypsin-EDTA (Gibco, Life Technologies, Grand Island, NY) for 5 minutes at 37C. The trypsin was inactivated with twice the volume of complete medium: Dulbecco Modified Eagle Medium containing 110mg/L sodium pyruvate and 0.2mM L-glutamine, 10% characterized FBS, 100units/ml penicillin/100µg/ml streptomycin and supplemented with additional L-glutamine for a total of 0.4mM (Gibco).

Cells were pelleted by centrifuging at 500g for 6 min, resuspended at 500000 cells/ml in freezing medium (90% FBS, 10% DMSO) and aliquoted into Cryule cell freezing vials (Wheaton Science Products, Millville, NJ.) After 24 hours at -80C in a Mr Frosty cell freezing container filled with 250ml isopropyl alcohol to limit the rate of freezing to -1 degree C/min (Nalge Nunc International, Rochester, NY), cells were transferred to liquid nitrogen for long term storage.

Frozen cells were revived by placing in a 37C water bath. Immediately upon thawing, cell vials received a brief spin in a centrifuge to shift suspension away from the cap, after which 1ml complete medium was added to reduce the concentration of the DMSO in the now thawed freezing medium. Cells were then aspirated transferred to a plastic T-25 tissue culture flask (Falcon, Becton Dickson Labware, Franklin Lakes, NJ.) Two vials of 500000 cells each were used for each T-25. Not including the complete medium added to each vial to thin out the DMSO, 4 additional milliliters of medium were added to the flask to bring the total volume to 7ml (2x1ml cells suspended in freezing medium, 2x1ml complete medium added to the vials, 4ml complete medium added after cells transferred to flask.) After 24hrs culture at 37C to foster cell adhesion, medium was aspirated and replaced with 5ml complete medium. This purpose of this step was to remove all DMSO from the medium as well as to flush non-adherent (mostly nonviable) cells from the culture.

Upon 90-95% confluence, cells were split 1:3 by trypsinization (as above), resuspended in 12ml complete medium, and plated in a T-75 flask (Becton Dickinson.) Cells were split again into 3 T-75 flasks prior to implantation.

Implant preparation: fresh, late passage cells

The McCauley lab protocol recommends ~5x5x7mm cubes of Gelfoam seeded with 2-3x10^6 mouse cells. Implants were prepared from 7mm thick porcine Type I collagen hemostatic foam (Gelfoam, Pharmacia & Upjohn, Kalamzoo, MI.) In order to ensure consistent implant size, a pre-cleaned leather punch was used to punch 5mm diameter cylindrical plugs from the Gelfoam. The smaller volume of these round implants compared to the approximate volume of those described in the McCauley protocol (137mm^3 versus ~175mm^3) was assumed to lead to a sufficient cell seeding density with the deer cells, which could not be guaranteed to provide the same cell yields as mouse cells.

Implant preparation: thawed cells

The McCauley lab protocol recommends ~5x5x7mm cubes of Gelfoam seeded with 2-3x10^6 mouse cells (~11000-17000 cells/mm^3.) Based on the experience of Experiment 1, we decided to use smaller implants in seeded with cells in the same range of densities given in the protocol.

A pre-cleaned leather punch was used to punch 3.2mm diameter plugs from the Gelfoam (or 56.3mm^3 volume.) We intended to seed these implants with 1x10^6 cells each, giving a cell density of ~17800cells/mm^3.

One unexpected issue was that the punch transferred small metal particles into the implants, which may have been responsible for image artifacts seen in the fresh cell ossicle study (see Results.) Consequently, all implants were tested for magnetic attraction using a powerful horseshoe magnet. Those that exhibited any attraction to the magnet were discarded. The remaining implants were x-rayed for 7 sec at 20kV to verify the absence of radiodense contaminants (Faxitron, Bioptics LLC, Tucson, AZ.)

Cell seeding

Prior to surgery, Gelfoam implants were sterilized using ethylene oxide gas. The night before surgery, the implants were placed in a 10cm dish filled with complete medium and transferred to a 37C cell culture incubator. This allowed medium to completely soak the foam before cells were seeded.

Immediately prior to use, implants were squeezed with a sterile instrument to displace some of the medium in order for the cell suspensions (see below) to be absorbed. "Blank" (no cell) implants were then placed in 50ml conical tubes and set aside.

Cells were trypsinized as described above. Aliquots of $1x10^6$ cells were resuspended in 50ml conical tubes and centrifuged at 500g for 6 minutes. Medium was aspirated and the cells resuspended in 25µl complete medium. This volume was approximately half that of the implant and assumed to be sufficiently small to be completely taken up by the partially dried sponges.

A sponge was taken dropped into each tube and a sterile scalpel handle used to force the cell suspension into each sponge. A cap was then placed on each tube, tightened and then loosened one quarter turn to allow gas exchange. Tubes were placed in a 37C incubator until ready to be taken to the operating room, where they were kept in a 37C water bath.

Implantation surgery

During surgery, mice were anesthetized using isoflurane inhalation and kept on a heating pad. Animals were placed under a sterile drape during each procedure. To implant each sponge, an incision was made on the dorsal aspect of the mouse and a blunt instrument used to create a subcutaneous pocket. A single sponge was placed in each pocket and the incision closed using a surgical adhesive (GLUture, Abbott Laboratories, Abbott Park, IL.) After surgery, mice were singly housed under a heat lamp until the effects of anesthetic dissipated. Animal health was monitored daily.

Four surgical locations were used for each animal and implant placed randomized.

Monitoring of ossicle growth and animal sacrifice

Four weeks following surgery, “lumps” were visible on the backs of place at sites corresponding to implant placement. One to two mice from each batch of surgeries were imaged under anesthesia in a pre-clinical micro-computed tomography scanner (eXplore Locus, GE Medical Systems, Milwaukee, WI.) Following image reconstruction on 27μm voxels, a qualitative assessment of ossicle growth progress was made.

Implants were ultimately kept in the mice for 6 weeks. At this point, the animals were sacrificed as described above. The implants were then dissected out and placed in 10% neutral buffered formalin to enable fixation. After 48 hours in NBF, implants were transferred to 70% ethanol for storage.

Micro-computed tomography

Implants were scanned using microCT and reconstructed on 18um voxels. Many of the implants had little apparent mineralization. The soft tissue and non-resorbed Gelfoam had similar degrees of x-ray attenuation. Therefore, implants were scanned in air rather than water to provide sufficient contrast for visualization.

Analysis was performed using GE Microview software on three dimensional regions of interest (ROI) interpolated from two dimensional splines. After generating image histograms to estimate mineralized tissue grayscales, a global threshold was applied to each ROI and mineral content and density calculated.

Histology

Ossicles were demineralized in 10% ethylenediamine tetraacetic acid in PBS for 48 hours. Demineralization progress was monitored via x-ray (Faxitron.) Ossicles were washed twice in dH20 and kept in 70% ethanol prior to processing. To process, demineralization ossicles were dehydrated and paraffin-infiltrated in an automated tissue processor for 7 hours (Shandon Hypercenter XP, Thermo Fisher.)

Next, ossicles were paraffin-embedded using a Leica EG1160 paraffin embedding center (Leica Microsystems Inc, Buffalo Grove, IL, USA.) Seven μm-thick sections were cut on a Leica Microtome (Leica Microsystems) and mounted on glass slides.

Matrix content was visualized using Safranin-O/Fast Green staining with Weigert's hematoxylin as a nuclear counter stain. In addition Alcian Blue-Periodic Acid Schiffs stain was carried out using a commercial kit (Poly Scientific R&D Corp, Bay Shore, NY.)

Putative osteoclasts were identified using a tartrate-resistant acid phosphatase (TRAP) detection kit and a protocol adapted from one developed by the McCauley laboratory (Sigma.) Slides were dewaxed in xylene and rehydrated to 50% ethanol and then ultrapure water. Next, slides were incubated in 0.2M Tris, pH 9.0 for 1 hour at 37C. TRAP staining was performed for 1 hour at 37C. Gill's No. 3 Hematoxylin was used as a nuclear counterstain. Slides were counterstain for 2 to 3 seconds and coverslipped using an anti-fading aqueous mounting reagent (ProLong Gold, Life Technologies, Carlsbad, CA.)

Images were captured on a Zeiss Axiovert 200M microscope (Carl Zeiss Microscopy, LLC, Thornwood, NY.)

Statistics

As each experiment involved a small sample size (3 biological replicates), multiple experimental replicates were performed for each assay. Generalized linear mixed models, which take into account nested data structures and repeated measures, were used for comparisons (SPSS, IBM Corp, Armonk, NY.) Sequential Bonferroni post hoc tests were used, with a p-value ≤ 0.05 considered significant.

Only ossicles with detectable bone were considered for analysis. As ossicle microCT involved APC, MSC and blanks, "celltype" was used as a fixed effect; no random effect was considered. Statistical comparisons were limited to implants with detectable mineralized tissue and values more than two standard deviations from the

mean were omitted. Figures show least squared means (LSM) and standard deviations.

Results: fresh, late passage cells

Probabilities of mineral formation: fresh, late passage cells

The probability of ossicle formation varied depending on the group (Fig. 1.) The likelihood of bone formation in C57BL/6, blank (no cell), and APC groups were similar—approximately 50%. MSC-seeded implants, on the other, produced detectable mineral about 25% of the time. Because these data were based on the aggregate probability of each group rather than the probability of each implant generating mineral, statistics cannot be employed to verify such comparisons.

Ossicle mineralization: fresh, late passage cells

Implants seeded with C57BL/6 marrow MSC had by far the greatest mineral content, though large variation was observed in specimens with detectable mineralization (mean 6.45 ± 6.15 μg.) Much less mineral was formed in the other groups and, interestingly, blank (no cell) controls actually formed significantly more mineral than implants seeded with either late passage APC or cervid MSC (Fig. 2A.). No difference was seen in the mineral densities of blank, APC or MSC implants (Fig. 2B.)

Ossicle histology: fresh, late passage cells

In implants seeded by C57BL/6 cells, small, discontinuous regions of apparent bone stained intensely for Fast Green (Fig. 3A, B.) Little Safranin-O staining occurred in these regions. Though bone was detected in BL/6-seeded scaffolds, no TRAP-positive cells were seen (Fig. 3C.)

Staining revealed deer cell-seeded scaffolds and blanks to be composed of regions of new tissue and non-resorbed Gelfoam. Safranin-O/Fast Green stain did not uncover consistent differences in scaffold composition between groups (Fig. 4.) In

general, however, APC and MSC-seeded implants were composed of a qualitatively greater proportion of Fast Green-positive tissue compared to the blanks (Fig. 4.)

Despite the lesser degree of mineralization detected in APC and MSC-seeded implants compared to the blanks, the latter did not display any apparent TRAP staining (Fig. 5.) In contrast, TRAP-positive cells were seen in ossicles from buck 1 APC and MSC-seeded ossicles from bucks 1 and 3. However, the number of TRAP-positive cells was still too small to quantify meaningfully.

Results: thawed deer cells

Probabilities of mineral formation: thawed cells

All implants seeded with C57BL/6 cells formed detectable mineral (Figs. 6, 7.) Similar probabilities of mineral formation were exhibited by implants seeded with APC, MSC or no cells at all (approximately 0.7). Of these three groups, APC had the highest probability (0.76.)

Ossicle mineralization: thawed cells

Implants seeded with BL/6 cells displayed robust mineral formation (mean 167 ± 155 µg.) In addition, unlike implants seeded with fresh, late passage cells, those that received thawed APC and MSC had greater mineral compared to the blanks (Fig. 8.) There was no difference detected in the mineral content between APC and MSC.

Mineral densities were of a similar magnitude between all groups, with MSC showing significantly greater TMD than the blanks (though there was not a substantial absolute difference) (Fig. 8.)

Ossicle histology: thawed cells

Safranin-O/Fast Green staining revealed a well formed cortical shell surrounding a defined marrow space in ossicles seeded with BL/6 cells (Fig. 9A-C.) Within this marrow numerous erthyrocytes, probably of host origin, could be seen. Numerous putative osteocytes were buried in the bony cortex (Fig. 9C.) The majority of staining

was due to Fast Green; little, if any, of the tissue has positive Safranin-O staining. The cortex stained intensely for Periodic Acid-Schiff, with alcian blue apparent in discrete regions surrounding the “lacunae” of buried cells (Fig.9D.) Numerous TRAP-positive bodies (putatitve osteoclasts) were found in the bone as well (Fig.9E.)

In blank and APC and MSC-seeded ossicles, Safranin-O/Fast Green stain did not reveal a continuous cortical shell or marrow space (Fig.10.) Instead, these specimens were defined by regions of new tissue and unresorbed Gelfoam. Qualitatively, APC and MSC-seeded ossicles exhibited a higher ratio of the former to the latter. However, no attempt was made to calculate relative areas of new tissue and Gelfoam. As with BL6-seeded implants, APC and MSC-seeded implants and blanks had little Safranin-O staining.

As microCT analysis revealed limited but nonetheless extant mineral in the ossicles, further histological analysis was performed to attempt to better define the composition of the new tissue. Alcian Blue-Periodic Acid/Schiff was, as with the Safranin-O staining, able to differentiate regions of new tissue from unresorbed Gelfoam (Fig.11.) Newly formed tissue stained intensely for PAS, but little specific Alcian Blue staining was observed. At 400X magnification, cells can be seen buried in the newly formed tissue in most images of APC and MS-seeded implants. Few buried cells could be found in blank implant sections. Rather, cells in the blank implants largely appeared on the surfaces of the regions of newly formed tissue.

TRAP-staining provided further evidence of mineralized tissue formation in the implants (Fig.12) TRAP-positive cells, most multinucleated, were observed in APC and MSC-seeded implants, indicating the presence of osteoclasts. No TRAP-positive cells were seen in the blank implants. The relatively small number of TRAP-positive cells in APC and MSC-seeded implants precluded meaningful quantification.

Discussion

The purpose of this aim was to investigate APC osteogenic differentiation in a milieu more representative of the *in vivo* environment compared to the *in vitro* conditions described in Chapter II. Using immunodeficient mice as a proxy for deer, we implanted cell-seeded or blank Gelfoam implants subcutaneously for 6 weeks. We carried this process out twice, first using fresh, late passage (P3-8) deer cells and then with thawed passage 1 cells.

When it comes to demonstrating osteogenic differentiation *in vivo*, the first study proved inconclusive. Counter intuitively, implants seeded with either APC or MSC produced less mineral than implants seeded with no cells at all. Even the positive control implants, those seeded with fresh marrow-derived MSC from C57BL/6 mice did not produce robust bone growth compared to that reported in the literature (Pettway 2005, 2008.)

Addressing the second issue first, the intention of the positive control in this study was to provide a reference point using a "known good" cell type (in this case murine MSC) that had been pre-cultured under the same conditions as the APC and MSC. In other words, the C57BL/6 used in conjunction with fresh, late passage deer cells were maintained in a standard complete medium used throughout our work (see Materials and Methods), rather than the "richer" formulation used in the literature (Krebsbach 1997, Pettway 2005, 2008.) In addition, the protocol used to wash away non-adherent cells from the freshly plated mouse cell cultures was similar to that used for deer cells.

Though it is possible that other factors contributed to the less than expected bone formation in BL/6-seeded implants, it seems most likely that robust mineral formation by these cells in the ectopic murine model benefits from two key protocols. The first is the enrichment of the adherent cell population in the initial culture by delaying the first wash up to one week. The second is the pre-culturing of these cells in a medium containing a high percentage of FBS.

Regarding the poor generation of mineralized tissue in fresh, late passage APC and MSC, there may have been two key issues at play. The first is that there is a clear

positive association between continued cell replication and senescence, a concept promoted by Hayflick in 1961 and ultimately linked to the shortening with each division of structures called telomeres on the ends of chromosomes (Watts 2011.) Senescence is thought to initiate in mesenchymal stromal cells upon culturing and MSC gradually lose their proliferative and differentiating capacity with increasing passage number (Bonab 2006, Wagner 2011.) Further, using cell cultured from red deer antlers (*Cervus elaphus*), Kuzmova found a significant reduction in H^3 thymidine incorporation in passage 2 cells versus primary cultures, indicating a ~50% reduction in proliferation in the later passage (Kuzmova 2011.) Therefore, it is likely that fresh passage 3-8 APC and MSC had lost much of their capacity for osteogenic differentiation.

A second issue is whether deer cells are capable of substantial growth or differentiation on a subcutaneously implanted gelatin scaffold, even under optimal conditions. Krebsbach has reported that bone growth in the murine ectopic model was dependent on cell type and scaffold material (Krebsbach 1997.) Unlike mouse MSC, human MSC seeded onto gelatin scaffolds failed to promote *in vivo* bone growth when dexamethasone and ascorbic acid were absent from the initial culturing medium (ibid.) Even when these factors were added to the medium, bone growth was achieved in only 5 of 28 scaffolds after implantation (ibid.) On the other hand, implanted hMSC were able to reliably generate bone when seeded onto scaffolds made from HA/TCP (hydroxyapatite/tricalcium phosphate), even after prior culturing in medium lacking dex and ascorbic acid (ibid.) Consequently, it is possible that gelatin scaffolds are inherently not conducive to APC or cervid MSC differentiation after implantation in a mouse.

The second set of experiments attempted to address these issues via three changes: first, the use of passage 1 (albeit previously frozen) APC and MSC; second, the adoption of C57BL/6 culturing protocols in line with those used in the literature (including the delay of cell washing in culture and the use of 20% FBS and dexamethasone in the medium); and third, the use of smaller implants to increase the density of seeded cells to the level used by Pettway/McCauley (~17000-18000 cell/cm^3) (Pettway 2005, 2008.) Though the use of those protocols rendered the BL/6 a less

direct positive control, it tested whether we could successfully recapitulate previous results with the ectopic ossicle model.

In this second round of experiments, our scaffolds seeded with BL/6 were able to reproduce the type and extent of bone growth reported in the literature—complete with a bony "cortex" and marrow space comprised of cells of most likely host origin (see Fig.9.) This demonstrates the validity of our cell seeding, implantation and assay methods.

Our results for the other implants were more in line with expectations. Though the probability of bone formation was approximately the same between APC and MSC-seeded scaffolds and blanks, scaffolds implanted with deer cells produced significantly more mineralized tissue compared to initially acellular scaffolds. However, the mineral generated by APC and MSC in vivo (a least squared mean of less than 1µg) was less than 1/100th of that produced by BL/6-seeded scaffolds.

With the relatively poor tissue mineral content of thawed passage1 APC and MSC-seeded scaffolds detected by microCT, we again used histology to look for additional evidence of bone formation. Though the numbers were too small to accurately quantify, we observed two key cell types in these implants.

First were putative osteocytes buried within the new tissue generated in the APC and MSC-seeded scaffolds that were virtually absent in blanks. Though definitive identification of these cells would require assaying for markers such as E11/gp38, sclerostin, DMP-1, phex and FGF-23 (Bonewald 2007), their placement within apparent lacunae in scaffold tissue lends credence to our assertion of some non-stochastic bone formation. Second, our observation of tartrate-resistant acid phosphatase (TRAP)-positive cells in APC and MSC-seeded scaffolds gives us further confidence that these cells gave rise to bone formation in the murine model. We failed to observe any TRAP positive cells in blank scaffolds, in line with the significantly lower mineralization measured in these scaffolds.

Detection of TRAP positive cells is indicative of the presence of osteoclasts, but is not ironclad proof. Immune cells such as macrophages and dendritic cells can also stain positively for TRAP (Hayman 2008.) However, scaffolds were implanted in

immunodeficient mice lacking functional thymus glands. The thymus is a primary lymphoid organ that serves as the site of maturation for T-cells (Widmaier 2008.) Though immune cells such as macrophages may still be present in athymic mice, the lack of mature helper T-cells may limit their specific activation (ibid.) Therefore, it is not unreasonable to assume that the presence of TRAP-positive cells in APC and MSC-seeded scaffolds strongly indicates existence of osteoclasts in those scaffolds.

Interestingly, there was no significant difference in the amount of mineral in APC and MSC-seeded implants. This contrasts to our in vitro findings (see Chapter II), in which MSC produced far more mineral under osteogenic conditions compared to APC, even correcting for cell number. It is possible that, compared to the MSC, APC osteogenic differentiation requires a more stringent set of factors--factors that were more available when these cells were seeded onto collagen sponges and implanted in mice. Put another way, APC differentiation is characterized by more specific milieu dependence relative to MSC.

Clearly, our ectopic ossicle formation studies would have benefitted from further protocol optimization. Had the resources been available, it would have been preferable to seed ossicles with fresh, primary APC and MSC. Still, though we failed to reject the null hypothesis of this aim, we have demonstrated that culture-expanded APC and MSC are capable of osteogenic differentiation in vivo.

Chapter 3 figures

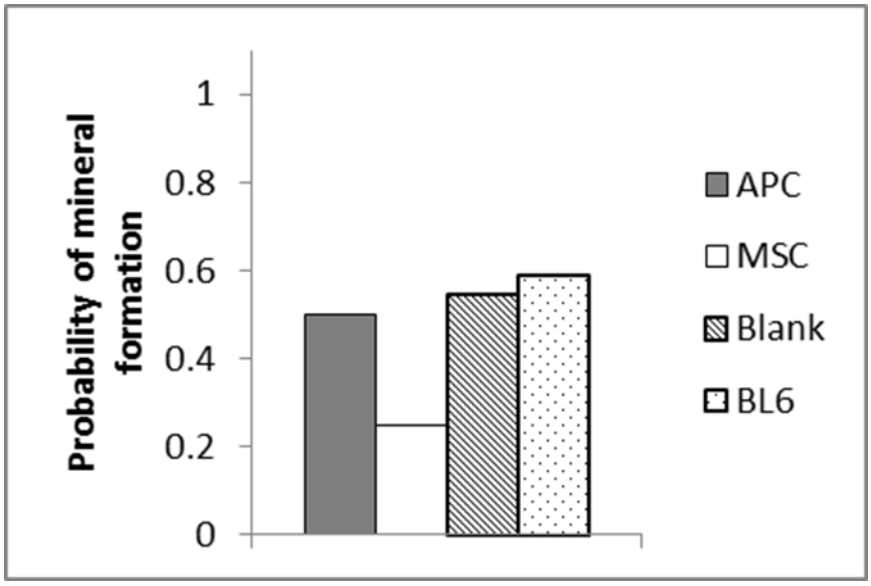

FIG. 3.1: Probability of mineral formation in fresh cell ossicles.

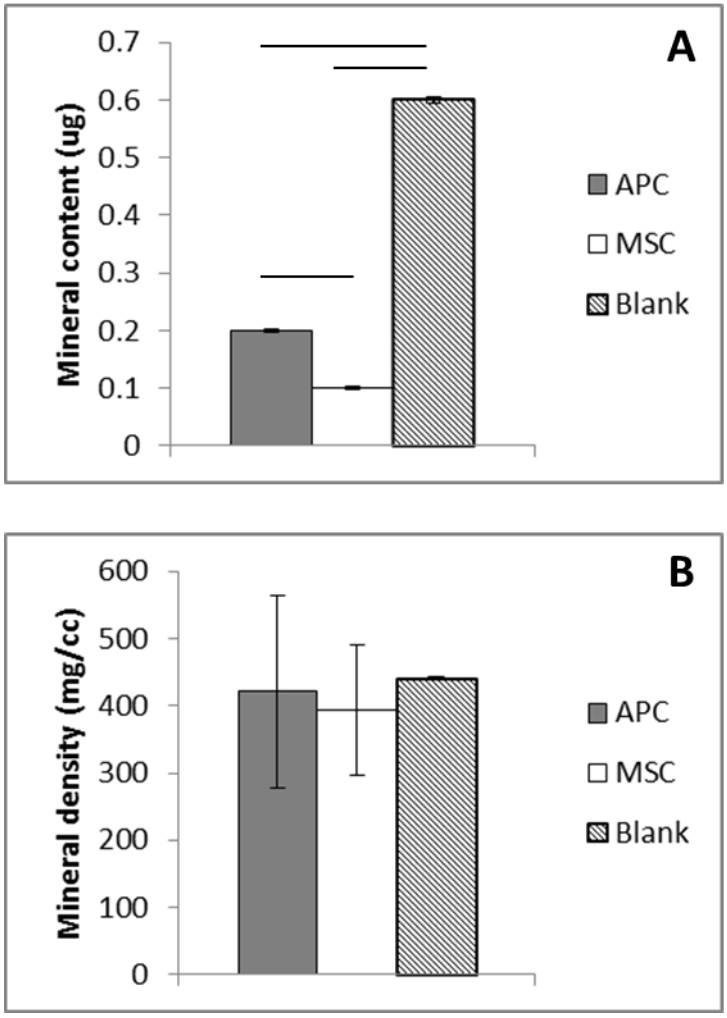

FIG. 3.2: Fresh cell ectopic ossicles microCT data (n=3.) (A) tissue mineral content and (B) tissue mineral density. Line: $p<0.05$.

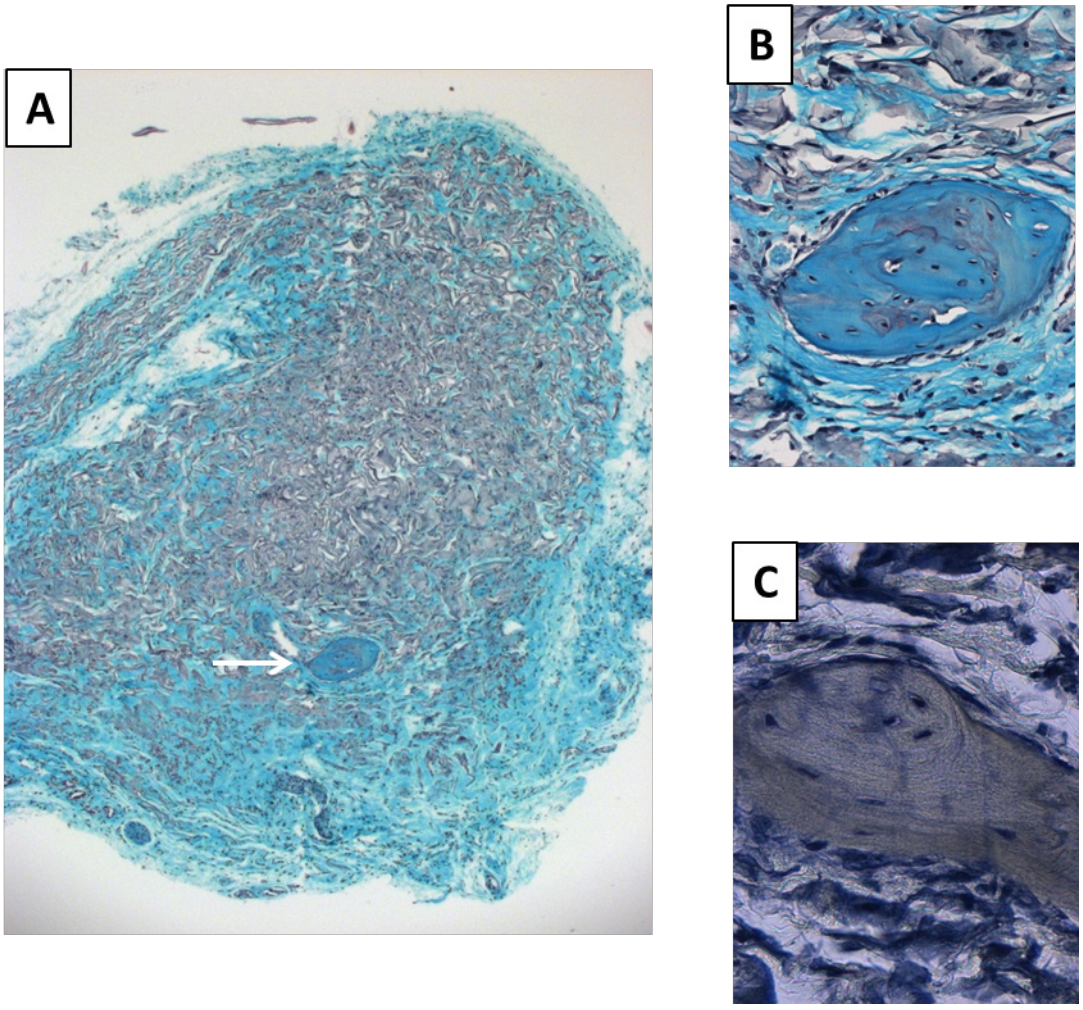

FIG. 3.3: Ossicle formation in C57BL/6 seeded positive control implants for fresh deer cell study. No pre-conditioning performed prior to implantation. (A) Whole implant showing small bone region (arrow). Safranin-O stain, 25x mag. (B) Inset of bone. Safranin-O stain, 200x mag. (C) Inset of bone, TRAP stain, 400X mag (non-adjacent section.) No staining observed.

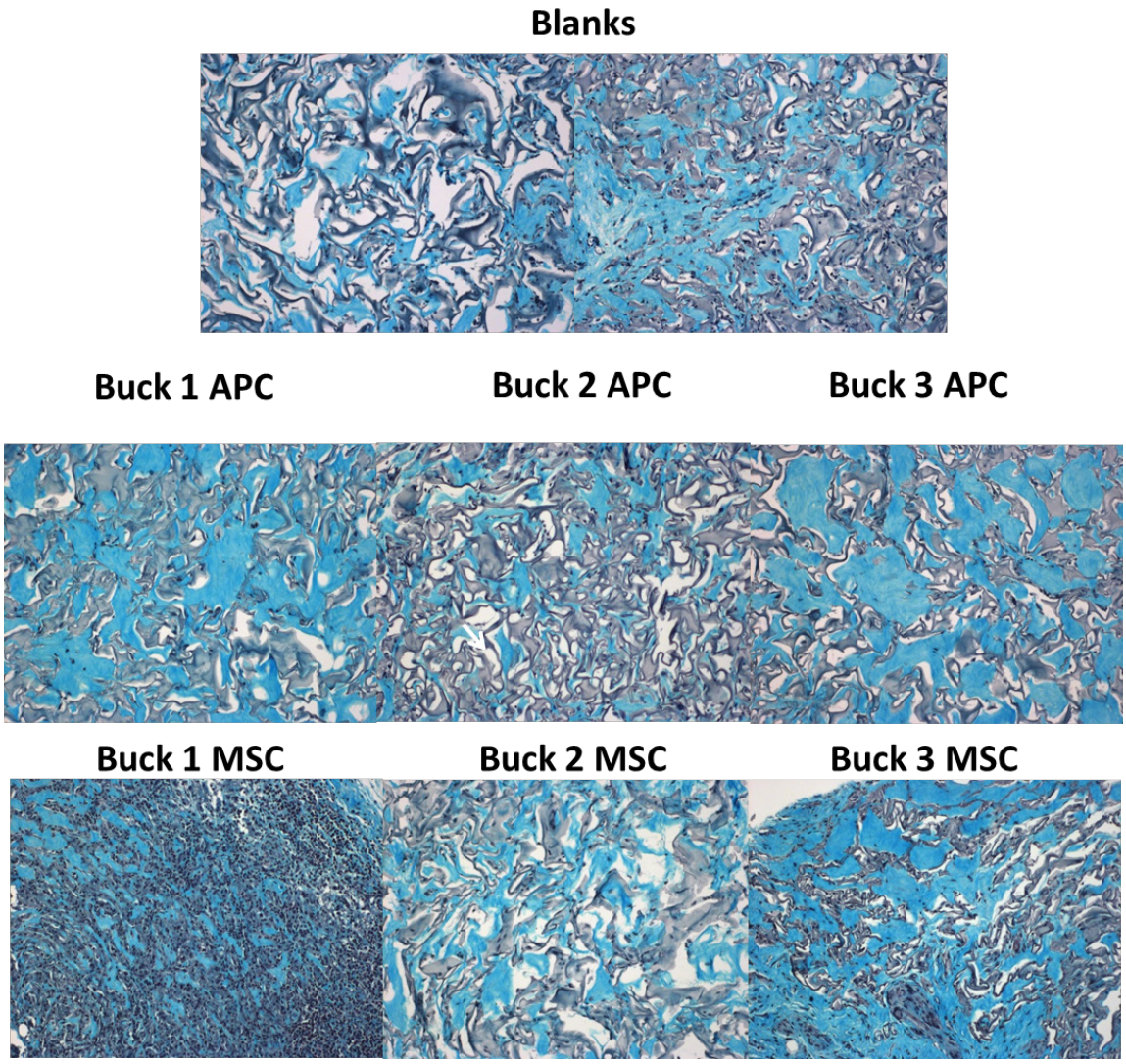

FIG 3.4: Safranin-O staining in fresh cell ossicles. 100X mag.

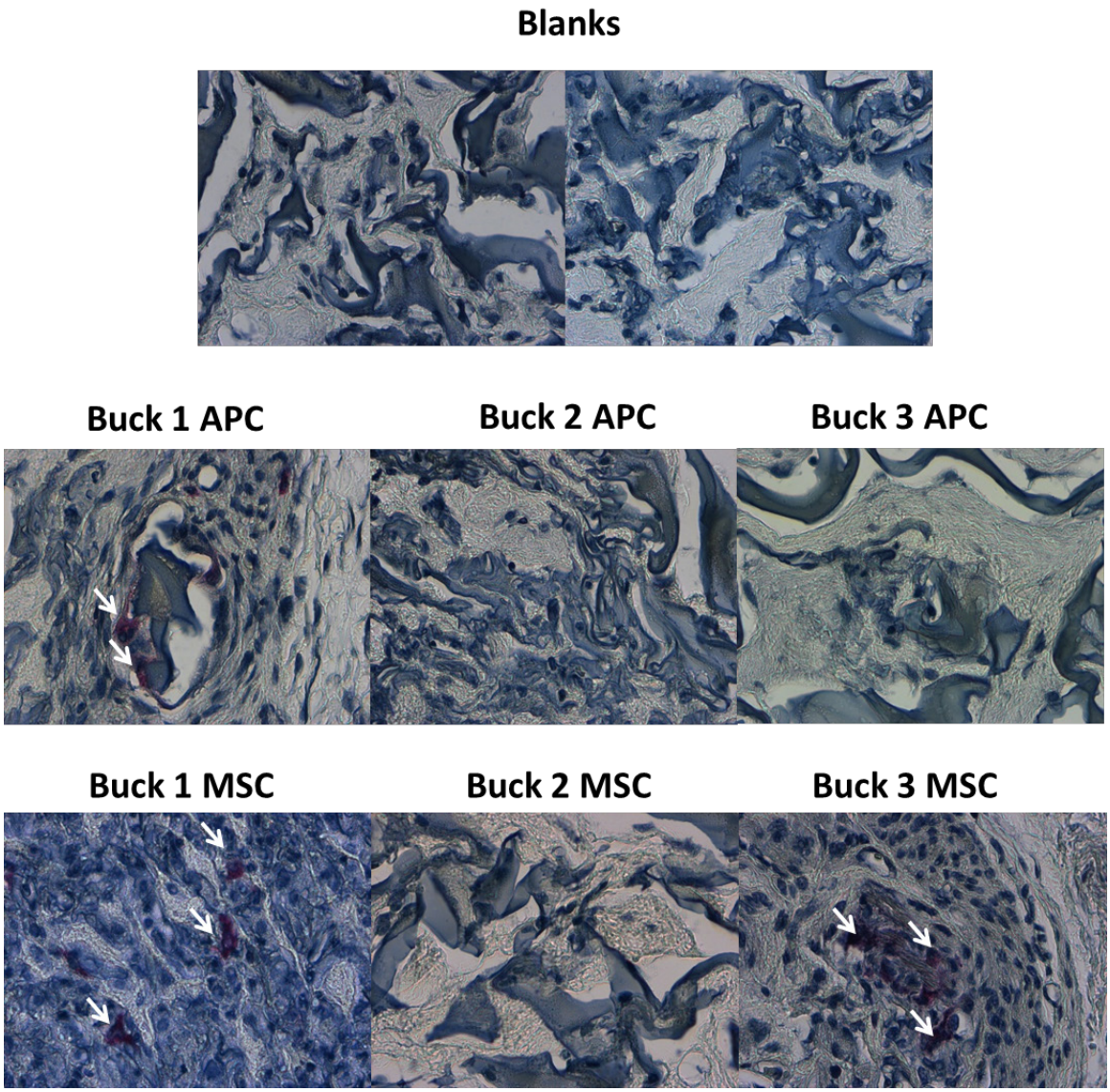

FIG. 3.5: TRAP staining of fresh cell ossicles. No staining in blanks and scaffolds seeded with APC from 2 of 3 deer (see arrows). Positive staining in scaffolds seeded with MSC from 2 of 3 deer (arrows). 400X magnification.

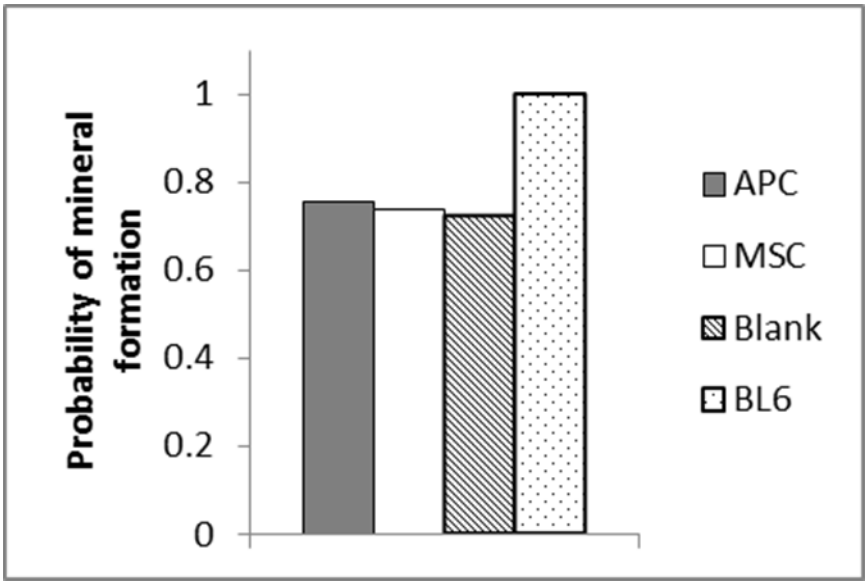

FIG. 3.6: Probability of mineral formation in thawed cell ossicles.

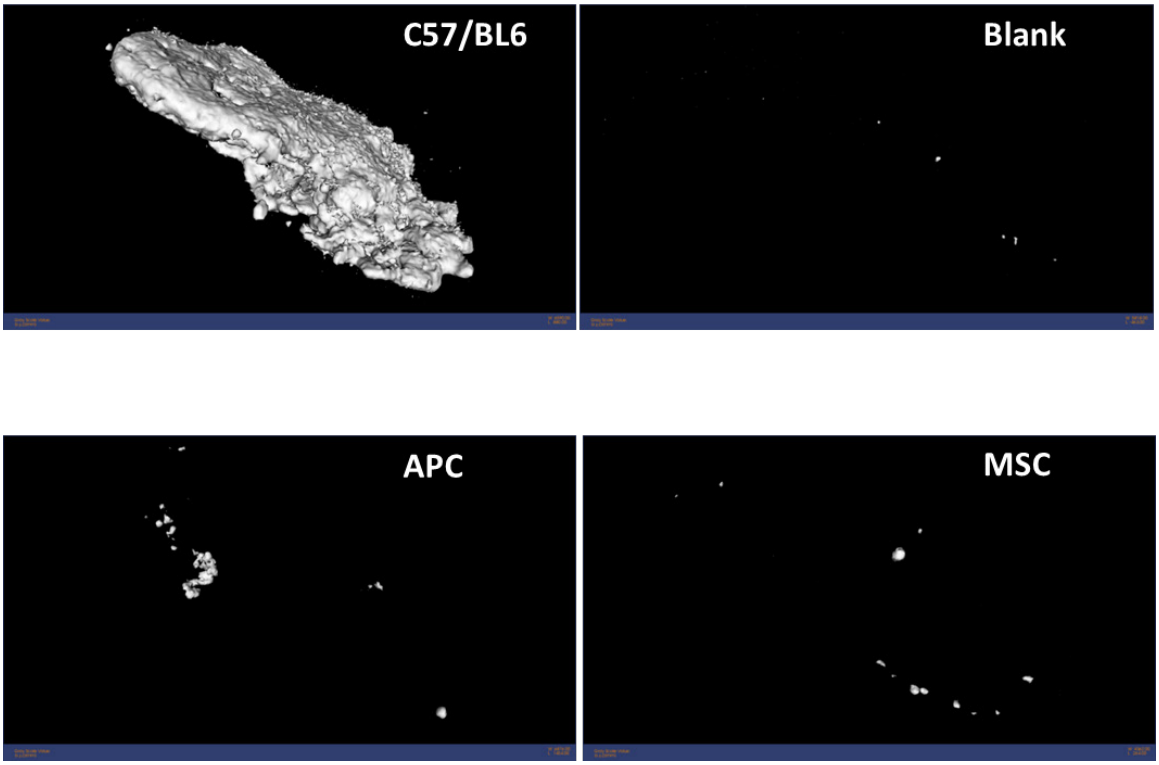

FIG. 3.7: Thawed cell ectopic ossicle mineralization. Images generated from microCT using 800 HU threshold.

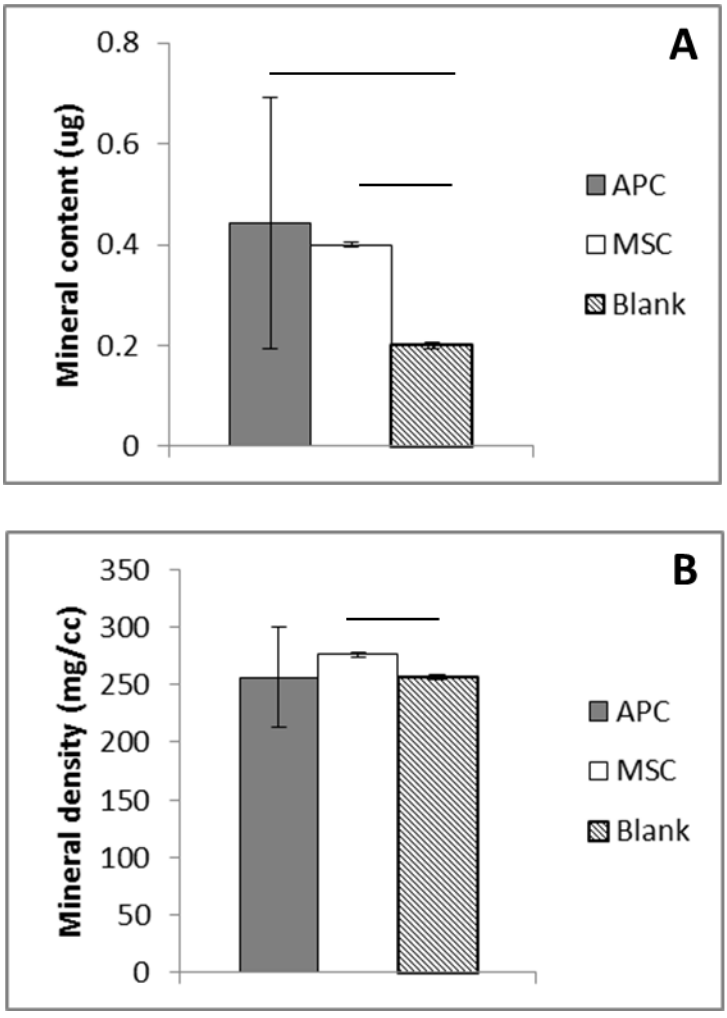

FIG. 3.8: Thawed cell ectopic ossicles microCT data (n=3). (A) tissue mineral content and (B) tissue mineral density. Line: $p<0.05$.

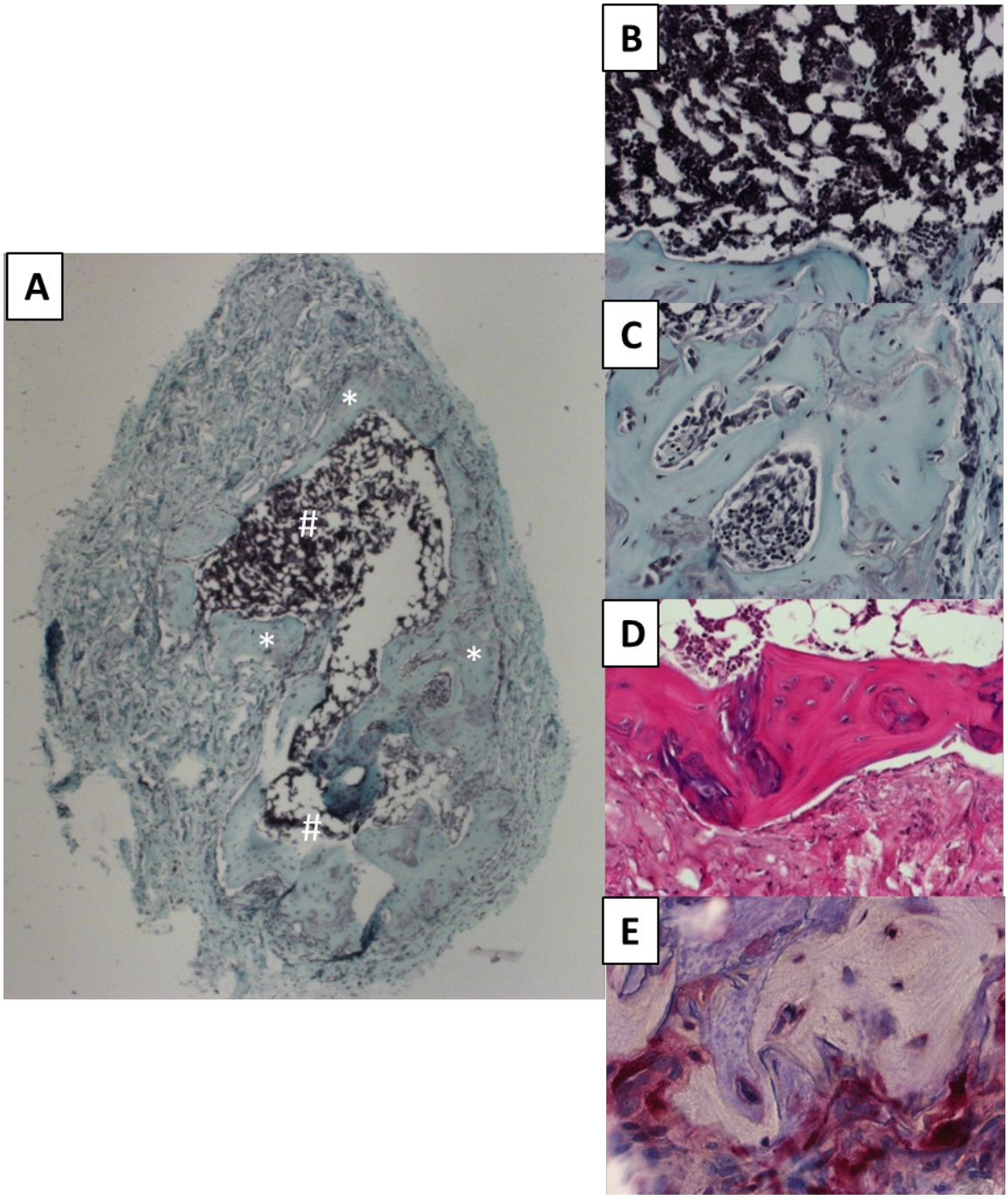

FIG 3.9: Ossicle formation in C57BL/6-seeded positive control implants for thawed deer cell study. Pre-conditioned prior to implantation. (A) Whole ossicle showing cortical shell (*) and marrow space (#). Safranin-O stain, 25x mag. (B) Inset of marrow. Safranin-O stain, 200x mag. (C) Inset of bone. Safranin-O stain, 200x mag. (D) Inset of bone, Alcian Blue-PAS stain, 200X mag. (E) Inset of bone, TRAP stain, 400X mag.

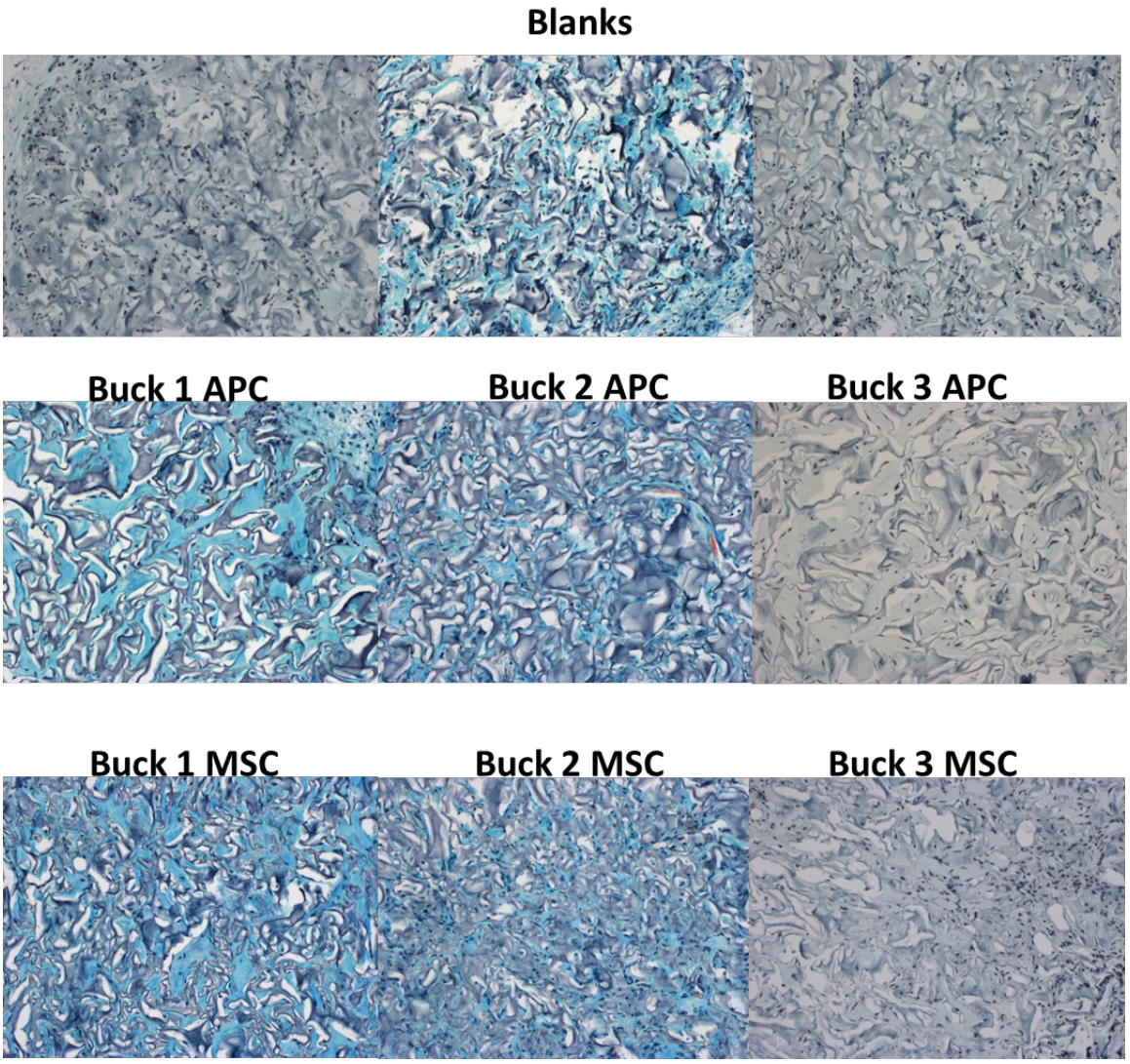

FIG. 3.10: Safranin-O staining in thawed ossicles. 100X mag.

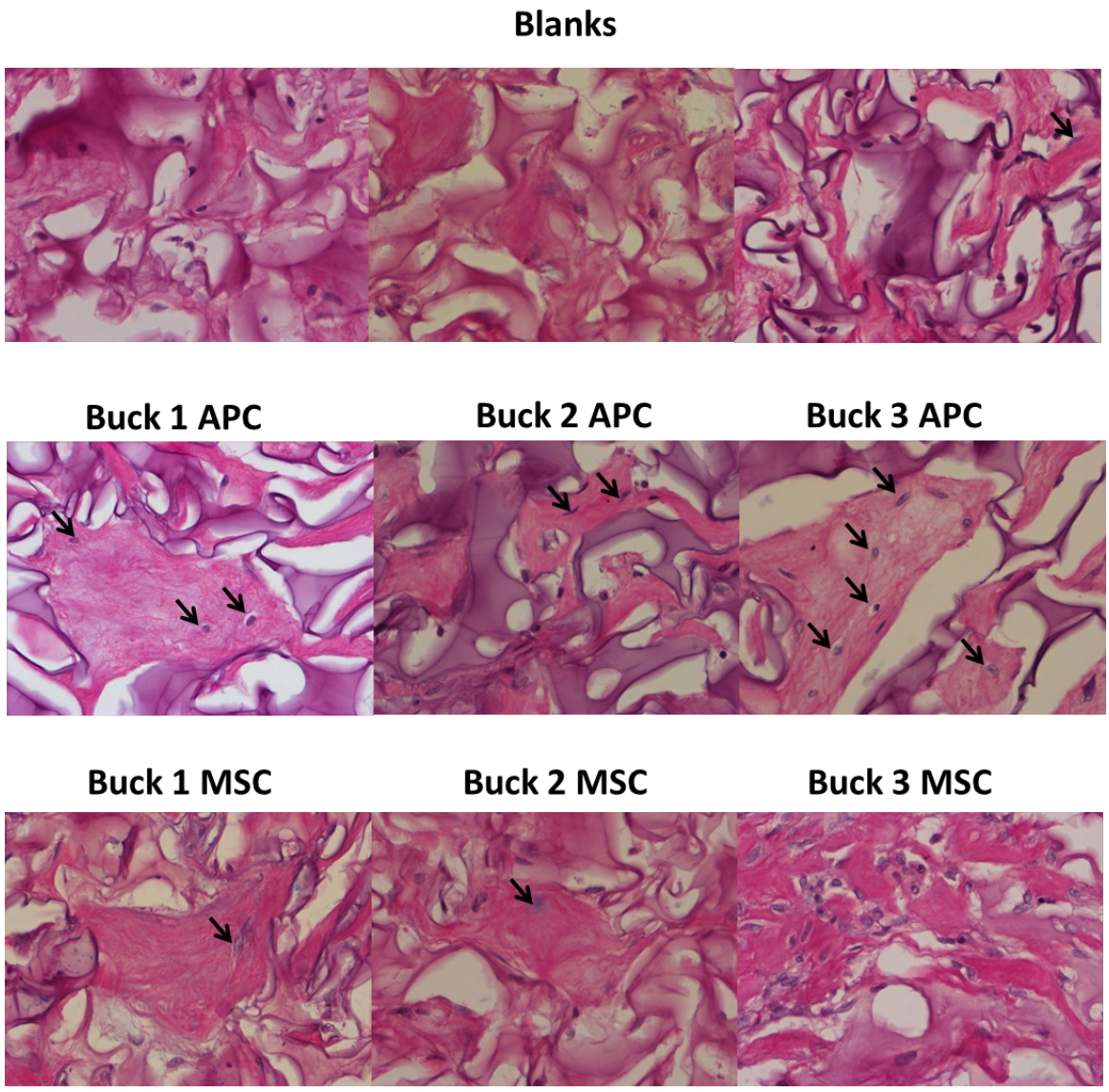

FIG. 3.11: Alcian Blue-PAS staining of thawed ossicles. Magenta regions are tissue while purple-stained regions are non-resorbed Gelfoam. 400X mag. Arrowheads indicate buried, putative osteocytes.

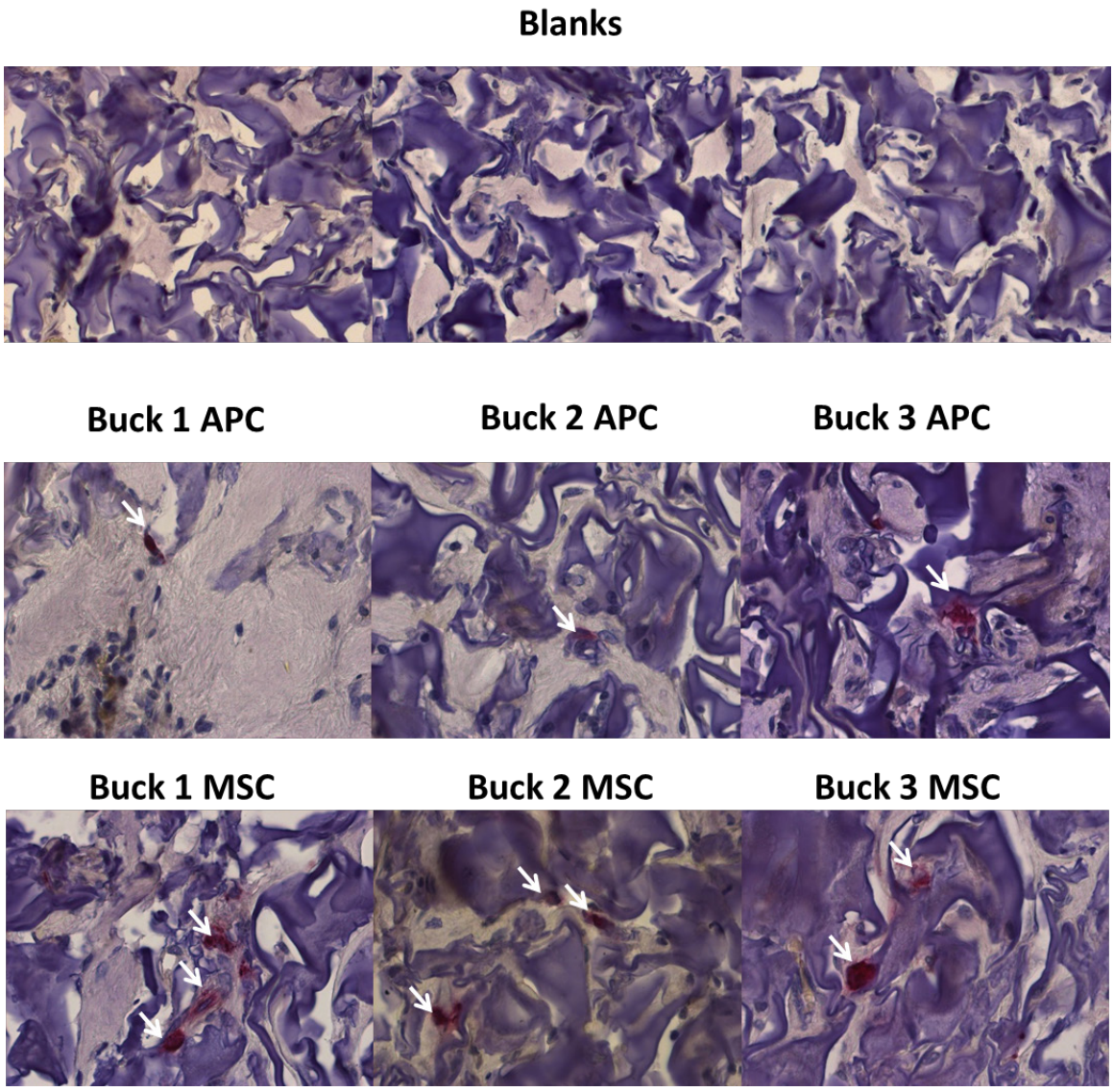

FIG. 3.12: TRAP staining of thawed cell ossicles. Arrow heads indicate TRAP-positive cells. 400X mag.

Bibliography

Ashton BA, Allen TD, Howlett CR, Eaglesom CC, Hattori A, Owen M. Formation of bone and cartilage by marrow stromal cells in diffusion chambers *in vivo*. Clin Orthop 1980;151:294-307.

Bianco P, Robey PG, Simmons PJ. Mesenchymal stem cells: revisiting history, concepts, and assays. Cell Stem Cell 2008; 2(4): 313-319.

Bianco P, Robey PG, Saggio I, Riminucci M. "Mesenchymal" stem cells in human bone marrow (skeletal stem cells): a critical discussion of their nature, identity, and significance in incurable skeletal disease. Human Gene Ther 2010;21:1057-1066.

Bonab MM, Alimoghaddam K, Talebian F, Ghaffari SH, Ghavamzadeh, Nikbin B. Aging of mesenchymal stem cell in vitro. BMC Cell Bio 2006 7;14: 1471-2121/7/14 .

Bonewald, LF. Osteocytes as dynamic multifunctional cells. Ann NY Acad Sci 2007 1116:281-290.

Currey JD, Brear K, Zioupos P. Notch sensitivity of mammalian mineralized tissues in impact. Proc R Soc Lond B 2004; 271:517-522.

Dominici M, Le Blanc K, Mueller I, Slaper-Cortenbach I, Marini F, Krause D, Deans R, Keating A, Prockop DJ, Horwitz E. Minimal criteria for defining multipotent mesenchymal stromal cells. The International Society for Cellular Therapy position statement. Cytotherapy 2006;8(4):315-317.

Hayman AR. Tartrate-resistant acid phosphatase (TRAP) and the osteoclast/immune cell dichotomy. Autoimmunity 2008 41;3:218-223.

Jaiswal N, Haynesworth SE, Caplan AI, Bruder SP. Osteogenic differentiation of purified, culture-expanded human mesenchymal stem cells in vitro. J Cell Biochem 1997; 64(2): 295-312.

Janderova L, McNeil M, Murrell AN, Mynatt RL, Smith SR. Human mesechymal stem cells as an in vitro model for human adipogenesis. Obesity Res 2003; 11(1): 65-74.

Kierdorf U, Kierdorf H, Szuwart T. Deer antler regeneration: cells, concepts, and controversies. J Morphology 2007; 268(8),726-738.

Krebsach PH, Kuznetsov SA, Satomura K, Emmons RVB, Rowe DW, Robey PG. Bone formation in vivo: comparison of osteogenesis by transplanted mouse and human marrow stromal fibroblasts. Transplantation 1997;63(8):1059-1069.

Kuzmova E, Bartos L, Kotrba R, Bubenik GA. Effects of different factors on proliferation of antler cells, culture *in vitro*. PloS ONE 2011; 6(3): e18053.

Mackay AM, Beck SC, Murphy JM, Barry FP, Chichester CO, Pittenger MF. Chondrogenic differentiation of cultured human mesenchymal stems cells from marrow. Tissue Eng 1998; 4: 415.

Pettway GJ, Schneider A, Koh AJ, Widjaja E, Morris MD, Meganck JA, Goldstein SA, McCauley LK. Anabolic actions of PTH (1-34): use of a novel tissue engineering model to investigate temporal effects on bone. Bone 2005;36(6):959-970.

Pettway GJ, Meganck JA, Koh AJ, Keller ET, Goldstein SA, McCauley LK. Parathyroid hormone mediates bone growth though the regulation of osteoblast proliferation and differentiation. Bone 2008;42(4):806-818.

Price JS, Allen S, Faucheux C, Althnaian T, Mount JG. Deer antlers: a zoological curiosity or the key to understanding organ regeneration in mammals? J Anat 2005; 207(5):603-618.

Snyder DL, Cowan RL, Hagen DR, Schanbacher BD. Effect of pinealectomy on seasonal changes in antler growth and concetrations of testosterone and prolactin in white-tailed deer. Bio Reproduct 1983;29:63-71.

Wagner W, Horn P, Castoldi M, Diehlmann A, Bork S, Saffrich R, Benes V, Pfister S, Eckstein V, Ho AD. Replicative senescence of mesenchymal stem cells: a continuous and organized process. PLoSOne 2008 3;5:e2213.

Watts G. Leonard Hayflick and the limits of ageing. Lancer 2011 377;9783:2075.

Widmaier EP, Raff H, Strang KT. Vander's Human Physiology 11th ed. 2008, McGraw-Hill: New York. p. 647-658.

Winer JP, Janmey PA, McCormick ME, Funaki M. Bone marrow-derived human mesenchymal stem cells become quiescent on soft substrates but remain responsive to chemical or mechanical stimuli. Tissue Eng 2009;15(1):147-154.

CHAPTER IV:
Aim 3

Introduction

Clearly, bones are living organs capable responding to biochemical and mechanical stimuli. The ways in which bone reacts to its mechanical environment are of interest as these play a significant role in determining the tissue's "structure-function" relationship. This mechanical adaption is manifested in three key ways: the optimization of bone strength through the judicious formation and resorption of structural material, the alignment of trabeculae in principal stress directions and the mechanoresponsiveness of individual bone cells as part of this self-regulating system (Martin1998.)

Though cell mechanoresponsiveness is a critical element of bone's structure-function relationship, the actual ways in which cells sense and respond to mechanical stimuli are, even today, not well understood. Though tissue strains of approximately 0.1% occur during physiologic loading (i.e. during ambulation), bone cells typically require strains of 10 to 100 times greater magnitude to respond (Riddle 2008.) Many believe that, rather than acting directly on bone cells, matrix deformation during locomotion is transduced to cyclical fluid flow through bone's lacunar-canalicular system (Forwood 1996.)

Bending stresses in the long bones, for example, induce pressure gradients that, in turn, generate fluid flows proportional to strain rate (ibid.) In addition, changes in oscillating intermedullary pressure are associated with bone formation and reduction of cortical porosity (Qin 2003.) Regardless of the exact source of strain, it is thought that the resulting fluid flow amplifies the mechanical signal to a magnitude that can be sensed by bone cells in some as yet undetermined fashion (Riddle 2008.)

The specific flow modality experienced by bone cells during locomotion is also a source of debate. Papers have reported the effects of steady (continuous fluid delivery), pulsatile (net positive) and oscillatory fluid flow (no net fluid delivery) on these cells (Jacobs 1998, Bakker 2001, Jiang 2002.) However, Jacobs argues that by virtue of its cyclical nature, oscillatory fluid flow may closely approximate physiologic conditions in an experimental setting (Jacobs 1998.)

The actual magnitudes of the shear stresses that cells are exposed to *in vivo* are unknown. In a frequently cited paper, Weinbaum described a porous media model that estimated peak shear stresses of up to 30 dyn/cm^2 in canaliculi due to combined axial and bending loads (Weinbaum 1994.) Using a connected cellular network model, Mi calculated a peak shear stress of approximately 20 dyn/cm^2 in the canalicular networks of avian long bones subjected to cyclical loading (Mi 2005.) It is unclear the extent to which Mi's value truly reflects loading in large animal long bones. However, the similar magnitudes of the Weinbaum and Mi shear stress estimates lend credence to their use as target parameters for fluid shear stress experiments.

Both of the above studies focused on fluid flow in the canalicular network, based on the assumption that terminally differentiated osteocytes perform the bulk of the mechanosensing in bone. In fact, numerous studies have demonstrated that cells further "upstream" in the osteoblast lineage respond to fluid flow—which is fortunate from an experimental standpoint, as the challenges of obtaining and culturing osteocytes *in vitro* (Stern 2012) favors the use of less differentiated cells. Though it is not yet known if the mechanoresponsiveness of mesenchymal progenitors and osteoblasts of varying degrees of lineage commitment contribute to bone's structure-function relationship *in vivo*, Riddle cites Qin's 2003 paper as evidence that marrow cells are exposed to fluid stresses in the body (Qin 2003, Riddle 2006.)

It is thought that cells respond both directly to flow-induced shear stress itself as well as to changes in chemotransport, in which fluid movement delivers needed factors and washes away waste products (Jacobs1998, Donahue 2003.) Researchers have focused on several basic interrelated cell responses to fluid flow which occur over different time scales. The specificity of the response may be positively related to the

time of exposure to the flow. Intracellular calcium and ATP release occurs within minutes of the onset of flow (Riddle 2008a.) The signaling factors nitric oxide and prostaglandin E_2 are secreted between minutes and hours (Riddle 2008b).

Nitric oxide (NO) is a small, short-lived molecule generated from molecular oxygen and the terminal guanidine nitrogen of the amino acid L-arginine in a reaction that also results in L-citrulline (Van'T Hof 2001.) The molecular targets of NO are not known, but the molecule has bisphasic effects on bone resorption and formation (ibid.) At low concentrations, NO is thought to contribute to IL-1 induced bone resorption; yet NO can inhibit resorption at high concentrations (ibid.) Likewise, constitutive production of low concentrations of NO contributes to osteoblast homeostasis while inhibiting proliferation in these cells at high concentrations due to increased apoptosis (ibid.) Of the three isoforms of nitric oxide synthase (NOS), the enzyme that catalyzes the reaction that forms NO, the endothelial form (eNOS) is constitutively expressed in bone cells. ENOS is regulated by changes in intracellular Ca2+ while the inducible synthase (iNOS) can be synthesized in response to pro-inflammatory cytokines (ibid.) Neuronal NOS is thought to be absent in bone cells.

Prostaglandin E_2 (PGE_2) are small lipid molecules that are part of a larger group of eicosanoid signaling molecules produced in nucleated cells (Miller 2006.) Prostaglandins are synthesized as follows: first, phospholipase A2 frees arachidonic acid from membrane phospholipids. Prostaglandin H_2 is then generated from arachidonic acid by cyclooxygenase-1 or -2 (COX-1, -2) as a result of stimuli such as inflammation (via IL-1 and TNF-α) and hormones (Harris 2002, Miller 2006.) Prostaglandins such as PGE_2 are produced by PGE synthases and released from the cell, where they act in a paracrine fashion (Harris 2002.)

What makes PGE_2 interesting in the context of mechanosensing is that this molecule is also produced in response to perturbations of the cell membrane (Miller 2006.) There are two stages of PGE_2 release due to fluid shear stress (Genetos 2005.) First, a burst of PGE_2 is released after 5-10 minute of flow as a result of Ca2+ entry into the cell. Second, after 45-60 minutes of continuous application of flow, PGE_2 release results from an increase in COX-2 synthesis and production.

In bone, PGE_2 is primarily produced by osteoblasts and affects these cells as well as osteoclasts (Miller 2006.) This molecule has a variety of seemingly contradictory effects on bone, promoting either bone resorption or formation, possibly due to the types of receptors present (ibid.) Suffice it to say, we do know that PGE_2 mediates cAMP production and DNA synthesis resulting from mechanical stimuli *in vitro* (Forwood 1996.) In short, though its exact role may be unclear, PGE_2 is a clear marker of mechanoresponsiveness.

At tens of hours after fluid flow cells can respond by proliferating. Jiang found that pulsatile flow increased proliferation in osteoblastic cells, while Kapur linked extracellular signal-related kinases (ERK) 1 and 2 to increased proliferation in osteoblastic cells after steady flow (Jiang 2002, Kapur 2004 .) Riddle also noted a positive association between both ERK and Ca2+ signaling and proliferation in human mesenchymal stromal cells after oscillatory flow (Riddle 2006.) However, these signals appeared to operate with some degree of independence—with Ca2+ release dependent on shear stress and ERK1/2 phosphorylation dependent on chemotransport (ibid.) In a later paper, Riddle attributed oscillatory flow-induced Ca2+ and ATP signaling almost entirely to chemotransport, rather than shear stress (Riddle 2008a.)

Having discussed the ways in which bone and bone-derived mesenchymal cells respond to mechanical stimuli, what role could mechanoresponsiveness play in antler regeneration? Though this is still a largely open question, there is circumstantial evidence mechanical forces indeed play some role in the antler.

First, though antler cortical bone consists mainly of primary osteons, secondary osteons can also be found (Launey 2010.) This indicates that some degree of remodeling may occur during the short, annual life span of the antler. While bone remodeling may be triggered by biochemical cues, mechanical forces are one of the central regulators of this process (Jacobs 2010.)

Second, osteocytes are found in antler bone (Rolf 1999.) In Aim 1 (see Chapter II) we also noted putative osteocytes in stained sections of antler bone. The presence of osteocytes in antler does not necessarily indicate that these cells serve the same mechanosensing function in this tissue as they do elsewhere. Without evidence of

normal physiologic function, it is at least conceivable that antler osteocytes are nonfunctional and are buried in antler bone as a result of a vacuum adaptation—i.e. simply the consequence of unimpaired terminal osteoblast differentiation. Still, we argue that it is more likely that the osteocytes in antler bone serve the same function they do in other bones.

Last, Li speculates that the transition from intramembranous to osteochondral ossification early in the regrowth stage is mediated by the pressure of the antler skin stretched over the tissue (Li 2000.) Similarly, based on anatomical descriptions of early antler regeneration, we have observed that new antler growth centers appear in places where one would expect high traction forces due to the re-epithelialization of the antler after casting (Price 2005.)

Consequently, in this aim we investigated the degree to which reserve mesenchyme-derived antlerogenic progenitor cells (APC) respond to mechanical stimuli. Based on Jacobs' contention that oscillatory fluid flow is the most physiologically relevant, we chose this flow modality as the means to mechanically load these cells. We will test the following hypothesis:

APC and MSC have different patterns of response when subjected to oscillatory fluid shear stress.

Materials and methods

Specimen acquisition

As described in Chapter II, APC and phalangeal-marrow-derived mesenchymal stromal cells were obtained from three wild, mature white-tailed bucks (*Odocoileus virginianus*.) Specimen acquisition took place on a University of Michigan-owned nature preserve and conformed to institutional animal care and use standards and state wildlife policies.

Cell freezing, thawing and initial culturing

As cellular antler tissue is only available on a seasonable basis, experiments were performed using previously frozen passage 1 cells.

To freeze, cells were washed twice in Ca2+ and Mg2+ free phosphate buffered saline and detached by incubating in 0.25% Trypsin-EDTA (Gibco, Life Technologies, Grand Island, NY) for 5 minutes at 37C. The trypsin was inactivated with twice the volume of complete medium: Dulbecco Modified Eagle Medium containing 110mg/L sodium pyruvate and 0.2mM L-glutamine, 10% characterized FBS, 100units/ml penicillin/100µg/ml streptomycin and supplemented with additional L-glutamine for a total of 0.4mM (Gibco).

Cells were pelleted by centrifuging at 500g for 6 min, resuspended at 500000 cells/ml in freezing medium (90% FBS, 10% DMSO) and aliquoted into Cryule cell freezing vials (Wheaton Science Products, Millville, NJ.) After 24 hours at -80C in a Mr Frosty cell freezing container filled with 250ml isopropyl alcohol to limit the rate of freezing to -1 degree C/min (Nalge Nunc International, Rochester, NY), cells were transferred to liquid nitrogen for long term storage.

Frozen cells were revived by placing in a 37C water bath. Immediately upon thawing, cell vials received a brief spin in a centrifuge to draw suspension away from the cap, after which 1ml complete medium was added to reduce the concentration of the DMSO in the now thawed freezing medium. Cells were transferred to a plastic T-25 tissue culture flask (Falcon, Becton Dickson Labware, Franklin Lakes, NJ.) Two vials of

500000 cells each were used for each T-25. Not including the complete medium added to each vial to dilute the DMSO, 4 additional milliliters of medium were added to the flask to bring the total volume to 7ml (2x1ml cells suspended in freezing medium, 2x1ml complete medium added to the vials, 3ml complete medium added after cells transferred to flask.) After 24hrs culture at 37C to foster cell adhesion, medium was aspirated and replaced with 5ml complete medium. This purpose of this step was to remove all DMSO from the medium as well as to flush nonadherent (mostly nonviable) cells from the culture.

Upon 90-95% confluence, cells were split 1:3 by trypsinization (as above), resuspended in 12ml complete medium, and plated in a T-75 flask (Becton Dickinson.)

Covalent modification of cell culture slides

Glass culture slides were silanized, a process in which organosilanes are covalently attached to a surface in a self-assembling monolayer (Cras 1999.) These silanes, in turn, allow molecules such as fibronectin, collagen, etc., to adsorb.

Silanization was carried out according to a protocol adapted by former Orthopaedic Research Laboratory student Michael Ominsky from the work of Werb (Werb 1989, Ominsky 2003.) In brief, 75x38x1mm glass microscope slides intended for cell adhesion and as slide covers (Fisher Scientific, Pittsburgh, PA), were first cleaned by immersion in 20% H_2SO_4 (15 minutes), tap water, 0.1N NaOH, distilled water, 100% ethanol and then dried in a 60-70C oven.

Next, slides intended for cell adhesion were exposed to 2% γ-aminopropyltriethoxysilane in dH20 (Sigma-Aldrich, St. Louis, MO) for 4 minutes and washed with dH20 and PBS. Slides were then incubated in 0.25% gluteraldehyde in PBS (Sigma) for 30 minutes at room temperature, washed in PBS and 100% ethanol and dried in a 60-70C oven.

Fibronectin coating of slides

Covalently modified slides were coated in fibronectin (5µg/cm^2) to promote cell adhesion. The following procedure was documented by former Orthopaedic Research Laboratory PhD student Michael Ominsky (Ominsky 2003).

Silicone chambers (Sylgard 184, Dow Corning, Midland, MI) were selected for adequate glass adhesion and autoclaved at 250C for 25 minutes. On the day of cell seeding, these chambers were transferred to a cell culture hood and placed on polycarbonate panels. These panels are subsequently used for transporting the finished chamber/slide assemblies to and from cell culture incubators.

Covalently modified slides were pressed onto the chambers to form a watertight seal, leaving an area of 12.3cm^2 open for cell culture. Each slide/chamber was then inverted to expose the open area and filled with 2ml of a sodium carbonate buffer with 31µg/ml bovine fibronectin (Sigma-Aldrich.) The composition of the buffer was as follows: 91 mM sodium bicarbonate (NaHCO3) and 9.1mM anhydrous sodium carbonate (Na2CO3) in dH20. The pH of the buffer was brought to 9.6 using sodium hydroxide, after which the buffer was sterile filtered and stored at 4C. To prevent the growth of microorganisms, the buffer was re-filtered every 3-4 months.

After the fibronectin-containing buffer was added to the cell adhesion slide, a slide cleaned as described above was used to cover the chamber/slide assembly. Following three hours of incubation at room temperature under a sterile hood, the fibronectin was aspirated and the slides were washed in pre-warmed PBS and complete medium.

Seeding of cells on slides

Cells were cultured in T-75 flasks preparatory to seeding on slides. At 90-95% confluence, cells were trypsinized, spun at 500g for 6min and resuspended in 10ml of complete medium. The cell count per milliliter of suspension was determined using an improved Neubauer hemacytometer. The average of both sets of grids was used to establish the count.

At this point, the complete medium used to rinse the chamber/slide assemblies was aspirated and a volume of suspension containing 250000 cells added to each (20300 cells/cm^2.) Chambers were then topped off to 2ml with complete medium.

Approximately 16 hours before fluid shear testing was to be conducted, the complete medium was exchanged for serum- free medium (SFM): phenol red-free low glucose DMEM, 100units/ml penicillin/100µg/ml streptomycin, and 4mM L-glutamine (Gibco.) Phenol red and fetal bovine serum can interfere with assays involving conditioned medium and were therefore omitted from the formulation.

Cells were transported to the cell culture hood adjacent to the fluid shear apparatus immediately after SFM was added (again, approximately 16 hours before fluid shear commenced.) The delay between this cell transfer and the conduction of OFF experiments allowed any potentially confounding effects induced from this movement to diminish before testing.

Oscillatory fluid shear apparatus

The fluid shear apparatus used here was adapted from the device originally developed for Michael Ominsky, in which the cell-seeded slides comprises one plate of a parallel plate flow chamber (Fig.1A) (Ominsky 2003). Fluid was delivered using a custom-built, programmable servomotor-powered syringe pump (linear actuator model SA-4-B.125-P-RBC4, Ultra Motion LLC, Cutchogue, NY) driven by a PC-based motion control application (Smart Motor Interface Version 1.314, Animatics) though a digital-analog converter (Fig.1B) (National Instruments, Austin, TX.) The Popper Perfketum glass syringes used in the pump had barrels and plungers precision ground to a slip fit that did not require elastomeric seals (Fig.1B) (Sigma-Aldrich.)

The shear stress provided was based on the principles of fixed parallel plate flow. Based on the assumptions of laminar flow and parabolic velocity profile, the governing equation is as follows:

$$\tau = 6\mu Q/bh^2$$

Where τ = shear stress, μ= fluid viscosity (equal to 0.00087 Pa-s for flow medium), Q= volume flow rate (cm^3/s), b= channel width (2.7cm) and h= channel height (0.0127cm.)

Two pascals of oscillatory fluid shear was generated using a Smart Motor Interface program adapted from a steady flow program written by Ominsky (Fig. 2.) Using a simple WHILE loop, this program delivered a 0.5Hz sawtooth waveform that gave rise to a 0.167ml/s flow rate in the flow chamber. As the goal was to isolate the effects of fluid shear rather than chemotransport, this program delivers zero net volume of medium to the chamber.

Validation was conducted using the actuator's linear potentiometer and a rudimentary Labview program (National Instruments) to ensure that the system was delivering the appropriate flow rate and cyclic rate. This testing revealed a motor amplitude error of approximately 10%, necessitating an over driven velocity constant (V) of 42591, rather than the theoretical 38332.

Though the fundamental mechanical hardware was unchanged compared to earlier uses of the system (Ominsky 2003, Pagedas 2010, Joiner 2010, Joiner 2012), some aspects were altered to suit the needs of our experiments. The system was mounted on a cart for portability and had numerous blind fasteners replaced with alignment pins and thumb screws to ease set-up and tear-down.

More importantly, the polycarbonate chambers and fixed seals used previously were replaced with machined stainless steel chambers and removable, high temperature-resistant O-rings. The O-rings were cast from two-part R-2374A/B silicone (Silpak Inc, Pomona, CA) in a custom-built mold. Casting was done under a -15inHg vacuum for one hour to remove bubbles. Unlike the earlier hardware, the steel chambers and silicone O-rings were autoclavable, and better able to be kept free of contamination. According to the manufacturer, R-2374 silicone has a service temperature of up to 204C (400F.)

Setting up the OFF system

Components that were too large (such as the fluid reservoir syringe holder) or otherwise unable to be autoclaved (fluid lines) were washed in soapy water, rinsed in dH20 and sprayed with 70% ethanol after each use. After drying overnight, these components were stored in a plastic bag to keep dust off of them. As described above, chambers, O-rings and chamber covers were autoclaved prior to use. By the way, if you're actually reading this, go ahead and give yourself a gold star for the day. The day before the system was to be run, the non-autoclavable components were resprayed with 70% ethanol, placed in the appropriate cell culture hood and exposed to the hood's UV light as a final cleaning measure.

The operation of the system was adapted from the Ominksy protocol. During each run, one chamber was exposed to fluid shear and a second chamber just assembled and connected to an unloaded syringe. This second chamber acted as a sham control. The sham simulated the conditions of the loaded chamber without exposing the cells inside to any loading beyond that caused by operator handling.

During system validation we experimented with the use of one or more loading syringes simultaneously. When more than one syringe was mounted to the manifold, the precision ground syringes required some looseness in the clamp affixing the plungers to the actuator. Due to the short stroke of the actuator during the desired loading modality, this "slop" would have reduced reproducibility between loaded specimens. If multiple plungers were instead clamped tightly to the actuator, we found that any small misalignments would be magnified across the clamp's width, raising the risk that the plungers would bind and crack the barrels.

Though it decreased experimental throughput, we reduced the tolerance stack by running one syringe, and therefore one loaded chamber, at a time. This allowed the loading syringe to be located in the center of the pump manifold.

On the day of shear loading, the apparatus was fully assembled in a cell culture hood. Uncoated, cell-free slides were mounted in the chambers. The system was filled with PBS plus 200units/ml penicillin, 200µg/ml streptomycin and 0.5µg/ml amphotericin B and run for 10-20 minutes. These initial "dummy" runs served two purposes. First,

they provided a chance to verify that the equipment was operating properly. Second, the 2X concentration of antibiotics and antimycotic acted as a final cleaning step should any microorganisms remain in the system.

Operating the OFF system

Loading was performed for 5, 15, and 60 minutes. Due to the lack of availability, cells from buck 2 were loaded for 15 and 60 minutes only.

After cleaning and set up (see above), the fluid shear system was flushed with serum free medium. Next, two cell-seeded slides were placed in the chambers. As described above, one chamber was connected to the syringe pump and the other to free standing sham syringe. The plunger of the sham syringe was fixed in place with a small clamp and a strip of tape.

During loading, the chambers, sham syringe and the rack holding the fluid reservoirs were placed in a 37C cell culture incubator (Fig. 1A) while the syringe pump remained outside the incubator (Fig.1B.) Note that the sham loading was the same duration as the actual loading.

Generating conditioned medium

Upon completion of loading, the chambers, sham syringe, reservoir rack, syringe pump manifold and fluid lines were returned to the cell culture hood. The slides were removed from the chambers and placed on a custom built ABS plastic holding block. Three milliliters of PBS was applied to the slides and aspirated to wash the cells. One milliliter of SFM was then pipetted onto the surface of the slides and kept in place via surface tension. The holding block was transferred to the incubator for 15 minutes to condition the SFM.

After incubation, the block was moved back to the hood. The now conditioned SFM was pipetted and cells scraped into the eppendorf tubes. The tubes were centrifuged at 1000-3000g for 5 min to pellet the cells and the supernatant (~750µl) aliquoted into two tubes. All tubes were then flash frozen I liquid nitrogen and kept in a -80C freezer.

During 15 minutes of medium conditioning, the OFF system was prepared for the next run. First, it was filled with PBS + antibiotic-antimycotic to flush out any remaining medium from the previous run. The PBS was aspirated and the system refilled and flushed with fresh SFM. The system was then filled a third time with SFM. After the cells and conditioned medium from the previous run were frozen, new cell-seeded slides were placed in the chamber and another round of OFF performed.

DNA quantification

The DNA content of each slide served as an estimate of cell number. A commercial kit (DNeasy Blood and Tissue Kit, Qiagen, Hilden, Germany) was used to extract DNA as per the manufacturer's instructions. In brief, cells were thawed, resuspended in 200µl PBS per tube, and exposed to 20µl proteinase K. A lysate was produced using the kit's buffers and pipetted onto spin columns placed in polypropylene microtubes. DNA that had adhered to the column was washed twice and dried by spinning at 20000g for 3 min. Last, the DNA was eluted in 200µl of buffer.

Freshly extracted DNA was quantified on a spectrophotometer (NanoDrop 2000, Thermo Fisher Scientific, Waltham, MA.) One microliter of the elution buffer was used to calibrate the device, after which DNA content was measured in each specimen. The purity of each DNA sample was assessed via A260/280 ratio (peak nucleic acid absorbance at 260nm divided by that for proteins at 280nm.)

Nitric oxide assay

The nitric oxide concentration in conditioned medium samples was measured using a commercial fluorometric assay kit (Cayman Chemical Company, Ann Arbor, MI.) NO has a 4 second half life and is rapidly oxidized into nitrite (NO_2^-) and nitrate (NO_3^-). This kit uses a reductase to enzymatically convert nitrate to nitrite. The resulting total nitrite content, in turn, converts DAN (2,3-diaminonaphtalene) to 1(H)-napthotriazole.

A total nitrate/nitrite standard curve was generated using the provided standard as well as a volume of non-conditioned SFM equivalent to the volume of conditioned medium used in the specimens. Standards and samples were aliquoted in duplicate

wells. After adding NaOH, the fluorescent intensity in each well was detected (363nm excitation, 430nm emission) using a spectrophotometer (SpectraMax M5, Molecular Devices, Sunnyvale, CA.) Results were normalized to the DNA content of each specimen.

Prostaglandin E2 ELISA

A commercially available competitive-binding ELISA kit (Amersham Biotrak, GE Healthcare Life Sciences, Pittsburgh, PA) was used to detect PGE_2 in conditioned medium specimens, as in previous studies (Bakker 2001, Donahue 2003, Saunders 2003, Genetos 2005.) The assay was performed as per the manufacturer's instructions, with a standard curve generated using from provided standard as well as blank and non-specific binding wells. Standards and samples were aliquoted in duplicate wells and the optical absorbances of each well read at 450nm (SpectraMex M5, Molecular Devices.) Non-conditioned SFM results were subtracted from the sample values, which were then normalized by the DNA content of each well.

Statistics

As each experiment involved a small sample size (2-3 biological replicates), multiple experimental replicates were performed for each assay (3-6 per cell type per time point.) Generalized linear mixed models, which take into account nested data structures and repeated measures, were used for comparisons (SPSS, IBM Corp, Armonk, NY.) Sequential Bonferroni post hoc tests were used, with a p-value ≤ 0.05 considered significant.

In sham-normalized data for combined animals, "celltype" was used as a fixed effect; no random effect was considered. For combined animal data that included both load and sham conditions, a "celltype*load" interaction term was included as a fixed effect. Figures show least squared means (LSM) and model-generated standard deviations.

Statistics were also conducted for results within each animal separately. For sham-normalized data, paired t-tests were performed for data at each time point while

data that included both load and sham conditions were compared using one-way analysis of variance and Dunnett's T3 *post hoc* test.

For all results, values more than two standard deviations from the mean were omitted.

Results

DNA

The DNA content of each load and sham slide was quantified to estimate of relative cell number. A260/280 ratios for each specimen exceeded 2.0, indicating high quality DNA extraction.

DNA content generally did not vary significantly regardless of whether load was applied (Fig.3.) In combined data, loaded cells typically had less DNA, though this was only significant for MSC sham slides at the 5min time point (Fig.3A.) MSC from bucks 1 and 3 displayed similar behavior (buck 2 cells were not available for that time point), however the difference was not significant (Fig.3B-D.) Shear stresses are capable of removing some quantity of cells, though it is unclear if APC and MSC differ in their susceptibility to detachment.

Comparing sham-normalized load DNA content in combined-animal data revealed differences in APC and MSC depending on the duration of loading (Fig.4A.) After 5 min of load, APC retained significantly more DNA than MSC ($p=0.002$), yet the opposite was true after 60 min ($p=0.032$.) In cells from individual animals similar, though not statistically significant, differences were observed for buck 1 and 3 at these time points (Fig.4B, D.) Large variabilities in the individual animal data precluded generalizations about DNA content at the 15 min time point.

When the DNA content of sham slides was divided by the days elapsed between seeding on fibronectin coated slides and testing, an unexpected result appeared (Fig.5.) In both combined and individual animal data, APC had greater than or equal DNA accumulation per day compared to MSC. These data contrast markedly with our earlier cell enumeration of time results (see Chapter II), for which cells had been seeded on

cell culture plastic. Note that both cell types did not appear to be subject to widespread cell detachment.

Nitric oxide

Nitric oxide content of conditioned medium was quantified as a measure of cell mechanoresponsiveness (Fig. 6.) Due to a defect in the spectrophotometer's fluorescent detection function, only relative (load/sham) values were able to be obtained for NO content.

No nitric oxide was detected in cells from all bucks after 60 min of loading and in cells from buck 2 at 15 min (buck 2 cells were not loaded for 5 min.) Significantly greater sham normalized NO was observed in MSC medium at 15 minutes (Fig.6A.) However, the lack of consistency in the individual animal data at this time point makes it difficult to determine whether this significance represents a true cell-based difference or is an artifact of the assumptions of the generalized linear mixed model.

Prostaglandin E_2

Prostaglandin E_2 content in conditioned medium was used as another measure of mechanoresponsiveness (Fig.7-9.)

First, we compared the PGE_2 in APC and MSC load and sham groups (Fig.7.) This served as a "reality check" to verify the extent to which oscillatory fluid shear affected PGE_2 levels in each cell type. In short, loading had few consistent effects on PGE_2. In combined animal data (Fig.7A), greater PGE_2 was observed in loaded versus sham APC after 5 and 15 minutes of load, though only the former difference was significant ($p=0.003$.) The only significant difference in load versus sham combined animal MSC data occurred at the 15 time point, in which conditioned medium from sham cells actually had a greater PGE_2 content. Individual animal data (Fig.7B-C) largely reflected the significant differences seen in the combined data. Large variation was seen in buck 2 MSC at the 15 time point (Fig. 7C), which contributed to the some ambiguity in the combined data.

When comparisons were made between sham-normalized PGE_2 (the relative magnitude of the load effect), few clear trends emerged (Fig.8.) Though combined-animal APC (Fig.8A) displayed a significantly greater normalized prostaglandin after 5 min of loading ($p=0.001$), this trend was seemingly reversed in the individual animal data (Fig.8A, C.) This inconsistency was due to large variations in MSC PGE_2 at the individual animal level, which themselves were consequences of a single widely dispersed value in each data set (though still within two standard deviations of the mean.) Thus, it is difficult to make definitive statements about relative APC and MSC PGE_2 production due to load.

On the other hand, it was clear that the basal levels of prostaglandin were much higher in APC compared to MSC (Fig.9.) For illustration and statistical purposes, sham PGE_2 levels were expressed as $pgPGE_2/pgDNA$ (rather than $pgPGE_2/ngDNA$) and log transformed. At every time point in both combined and individual animal data, APC exhibited significantly higher PGE_2 levels. The difference in combined data was $10^{0.96}$ at for 15 minute shams, equal to a 9X fold change. The largest was 18X at 5 min. In the individual animal data, the smallest APC-MSC fold change difference was for buck 1 15 min sham (4.9X) and the largest for buck 3 60 min shams (313X.)

Discussion

Mechanical forces are known to play a central role in literally shaping the musculoskeletal system. During ambulation, bending and compressive loads are transduced to cyclical alterations in fluid flow in the marrow space and lacunar-canalicular system (Forwood 1996, Qin 2003.) It is therefore thought that oscillatory fluid flow represents a physiologically relevant mechanical stimulus *in vitro* (Jacobs 1998.)

Little is known about the role, if any, that mechanical forces play in the formation of deer antler. Circumstantial evidence, such as the presence of osteocytes and some secondary osteons in antler bone, led us to pursue this question on a cellular level (Rolf 1999, Launey 2010). Using an oscillatory fluid flow (OFF) regime, we explored the

effects of 2Pa of shear stress on thawed first passage APC and MSC after 5, 15, and 60 minutes of load.

Looking at nitric oxide and prostaglandin E_2, we failed to discern an overall effect of OFF on either APC or MSC. While NO is clearly produced by these cells, high within-animal and across-animal variability complicated the elucidation of repeatable patterns of this factor's secretion by APC or MSC.

We did not detect NO in any animal after 60 min of load, and in buck 2 after 15 min as well. It is possible that bone or antler cells respond to load with fast acting constitutive nitric oxide synthase (eNOS) rather than the inducible form of this enzyme. Or, it is possible that iNOS is expressed quickly and transiently in response to load. In either case, it is certainly conceivable that the earliest time point examined in this study, 5 min, was simply too late to catch any spikes in NO secretion. Future explorations of NO in deer APC or MSC would benefit from even earlier time points (1-3 min) or the use of a fluorometric nitric oxide probe to monitor secretion in real time. The latter would require substantial re-engineering of our fluid shear apparatus.

It seems that, contrary to our assumption that PGE_2 is a longer term marker of mechanoresponsiveness, the only significant load-induced increase in this factor was seen in APC after five minutes, the shortest OFF duration. At this same time point, the magnitude of APC sham-normalized PGE_2 was also greater than in MSC. Though these data would benefit from additional confirmation, they at least suggest that APC are capable of a more robust PGE_2 response to short duration loads. As the highest intensity loading of antler likely is due to clashes among males during the rutting season, it may be that this tissue has adapted to respond to short-lived impact forces.

Though they were not part of the original intention of this study, our work revealed two intriguing results regarding the basal (unloaded) APC phenotype. First, APC cultured on fibronectin-coated sham slides showed similar and often greater DNA accumulation over the time compared to MSC under the same conditions. Second, unloaded APC demonstrated significantly greater PGE_2 secretion (both in the denotative and statistical sense) at all time points in all animals.

DNA content served as a proxy for cell number. The similar and frequently higher rate of DNA accumulation in APC contrasts versus MSC sharply to our earlier *in vitro* work (Chapter II.) There, we used a fluorescent DNA marker to estimate the relative numbers of APC and MSC. We found significantly lower APC cell number at each 24 hour interval over 7 days, as well as a decline and recovery of APC number that occurred over the first 5 days in culture (see Chapter II, Fig.1B.)

Three potential explanations for these differences are 1) the use of frozen and thawed cells in the current study, 2) different initial seeding densities, and 3) altered cell response to the culture substrate.

Addressing the first, it is theoretically possible that freezing selects for a more robust cell population. However, prior work has shown that freezing of human bone marrow mononuclear cells has little effect on the expression of cell surface markers or on indicators of osteogenic differentiation such as alkaline phosphatase (Haack-Sorensen 2007, Ginis 2012.) The cited studies showed somewhat different effects of freezing on cell proliferation, with Haack-Sorensen finding a slight enhancement and Ginis noting no difference when compared to unfrozen cells. However, the most pronounced increases in cell proliferation in the former study were found in cells frozen for short periods of time (one month) and cultured beyond 7 days. Still, we cannot rule out the possibility that freezing and thawing may induce changes to the cell population that benefit APC proliferation to a greater extent than MSC, even over the 2-3 days of culture from seeding to sham loading.

Regarding the role that initial plating densities may play in affecting APC and MSC number over time, recall that in our *in vitro* cell enumeration study we seeded cells at 3200 cells/cm^2. In the current study, seeding densities were approximately 6 times higher: 20300 cells/cm^2. It is possible that APC and MSC differ in their response to seeding densities, and that the lower density used was insufficient for APC to mount robust proliferation. Though plausible, the explanation is at variance with the notion that lower seeding densities actually promote bone MSC growth due to the reduction of the likelihood of contact inhibition, increased log growth phase duration and greater nutrient availability per cell (Fossett 2012.) An alternative explanation is that APC plated at the

higher density are in fact more resistant to contact inhibition compared to MSC. If true, resistance to contact inhibition in antler cells would represent a diametrically opposed adaptation compared to the naked mole rat (*Heterocephalus glaber*), whose cells possess a hypersensivity to contact inhibition that is thought to contribute to this rodent's singular tumor resistance (Seluanov 2009.)

The most likely explanation for the differences in relative cell number compared to our earlier *in vitro* work points to the substrate on which the cells were cultured. In the latter study, cells were plated onto standard cell culture plastic: plasma-treated, polystyrene BD Falcon 96 well plates. In the current work, recall that cells were seeded onto silanized glass slides coated with 5μg/cm^2 bovine fibronectin.

The adherence of MSC onto cell culture plastic has been a defining feature of these cells since the days of Friedenstein and is now considered a key phenotypic marker (Colter 2000, Dominici 2006.) MSC are known to possess a variety of adhesion molecules. Human bone marrow MSC cultured on plastic, for example, express a suite of α and β integrins (α1-3,5,6, 11, V, X and β1-2, 4-5 and 7-8) as well as several other adhesion molecules (ICAM-1, E-, P-, L- selectins, E- and VE-cadherins, etc.) (Brooke 2008.) On the other hand, cell culture plastic is less representative of the *in vivo* milieu compared to actual extracellular matrix (ECM) proteins.

The composition of the ECM has wide ranging effects on cell growth and differentiation (Sottile 2000.) Fibronectin is a cell adhesive glycoprotein that, like molecules collagen and laminin, is a fibrillar constituent of many ECM (Singh 2012.) Binding to integrins α5β1, α4β1, and αvβ3 and proteoglycans such as syndecans, fibronectin can give rise to a host of cell behaviors including cell growth (Sottile 2000.) In light of this, there are several explanations for our observations that APC grow as or more rapidly as MSC on fibronectin-coated glass slides compared to cell culture plastic. First, compared to MSC, APC may express a suite of adhesion molecules more specific to fibronectin. Or, perhaps APC present a larger proportion of fibronectin-specific molecules. Still another possibility is that APC possess a more robust downstream response to fibronectin binding. No matter the mechanism, it appears that APC cell

enumeration over time has a milieu dependence distinct from animal-matched marrow stromal cells.

The second key unexpected result from the current study was the robust secretion of PGE_2 in non-loaded APC compared to MSC. It is possible that the minor handling sham cells do incur could contribute to some degree of PGE_2 production. However, we believe that our results under these conditions were qualitatively indicative of basal prostaglandin secretion levels. Therefore, it is reasonable to propose that APC, at least thawed APC cultured on fibronectin-coated glass slides, have constitutively greater PGE_2 production relative to MSC.

If this observation is valid for APC *in vivo*, it has several intriguing implications. The first is a possible mechanism for our observation that APC are resistant to adipogenic differentiation (see Chapter II.) There is evidence that PGE_2 can directly suppress PPARγ2 expression in an autocrine fashion in fibroblasts, and thus serve as an antagonist of adipogenesis (Inazumi 2012.)

The second implication involves the effects of PGE_2 on the immune response. Once widely thought to be immunosuppressant, PGE_2 is more accurately immunomodulatory: it alters immune cell proliferation and function in a manner that shifts the response from the phagocytic type 1 to the anti-inflammatory, more antibody-dependent type 2 (Harris 2002.) Prostaglandin E_2 is one of the factors secreted by MSC that contribute to the immunomodulatory nature of these cells (Aggarwal 2004.) Interestingly, speculation exists that the absence of scar tissue or bacterial infection after antler casting is due to antler being immunodeficient in some way (Price 2004.) In other words, it is thought that the suppression of a stereotypical inflammatory response at the site of antler casting may contribute to the formation of a blastema instead of fibrotic scar (ibid.) Robust constitutive production of PGE_2 by APC, if the case *in vivo*, would offer a mechanism for an altered immune response at the site of antler casting.

A third ramification of high constitutive PGE_2 production in APC relates to the well-characterized relationship between this factor and bone. Depending on the concentration, PGE_2 has both anabolic and catabolic effects on bone (Scutt 1995). The anabolic effects of PGE_2 may be mediated though bone MSC rather than directly

though osteoblasts and are associated *in vitro* with a transient increase in bMSC cell number and collagen production (ibid.) It is therefore possible that PGE_2 is can stimulate high (though most likely milieu dependent) APC proliferation.

An additional well-studied aspect of PGE_2 in bone is its ability to oppose the catabolic effects of high doses of glucocorticoids such as dexamethasone (Scutt 1996.) Recall from Chapter I that the calcium demands of rapid antler growth cannot be met entirely through the animal's diet and are supplemented by transient bone resorption elsewhere in the body (Landete-Castillejos 2007.) Also note the coincidence between peak circulating IGF-1 levels and rapid antler growth (Price 2004.) Though the relationship between growth factors and stress hormones is complicated, often seemingly contradictory and species specific, it has been demonstrated that IGF-1 stimulates ACTH-induced cortisol in bovine adrenal glands (Le Roy 2000.) In fact, peak serum cortisol levels in some species coincide with antler growth, during a period of reversible skeletal bone resorption (Ingram 1999.) Therefore, we argue that high constitutive PGE_2 production in the antler, again if the case *in vivo*, might provide a local osteoprotective counterbalance to systemic resorptive signals.

In this study, we have provided evidence that APC and MSC have different patterns of response to oscillatory fluid flow. In particular, that APC exhibit heightened PGE_2 production after short duration fluid shear compared to MSC. However, we were not able to construct a more generalizable statement about APC and MSC mechanoresponsiveness. Fortunately, unanticipated findings in terms of APC cell number over time and sham PGE_2 levels have raised intriguing questions regarding the unique manner in which these cells interact with their microenvironment.

Chapter IV figures

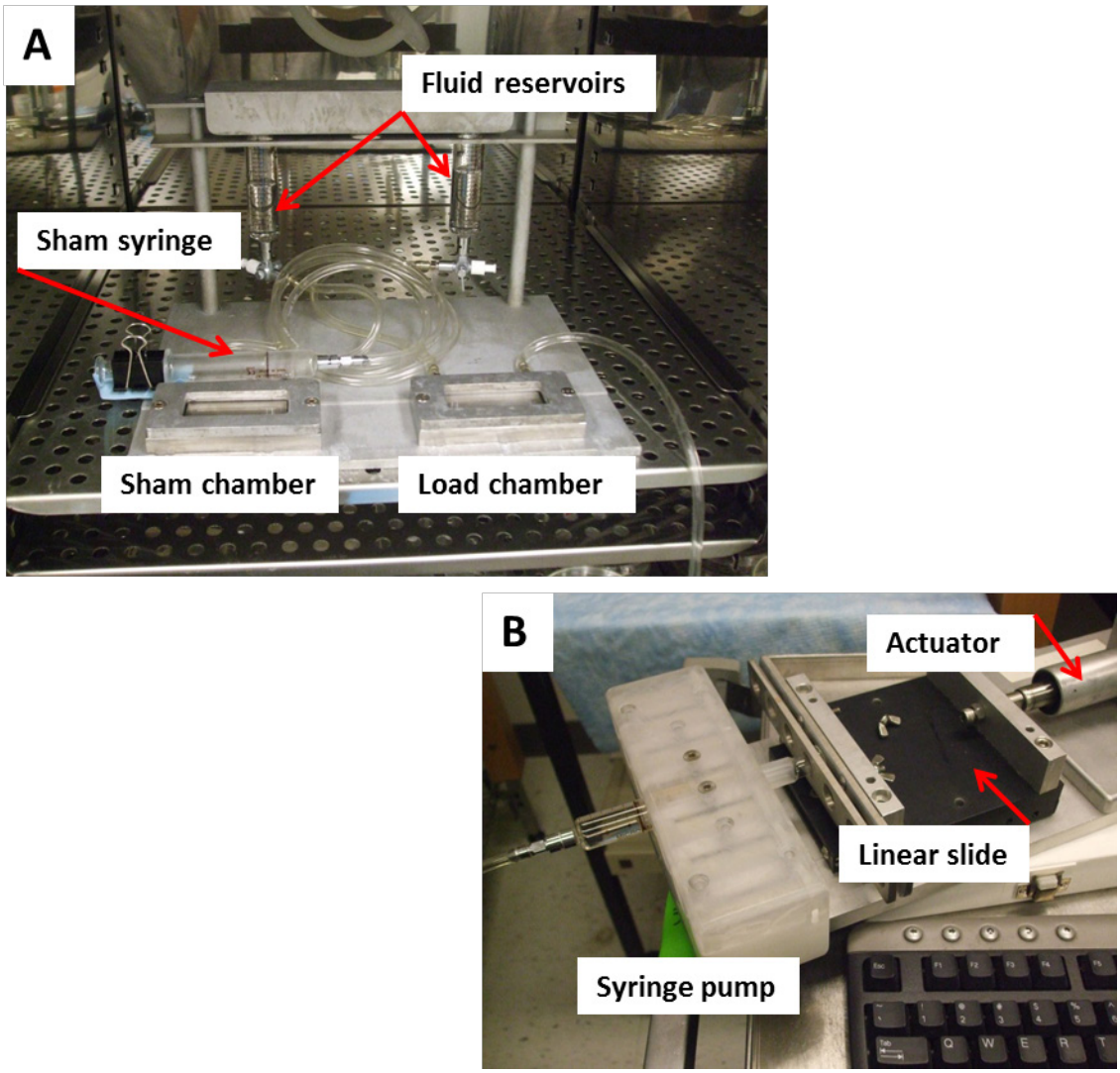

FIG. 4.1: Apparatus used to generate fluid flow. (A) Fluid reservoirs and chambers (sham and load.) Shown inside cell culture incubator. (B) Actuator, linear slide and syringe pump. This equipment was kept outside incubator during experiment.

```
'this program will give 2 Pa shear @ 0.5 Hz

PID1
KP=50
KI=28
KD=100
KL=200
KS=1
KV=300
KA=0
KG=0
O=0             ' reset motor at current position
'v=38332        ' velocity constant = 32212*(1.19rev/s) for 2 Pa shear
v=42591         'velocity constant for 2Pa times 110% to compensate for  motor amplitude error at
0.5 Hz
'v=256000       'high speed velocity for calibration
A=96            ' acceleration to 1.19rev/s in 0.1sec
z=0             ' cycle # = 0
q=1188          'position constant = (1.19rev/s)*1sec*1000 encoder codes/sec--this gives 0.5Hz
cycles
'q=64000        'position constant = 1 inch for calibration

WHILE z<2400          ' for 10 HOURS
P=q
V=v
MP
G               ' GO
TWAIT           ' Waits for motor to fully stop
F               'lets PID filter update, helps prevent slight loss of position errors

P=-q
V=-v
MP
G               ' GO
TWAIT           ' Waits for motor to fully stop
F               'lets PID filter update, helps prevent slight loss of position errors
z=z+1
LOOP
END
```

FIG. 4.2: Simple code used to generate 2Pa shear stress using a saw tooth waveform at 0.5Hz. Adapted from steady flow program originally written by Michael Ominsky.

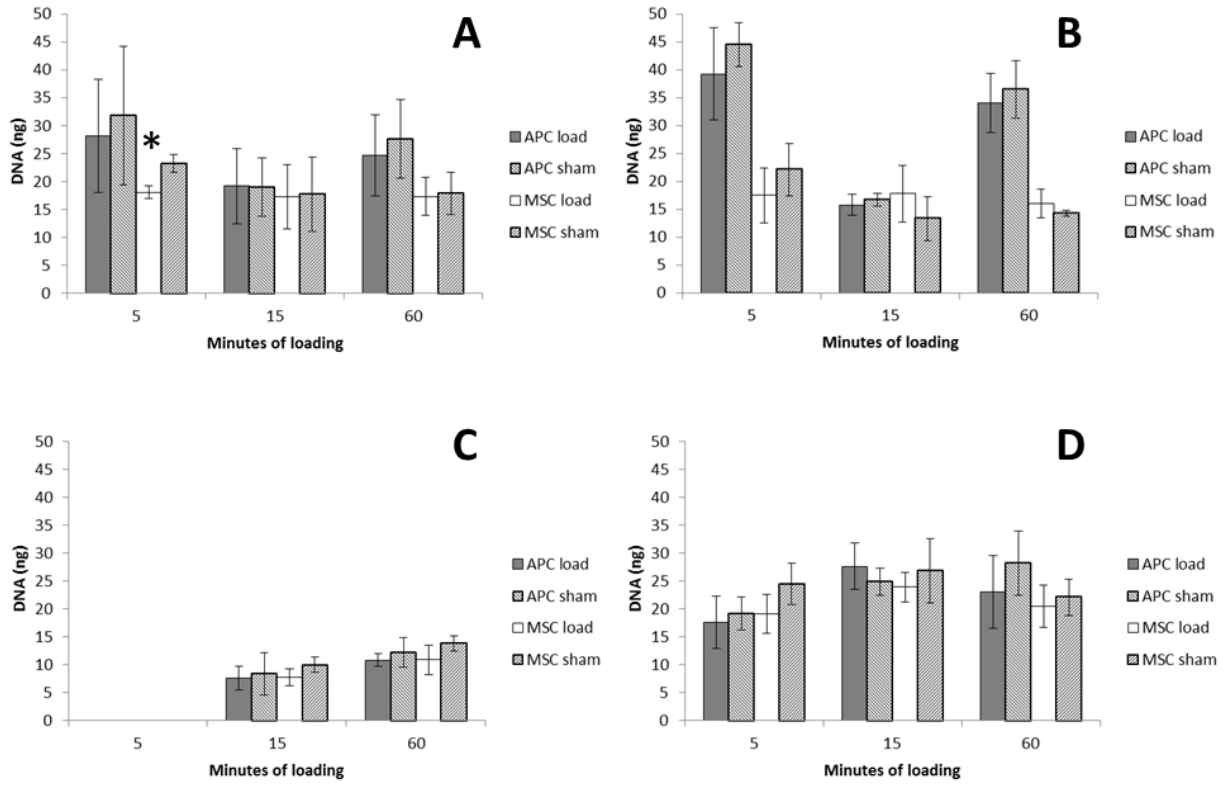

FIG. 4.3: Effects of loading on DNA. (A) Data from animals combined (n=2 for 5 min timepoint, n=3 for others.) Generalized linear mixed model. Least squared means and estimated std devs. (B), (C), (D) Bucks 1, 2 and 3. One way ANOVA, Dunnett's T3 post-hoc test. * Significant relative to sham.

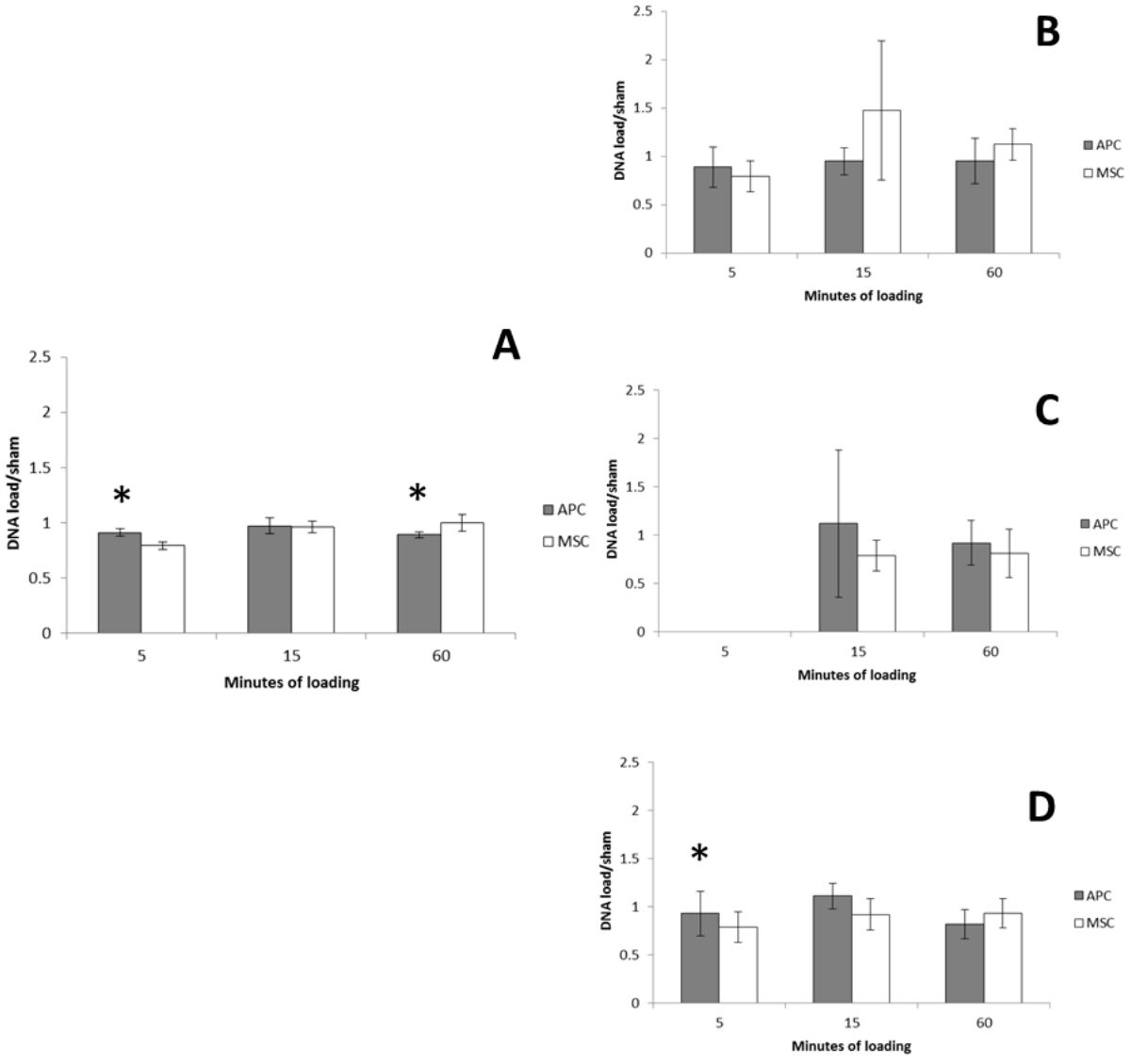

FIG. 4.4: Load DNA normalized by sham. (A) Data from animals combined (n=2 for 5 min time point, n=3 for others.) Generalized linear mixed model. Least squared means and estimated std devs. (B), (C), (D) Bucks 1, 2 and 3. Paired t-tests at each time point. * Significant relative to MSC.

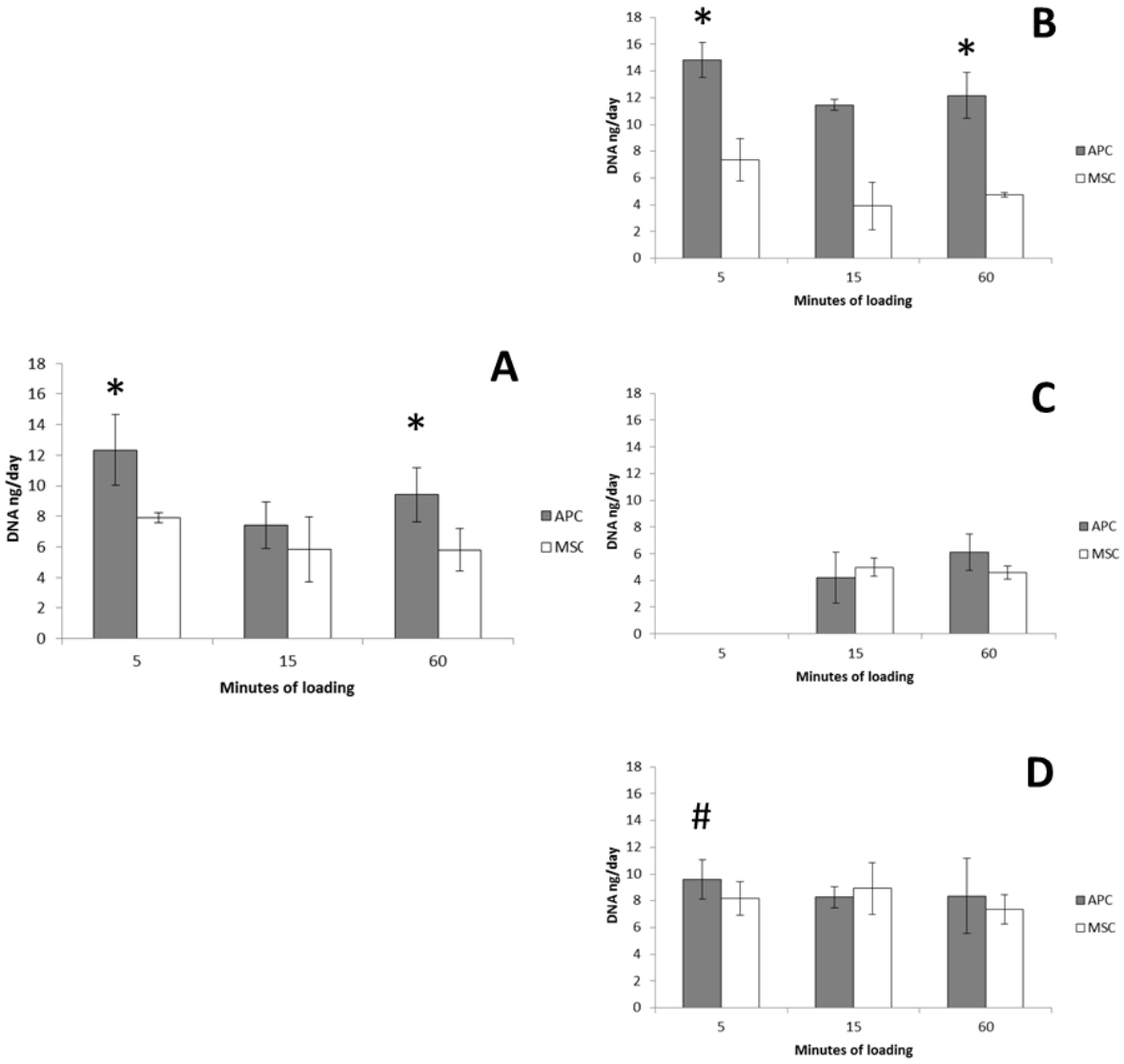

FIG. 4.5: Rate of DNA accumulation of in sham-loaded cells (ng/day). Measured from time of cell seeding to completion of sham loading. (A) Data from animals combined (n=2 for 5 min time point, n=3 for others.) Generalized linear mixed model. Least squared means and estimated std devs. (B), (C), (D) Bucks 1, 2 and 3. Paired t-tests at each time point. * Significant relative to MSC. # p<0.1 relative to MSC.

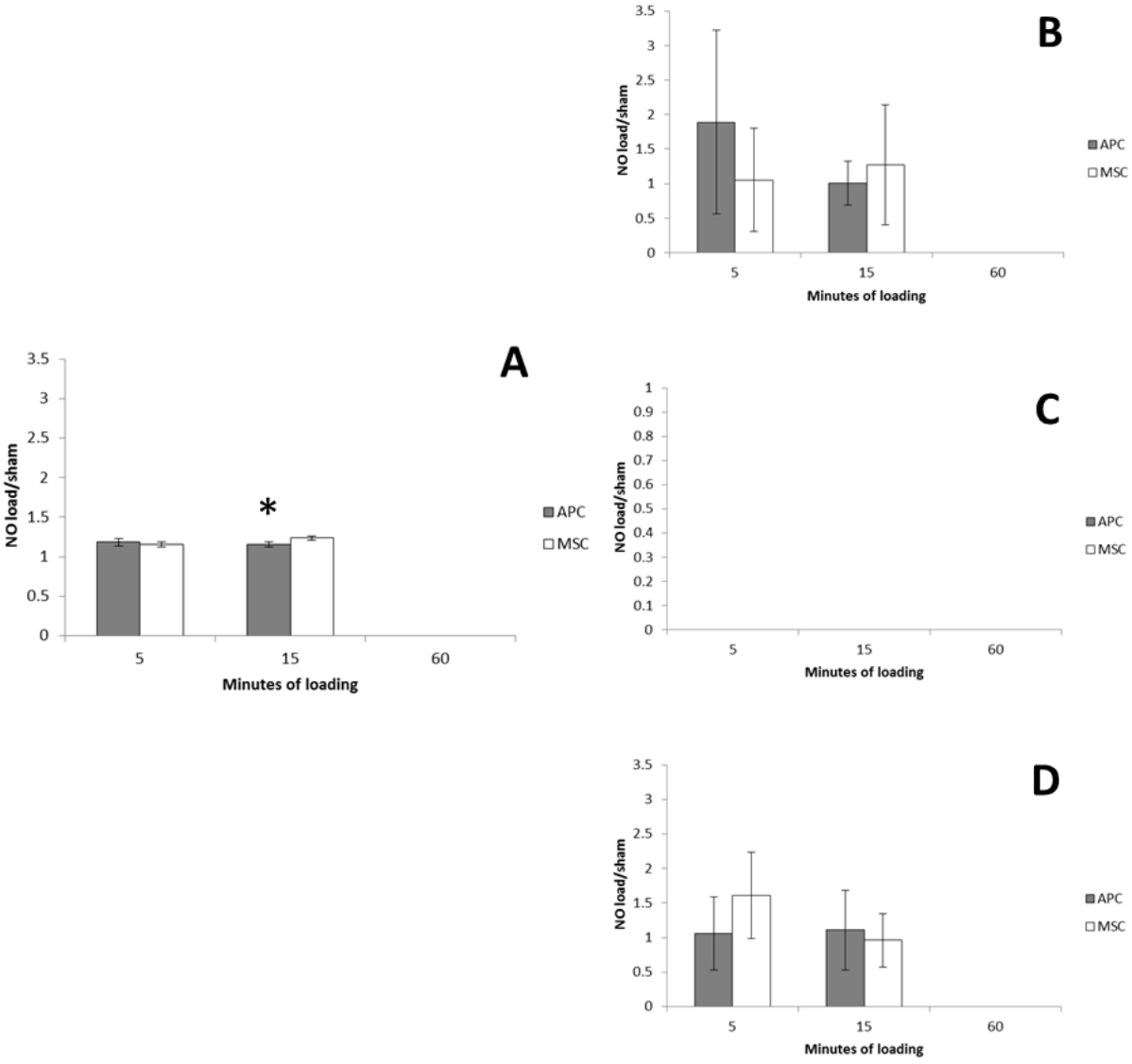

FIG. 4.6: Nitric oxide, load normalized by sham. (A) Data from animals combined (n=2 for all time points due to lack of detectability in buck 2 cells.) Generalized linear mixed model. Least squared means and estimated std devs. (B), (C), (D) Bucks 1, 2 (15 and 60 min only) and 3. Paired t-tests at each time point. No detectable NO at 60 min in cells from all bucks, none for NO at 15 min. * Significant relative to MSC.

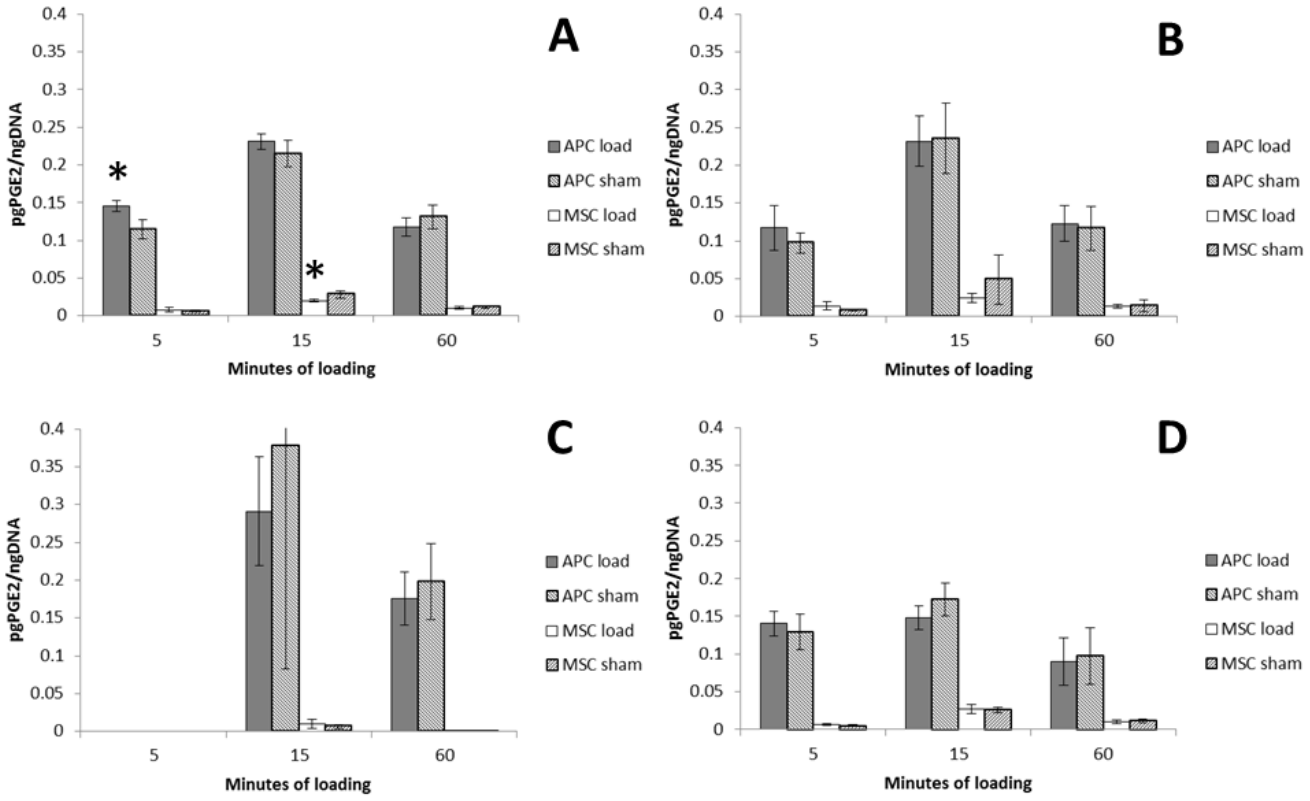

FIG. 4.7: Effects of load on PGE2, load and sham. (A) Data from animals combined (n=2 for 5 min time point, n=3 for 15 and 60 min.) Generalized linear mixed model. Least squared means and estimated std devs. (B), (C), (D) Bucks 1, 2 and 3. One way ANOVA, Dunnett's T3 post-hoc test. * Significant relative to sham.

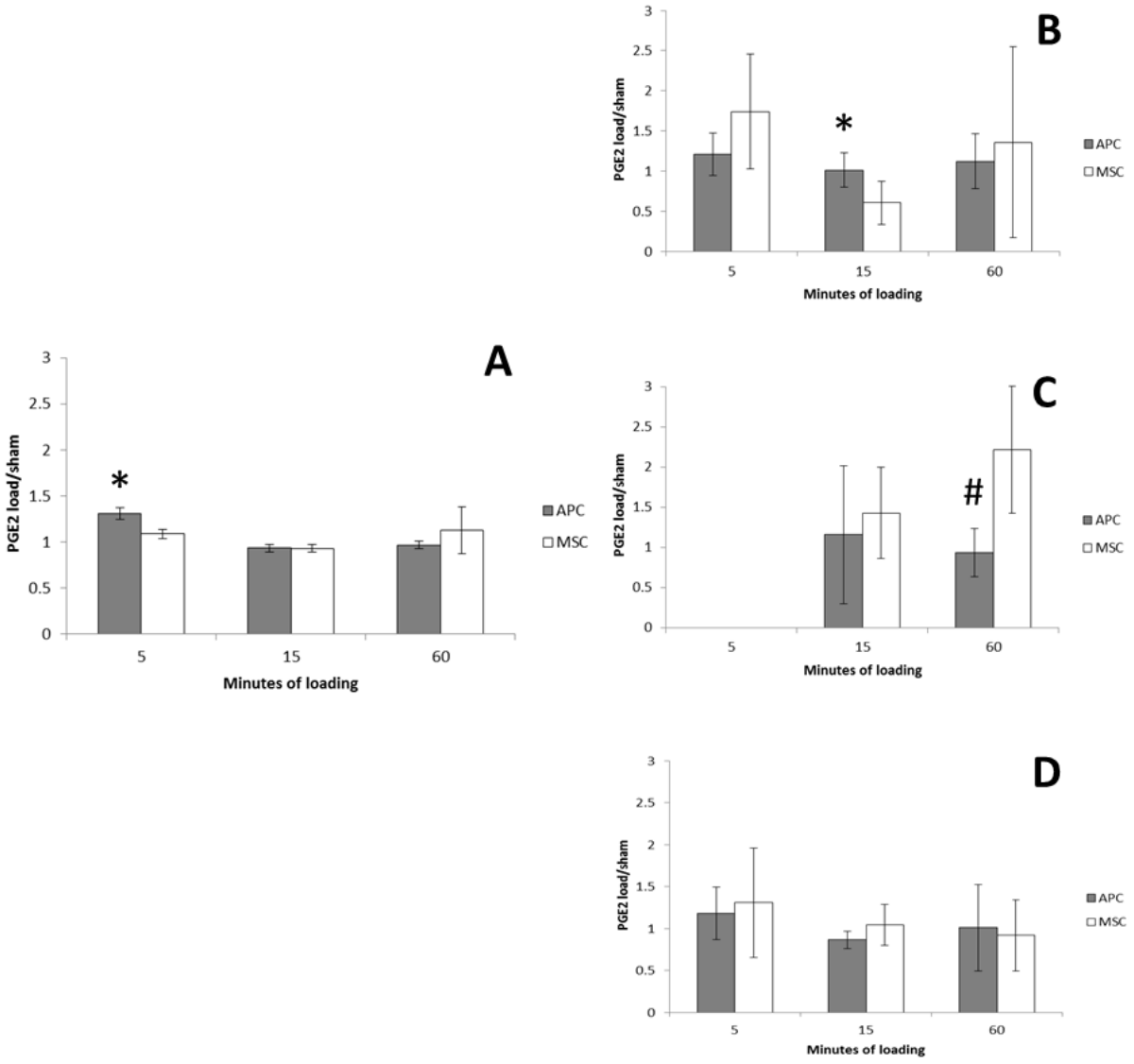

FIG. 4.8: PGE2 load normalized by sham. (A) Data from animals combined (n=2 for 5 min time point, n=3 for 15 and 60 min.) Generalized linear mixed model. Least squared means and estimated std devs. (B), (C), (D) Bucks 1, 2 and 3. Paired t-tests at each time point. * Significant relative to MSC. # p<0.1 relative to MSC.

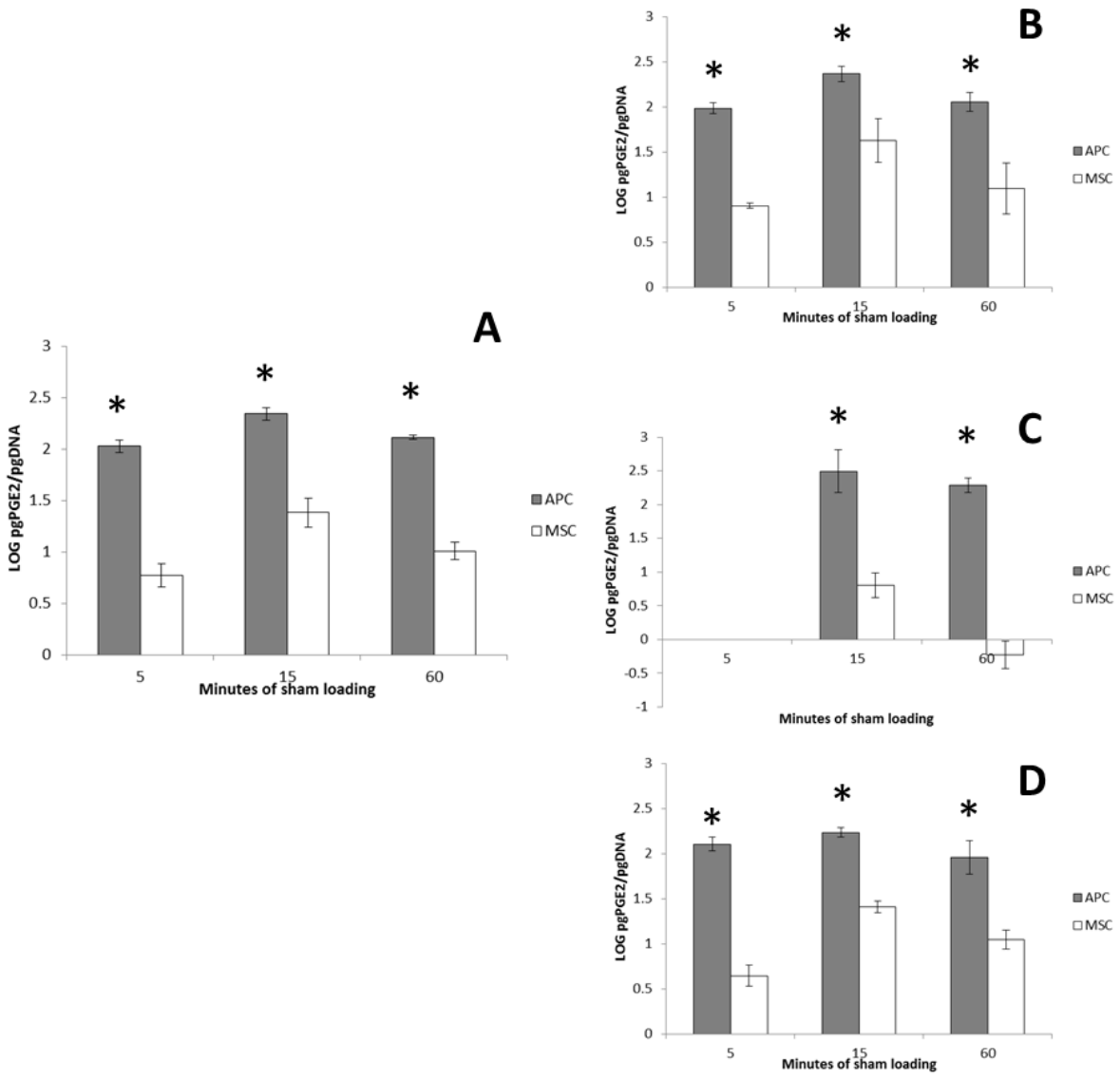

FIG. 4.9: Comparison of basal PGE2 levels in MSC and APC using sham data (log pgPGE2/pgDNA.) (A) Data from animals combined (n=2 for 5 min time point, n=3 for 15 and 60 min.) Generalized linear mixed model. Least squared means and estimated std devs. (B), (C), (D) Bucks 1, 2 and 3. Paired t-tests at each time point. * Significant relative to MSC.

Bibliography

Aggarwal S, Pittenger MF. Human mesenchymal stem cells modulate allogeneic immune cell responses. Transplantation 2005;105(4):1815-1822.

Bakker AD, Soejima K, Klein-Nulend J, Burger EH. The production of nitric oxide and prostaglandin E_2 by primary bone cells is shear dependent. Jour Biomech 2001;34:671-677.

Brooke G, Tong H, Levesque JP, Atkinson K. Molecular trafficking mechanisms of multipotent mesenchymal stem cells derived from human bone marrow and placenta. Stem Cells Dev 2008;17:929-940.

Colter DC,Class R, DiGirolamo CM, Prockop DJ. Rapid expansion of recycling stem cells in cultures of plastic-adherent cells from human bone marrow. PNAS 2000;97(7): 3213-3218.

Cras JJ, Rowe-Taitt CA, Nivens DA, Ligler FS. Comparison of chemical cleaning methods of glass in preparation for silanization. Biomesensors Bioelectronics 1999;14:683-688.

Dominici M, Le Blanc K, Mueller I, Slaper-Cortenbach I, Marini F, Krause D, Deans R, Keating A, Prockop DJ, Horwitz E. Minimal criteria for defining multipotent mesenchymal stromal cells. The International Society for Cellular Therapy position statement. Cytotherapy 2006;8(4):315-317.

Forwood MR. Inducible cyclo-oxygenase (COX-2) mediates the induction of bone formation by mechanical loading *in vivo*. Jour Bone Min Res 1996;11(11):1688-1693.

Fossett E, Khan WS. Optimising human mesenchymal stem cell numbers for clinical application: a literature review. Stem Cell Int 2012;2012:article ID465259.

Genetos DC, Geist DJ, Liu D, Donahue HJ, Duncan RL. Fluid shear-induced ATP secretion mediates prostaglandin release in MC3T3-E1 osteoblasts. Jour Bone Min Res 2005;20(1):41-49.

Ginis I, Grinblat B, Shirvan MH. Evaluation of bone marrow-derived mesenchymal stem cells after cryopreservation and hypothermic storage in clinically safe medium. Tissue Eng Part C Methods. 2012 Jun;18(6):453-63.

Haack-Sorensen M, Bindslev L, Mortensen S, Friis T, Kastrup J. The influence of freezing and storage on the characteristics and functions of human mesenchymal stromal cells isolated for clinical use. Cytotherapy. 2007;9(4):328-37.

Harris SG, Padilla J, Koumas L, Ray D, Phipps R. Prostaglandins as modulators of immunity. Trends Immuno 2002;23(3):144-150.

Haut Donahue TL, Haut TR, Yellowley CE, Donahue HJ, Jacobs CR. Mechanosensitivity of bone cells may be modulated by chemotransport. Jour Biomech 2003;36:1363-1371.

Inazumi T, Shirata N, Morimoto K, Takano H, Segi-Nishida E, Sugimoto Y. Prostaglandin E2-EP4 signaling suppresses adipocyte differentiation in mouse embryonic fibroblasts via an autocrine mechanism. Jour Lipid Res 2012;52:1500-1508.

Ingram JR, Crockford JN, Matthews LR. Ultradian, circadian and seasonal rhythms in cortisol secretion and adrenal responsiveness to ACTH and yarding in unrestrained red deer (Cervus elaphus) stags. Endochrin 1999;162:289-230.

Jacobs CR, Yellowley CE, Davis BR, Zhou Z, Cimbala JM, Donahue HJ. Differential effect of steady versus oscillating flow on bone cells. J Biomechanics 1998; 31:969-976.

Jacobs CR, Temiyasathit S, Castillo AB. Osteocyte mechanobiology and pericellular mechanics. Ann Rev Biomed Engin 2010;12:369-400.

Joiner DJ. 2010. The Effect of Age on Bone and its Response to Mechanical Stimulation. Doctoral dissertation. University of Michigan, Ann Arbor, MI. http://hdl.handle.net/2027.42/75822

Jiang GL, White CR, Stevens HY, Frangos JA. Temporal gradients in shear stimulate osteoblastic proliferation via ERK1/2 and retinoblastoma protein. Am Jour Physio Endocrinol Metab 2002;283:E383-E389.

Joiner DM, Tayim RJ, Kadado A, Goldstein SA. Bone marrow stromal cells from aged male rats have delayed mineralization and reduced response to mechanical stimulation through nitric oxide and ERK1/2 signaling during osteogenic differentiation. Biogerontology 2012;13(5):467-478.

Kapur S, Chen ST, Baylink DJ, Lau William KH. Extracellular signal-regulated kinase-1 and -2 are both essential for the shear stress-induced human osteoblast proliferation. Bone 2004;35:525-534.

Launey ME, Chen PY, McKittrick J, Ritchie RO. Mechanistic aspects of the fracture toughness of elk antler bone. Acta Biomaterialia 2010;6:1505-1514.

Le Roy C, Li JY, Stocco DM, Langlois D, Saez JM. Regulation by Adrenocorticotropin (ACTH), Angiotensin II, Transforming Growth Factor-β, and Insulin-Like Growth Factor I of Bovine Adrenal Cell Steroidogenic Capacity and Expression of ACTH Receptor, Steroidogenic Acute Regulatory Protein, Cytochrome P450c17, and 3β-Hydroxysteroid Dehydrogenase. Endocrinology 2000;141(5):1599-1607.

Li C, Suttie JM. Histological studies of pedicle skin formation and its transformation to antler velvet in red deer (Cervus elaphus). The Anat Rec 2000;260:62-71.

Martin RB, Burr DB, Sharkey NA. Skeletal Tissue Mechanics. 1998 Springer-Verlag, Inc.: New York, NY, pp 225-232.

Mi LY, Fritton SP, Basu M, Cowin SC. Analysis of avian bone response to mechanical loading-Part one: Distribution of bone fluid shear stress induced by bending and axial loading. Biomech Model Mechanobiol 2005;4(2-3):118-131.

Miller SB. Prostaglandins in Health and Disease: An Overview. Sem Arthritis Rheum 2006;36(1):A1-A8.

Ominsky MS. 2003. Effects of hydrostatic pressure, biaxial strain, and fluid shear on osteoblastic cells: mechanotransduction via NF-κB, MAP inase, and AP-1 pathways. Unpublished doctoral dissertation. University of Michigan, Ann Arbor, MI.

Pagedas-Soves C. 2010 Unpublished doctoral dissertation. University of Michigan, Ann Arbor, MI.

Price JS, Allen S. Exploring the mechanisms regulating regeneration of deer antlers. Phil Tran Roy Soc London B 2004; 359(1445): 809-822.

Price JS, Allen S, Faucheux C, Althnaian T, Mount JG. Deer antlers: a zoological curiosity or the key to understanding organ regeneration in mammals? Jour Anat 2005;207(5):603-618.

Qin YX, Kaplan T, Saldanha A, Rubin C. Fluid pressure gradients, arising from oscillations in intramedullary pressure, is [sic] correlated with the formation of bone and inhibition of intracortical porosity. Jour Biomech 2003:36:1427-1437.

Riddle RC, Taylor AF, Genetos DC, Donahue HJ. MAP kinase and calcium signaling mediate fluid flow-induced human mesenchymal stem cell proliferation. Am Jour Physio Cell Physio 2006;290:C776-C784.

Riddle RC, Hippe KR, Donahue HJ. Chemotransport contributes to the effect of oscillatory fluid flow on human bone marrow stromal cell proliferation. Jour Ortho Res 2008;26(7):918-924.

Riddle RC, Donahue HJ. From streaming potentials to shear stress: 25 years of bone cell mechanotransduction. Jour Ortho Res 2008;27:143-149.

Rolf HJ, Enderle A. Hard fallow deer antler: a living bone till antler casting? The Anat Rec 1999;255:69-77.

Seluanov A, Hine C, Azpurua J, Feigenson M, Bozzella M, Mao Z, Catania K,Gorbunova V. Hypersensitivity to contact inhibition provides a clue to cancer resistance of naked mole-rat. PNAS 2009;106(46):19352-19357.

Scutt A, Bertram P. Bone marrow cells are the targets for the anabolic actions of prostaglandin E_2 on bone: induction of a transition from nonadherent to adherent osteoblast precursors. Jour Bone Min Res 1995;10(3):474-487.

Scutt A, Bertram P, Bräutigan M. The role of glucocorticoids and prostaglandin E_2 in the recruitment of bone marrow mesenchymal cells to the osteoblastic lineage: Positive and negative effects. Calc Tissue Int 1996;59(3):154-162.

Singh P, Schwarzbauer JE. Fibronectin and stem cell differentiation – lessons from chondrogenesis. Jour Cell Sci 2012;125:3703-3712.

Sottile J, Hocking DC, Langenbach KJ. Fibronectin polymerization stimulates cell growth by RGD-dependent and-independent mechanisms. Jour Cell Sci 2000;111:4287-4299.

Stern AR, Stern MM, Van Dyke ME, Jähn K, Prideaux M, Bonewal LF. Isolation and culture of primary osteocytes from the long bones of skeletally mature and aged mice. Biotechniques 2012;52(6):361-373.

Van'T Hof RJ, Ralston SH. Nitric oxide and bone. Immunology 2001;103:255-261.

Werb Z, Tremble PM, Behrendsten O, Crowley E, Damsky CH. Signal transduction through the fibronectin receptor induces collagenase and stromelysin gene expression. Jour Cell Bio 1989;107(105a):877-889.

Wienbaum S, Cowin SC, Zeng Y. A model for the excitation of osteocytes by mechanical loading-induced bone fluid shear stresses. Jour Biomech 1994;27(3):339-360.

Chapter V: summary and future directions

Summary

Project outline

Repair of large bone defects is one of the key unmet clinical needs in musculoskeletal medicine (Guldberg 2012). One critical barrier to the realization of viable tissue engineering repair therapies is the poor regenerative capacity of most mammalian tissues compared to those of vertebrates such as certain amphibians, which can completely regrow severed appendages (Poss 2010.) A rare exception to the limits of mammalian regeneration is the deer antler, the only example of complete, repeated organ regrowth in an adult mammal (Kierdorf 2007.) Though they have largely escaped the attention of the tissue engineering field, the antlerogenic progenitor cells (APC) at the heart of antler regeneration have the potential to provide tremendous insights into potential strategies for directing adult somatic progenitor cells to achieve large scale tissue repair.

As basic questions about the APC phenotype remain unanswered, we embarked on a wide ranging investigation of properties and behavior displayed by these cells *in vitro* and in an *in vivo* murine ossicle model. In addition, we submit that any understanding of the uniqueness of APC is incomplete without also investigating how they differ from other cervid MSC. We therefore cultured a parallel, animal-matched population of marrow-derived MSC and subjected them to the same methods as with APC.

Using cells isolated from the antlers and marrow of whitetail deer (*Odocoileus virginianus)*, the work was guided by the following global hypothesis:

APC and cervid marrow-derived MSC conform to a mesenchymal stromal cell model but differ measurably from each other in terms of their intrinsic behavior and responses to stimuli.

In Aim 1 (Chapter II), we investigated how white-tailed deer APC conform to basic criteria defining mesenchymal stromal cells (MSC), particularly in terms of self-renewal and multipotency. Working *in vitro*, we compared colony formation, cell expansion rates and differentiation capacities of reserve mesenchyme APC to animal-matched, phalangeal marrow-derived MSC. As antler growth is closely tied to hormone status, we also examined the effects of the glucocorticoid dexamethasone on osteogenesis. In chondrogenic cultures, which we argue recapitulate aspects of the antler tip microevironment, we explored the effects of dexamethasone on cell number, apoptosis and matrix production.

According to Bianco and others, *in vivo* differentiation is a more representative measure of a cell's multipotency than *in vitro* culturing (Bianco 2008.) In Aim 2 (Chapter III), we therefore explored APC and MSC osteogenic differentiation in a murine ectopic ossicle formation model (Krebsach 1997, Pettway 2005 and 2008.) Here, cells were seeded onto collagen scaffolds and implanted subcutaneously in immunodeficient mice for 6 weeks. Evidence of mineralized tissue formation was collected using microCT and histological techniques.

Last, with mechanical forces so intimately linked to musculoskeletal structure-function relationships, we sought in Aim3 (Chapter IV) to investigate the degree to which reserve mesenchyme-derived antlerogenic progenitor cells (APC) respond to mechanical stimuli. Based on Jacobs' contention that oscillatory fluid flow is the modality most representative of the mechanical conditions experienced on a cellular level, we employed it to load these cells (Jacobs 1998.)

Key results

Aim 1

Contrary to expectations, APC did not exhibit greater *in vitro* proliferative capacity compared to MSC. Mean numbers of visible colonies generated by APC and MSC were similar, but APC demonstrated more inter-animal variability.

APC and MSC exhibited different patterns of differentiation. Unlike MSC, no evidence of adipogenesis was seen in APC. Under osteogenic conditions, APC displayed greater alkaline phosphatase activity at earlier time points yet generally less mineralization. While dexamethasone reduced mineralization in MSC, this glucocorticoid had time dependent effects on APC. In chondrogenic micromass culture, APC were more cellular than MSC, yet were also more apoptotic. Dexamethasone has opposing effects on APC and MSC chondrogenesis, increasing markers of differentiation in latter cells with reducing them in the former. Dexamethasone also increased apoptosis in APC but not MSC.

Aim 2

Fresh, late passage APC and MSC did not experience substantial mineralization in an *in vivo* ectopic ossicle formation model. However, early passage, albeit previously frozen, APC and MSC displayed greater markers of osteogenic differentiation (tissue mineral content and presence of putative osteocytes and osteoclasts) compared to blank (no cell) controls. In contrasts to *in vitro* results, no difference was seen between APC and MSC mineralization *in vivo*.

Aim 3

Oscillatory fluid shear did not have a generalizable influence on the nitric oxide and prostaglandin E2 content of APC and MSC conditioned medium. Loaded APC did exhibit greater increases in PGE2 versus sham at early time points, yet no consistent effect was found in MSC.

On the other hand, non-loaded APC showed equal or increased relative cell numbers compared to MSC. In addition, basal levels of APC PGE2 were substantial greater.

Conclusions and observations

We presented evidence that antler tip APC are likely more lineage-committed osteo-/chondroprogenitors compared to animal-matched marrow MSC with different, often opposing, responses to glucocorticoid steroids.

The inverse relationship between APC apoptosis and chondrogenesis raises the possibility that programmed cell death may help sustain a potential "work force" of non-differentiating APC within the reserve mesenchyme. Apoptosis, rather than being antagonistic to tissue regeneration, may, though a mechanism such as compensatory proliferation, actually contribute to short duration progenitor cell homeostasis.

In contrast to our *in vitro* findings, APC and MSC produced similar amounts of mineral in a murine ossicle model. It is possible that, compared to the MSC, APC osteogenic differentiation requires a more stringent set of factors--factors that may be more accessible to these cells when seeded onto collagen sponges and implanted in mice. This further reinforces the notion that APC and MSC growth and differentiation are subject to distinct set of responses to environmental cues.

We were not able to make definitive statements regarding APC and MSC mechanoresponsiveness. However, our investigation of the effects of oscillatory fluid shear stress on these cells uncovered more evidence of the differing effects of milieu on growth (in this case, the growth substrate) as well as the robust basal production of a factor (PGE2) by APC that could contribute to antler-specific behavior.

APC cultured on fibronectin-coated glass accrued DNA at a rate equal to or greater than MSC, contrasting with the reduced cell enumeration over time seen when antler cells were grown on cell culture plastic. Experimental differences (fresh versus thawed cells or seeding densities) may have contributed to these results, but it is also possible that APC possesses an altered sensitivity to extracellular matrix materials like fibronectin.

Our observation of greater PGE2 production in APC contributes to the speculation that antler is an "immunodeficient" or "immune privileged" tissue and offers a potential mechanism for a local osteoprotective counterbalance to systemic resorptive signals during the antler cycle. The latter may involve an association with the differential response of APC to glucocorticoids compared to marrow cells. While these

findings await further verification, they implicate PGE2 as a compelling factor for additional study in the context of tissue regeneration.

The observed pattern of time, factor, and milieu dependence of APC expansion and differentiation may reflect a system of regulation required to confine antler growth to a specific anatomical and temporal range. Antler regrowth does not proceed "automatically" in response to antler casting, it is initiated by seasonally determined signaling (Kierdorf 2007.) Complete mineralization of the antler is delayed until circulating androgens peak during the fall rutting season, after it is fully regrown (Price 2004.) Moreover, antler regrowth occurs concurrently with bone resorption elsewhere in body, indicating a differential responsiveness to circulating factors in the antler compared to other bone tissue (Landete-Castillejos 2007.)

Throughout this project the lack of readily available laboratory animals and protocols was a constant challenge. We were able to carry out our work by subjecting cells from wild animals to methods developed for mouse, rat and human cells. This resulted in two central limitations to our work: small sample size and the use of non-optimized techniques. Compared to projects involving more conventional animal models, considerable time was expended conducting protocol development. Consequently, our results were derived largely from merely serviceable methods. It is our hope that the extensive cataloging of the techniques used here would offer a beneficial starting point for the next person who intends to conduct antler cell research.

Overall, we have demonstrated that APC are musculoskeletal mesenchymal stromal cells with a distinctly different phenotype compared to animal-matched bone marrow-derived MSC.

Ramifications for regenerative medicine

The deer accomplishes something that is unique among adult mammals: the repeated regrowth of an appendage. The ubiquity of deer in the landscape around us belies the potential boon these animals are to regenerative medicine. As mammals, cervids are far closer to our own species evolutionarily compared to the more commonly studied regenerative animal models such as the newt and axolotl.

As illustrated in Chapter I, research into antler progenitor cell behavior and response to putative factors has shed light on a variety of intriguing facets of the antler cycle. However, one of the key aspects of antler research that has remained unexplored is the difference between APC and other cervid progenitor cells.

We found that the APC phenotype is strikingly different compared to marrow-derived MSC. Our results suggest that these differences may be part of a pattern of local regulation that limits regenerative signaling to a specific place and time. After all, rapid cell growth and differentiation on a systemic level would be destructive to the organism. This local confinement of antler regrowth underscores the potential of this model in guiding the development of novel regenerative strategies, in which one goal is to isolate the effects of exogenous materials and factors to the damaged region so as to reduce systemic morbidities.

Recall that the buck has the means to stop antler growth as well. As described in Chapter I, this is accomplished by harnessing rising testosterone levels to fully mineralize the antler and cause the velvet to shed. Though the exact mechanisms governing this process are not yet known, the capacity for selective growth cessation further highlights the pertinence of the antler to regenerative medicine, as well as to other fields involving the study of unchecked tissue growth.

It would be presumptuous to make bold productions as to whether our results would be off some benefit to the field of regenerative medicine. At this point we merely submit that the above is worthy of further investigation.

Future directions

In this section, we will detail several experiments that could be conducted in the near future using available knowledge, techniques and equipment.

Confirmation of results and optimization of protocols

In order to address the limitations described above, a priority of any future work would be to confirm our results using a larger sample size. Due to the use of wild animals, the limited temporal availability of cellular antler tissue and the commensurate

legal hurdles involved in the off-season culling of bucks, we were only able to have a maximum of three bucks collected at a time. Additional animals would certainly improve the statistical power of our results and thus reduce the likelihood of Type II errors (when one fails to reject a null hypothesis when it is actually false.)

As an example, consider the load/sham PGE_2 levels we saw in Aim 3. We found a statistically significant difference between APC and MSC for the 5 minute time point. To repeat this experiment to ensure a power of at least 80%, we can calculate the needed sample size (N) based on the following equation:

$$N \approx 2*SD^2*(z_\alpha + z_\beta)^2/\Delta^2$$

Where SD is the standard deviation of the population, $z_\alpha + z_\beta$ are the values of the z distributions for the desired α and β levels, and Δ is the difference between means to be detected. Using the pooled standard deviation for all our APC and MSC results as an estimate of "population" SD, we get a value of 0.72. We desire an α of 0.05 (for a $P<0.05$) and a β of 0.80 (or 80% power), yielding a "power index" (equal to $(z_\alpha + z_\beta)^2$) of 7.9. Last, we would like to at least be able to detect a difference of 1 in our sham-normalized PGE_2 levels. Putting this all together, we find that nine animals per group would be necessary for the desired experimental power.

Optimization of protocols would require a larger number of cells than was available for our work so far. Methods could be refined using cells from antler only, which would not require the killing of the animal. This would allow the use of farmed deer, whose owners have been understandably reluctant to allow culling of scientifically-robust numbers of their herds.

While collecting pilot data we experimented with the use of a drill-powered trephine to collect cells from the antler tips of anaesthetized captive white-tails. Such equipment could be used to gather large numbers of cells from the same deer over the course of the summer growing season. In addition, a trephine could be used to collect bone marrow and allow the continued refinement of methods for cervid MSC without the sacrifice of animals.

Investigation of apoptosis

Our results (see Chapter II) have led us to speculate that apoptosis may play an important role in the homeostasis of APC. To explore these questions further, we propose investigating the effects of the modulation of apoptosis on cell number and proliferation.

An initial study would probe the effects of different culture conditions on apoptosis and attempt to hone in on the specific pathways (extrinsic or intrinsic, etc.) involved in the programmed death of these cells. APC and animal-matched, marrow derived would be grown in monolayers and micromass cultures. The former would be conducted on fibronectin-coated slides, which we have shown to allow cell growth of a degree equal to or greater than MSC. As described in Chapter II, micromass cultures offer a milieu that approximates that of the distal antler, where robust apoptosis has been shown to occur (Colitti 2005.)

Assessments of apoptosis would be carried out histologically (using TUNEL-staining) as well as via the expression of genes coding for proapoptotic proteins such as TNF, BAK and BAX (Lindsten 2000, Willis 2003.) Basal levels of proliferation under these conditions would be measured using H^3 -conjugated thymidine incorporation or BrdU (or a non-toxic equivalent such as Invitrogen's Click-iT EdU kit.) Cell would be seeded from the 3200/cm^2 to the 20300/cm^2 values used in the cell enumeration and fluid shear studies, respectively, to determine the effects of seeding density on proliferation.

Next, we would investigate the effects of graded doses of pro- and anti-apoptotic compounds on apoptosis and cell proliferation. Compounds would be chosen to target pathways specific to the upregulated proapoptic genes found in the initial study. Examples of commercially available proapoptotic compounds include BAM7 and AT101 (BAX activators) and recombinant human BAX (Sigma-Aldrich, St. Louis, MO.) Anti-apoptotic factors include BAX inhibiting peptide and GNF-2 (a Bcr inhibitor) (also from Sigma.) If our earlier *in vitro* observations are valid, we would expect that some degree of apoptosis suppression would negatively impact APC proliferation and vice versa. However it is likely that the effects of the selected compounds will be multi-phasic—that

the suppression or enhancement of apoptosis may only occur within a range of concentrations.

Investigation of prostaglandin E2

Confirmation will be needed to verify whether the comparatively robust production of PGE2 by APC occurs on a constitutive basis *in vitro*, or if the levels of this factor measured in these cells (see Chapter IV) was an artifact of the sham loading protocol. In addition, it would also be worthwhile to explore whether the production of PGE2 is substrate and cell-density dependent. To carry this out, we propose seeding APC and MSC on standard cell culture-treated polystyrene plates as well as glass slides onto which graded concentrations of gelatin and fibronectin had been coated. PGE2 and COX-2 levels will be measured in conditioned medium specimen and in cell lysates, respectively. Expression of prostaglandin synthases and COX-2 will also be determined using qPCR. If our Chapter IV data was representative of the basal APC phenotype, we would expect APC to produce more PGE2 regardless of the culture conditions.

We also propose to investigate *in situ* production of PGE2. Immunohistochemistry would be used to locate PGE2, COX-2 and PGE2 receptors EP1-4 in antler tissue sections (Harris 2002.) Comparisons would be made between relative numbers of cells in each antler tissue compartment that were positive for each marker. The proportion of each PGE2 receptor subtype would also be determined to give a sense of the specific downstream pathways activated.

The next logical step would be the modulation of PGE2 levels in APC and MSC *in vitro*. From the results generated in the first part of the study, APC and MSC culture conditions (cell plating density and substrate) would be selected for maximal growth. Next, proliferation would be measured graded concentrations of PGE2 antagonists such as indomethacin and SC-560 (both COX-2 inhibitors) and agonists including Perkin Elmer's Prostanoid (Levine 1972, Brenneis 2006.) We predict that suppression of PGE2 production would be more detrimental to APC proliferation compared to that of MSC. On the other hand, we hypothesize that increasing PGE2 levels would not

enhance (and could actually degrade) APC proliferation, while offering some benefit to MSC proliferation, at least over a range of concentrations (Scutt 1995.)

Gene array comparison between APC and MSC

So far the scope of our analysis has been limited to a narrow number of mainly biochemical markers of cell growth and differentiation. In order to maximize the utility of the APC as a model for musculoskeletal regeneration, we must cast a wider net to better encompass the panoply of differences that may exist between APC and cervid MSC. One means of doing so would be to use microarrays to capture alterations in gene expression between these cell types.

A key technical challenge to such work would be the lack of commercially available cervid microarrays. There is, however, a high degree of synteny between deer, sheep, cows and humans chromosomes (Slate 2002.) While this by no means guarantees the necessary homology at the single gene level, it is encouraging enough for us to propose the use of microarrays designed for bovines, sheep or even humans.

Microarrays could assist in the understanding of differences in the regulation of pathways involved in development, inflammation, osteogenesis, chondrogenesis, etc. between cultured APC and MSC. This knowledge would be of great help in guiding the development of future experiments.

Bibliography

Bianco P, Robey PG, Simmons PJ. Mesenchymal stem cells: revisiting history, concepts, and assays. Cell Stem Cell 2008; 2(4): 313-319.

Brenneis C, Maier TJ, Schmidt R, Hofacker A, Zulauf L, Jakobsson PJ, Scholich K, Geisslinger G. Inhibition of prostaglandin E2 synthesis by SC-560 is independent of cyclooxygenase 1 inhibition. FASEB J 2006;20(9):1353-1360.

Colitti M, Allen SP, Price JS. Programmed cell death in the regenerating deer antler. J Anat 207(4):339-351, 2005.

Guldberg, RE. “Limb regeneration: effects of local biomechanical and biologic factors.” International Bone & Mineral Society Workshop: Musculoskeletal Biology. Sun Valley, Idaho. 6 Aug. 2012.

Harris SG, Padilla J, Koumas L, Ray D, Phipps R. Prostaglandins as modulators of immunity. Trends Immuno 2002;23(3):144-150.

Jacobs CR, Yellowley CE, Davis BR, Zhou Z, Cimbala JM, Donahue HJ. Differential effect of steady versus oscillating flow on bone cells. J Biomechanics 1998; 31:969-976.

Kierdorf U, Kierdorf H, Szuwart T. Deer antler regeneration: cells, concepts, and controversies. J Morphology 2007; 268:726-738.

Krebsach PH, Kuznetsov SA, Satomura K, Emmons RVB, Rowe DW, Robey PG. Bone formation *in vivo*: comparison of osteogenesis by transplanted mouse and human marrow stromal fibroblasts. Transplantation 1997;63(8):1059-1069.

Landete-Castillejos T, Garcia A, Gallego L. Body weight, early growth and antler size influence antler mineral composition of Iberian red Deer (Cervus elaphus hispanicus). Bone 2007;40(1):230-235.

Levine L. Prostaglandin production by mouse fibrosarcoma cells in culture: Inhibition by indomethacin and aspirin. Biochem Biophys Res Com 1972;47(4):888-896.

Lindsten T, Ross AJ, King A, Zong WX, Rathmell JC, Shiels HA, Ulrich E, Waymire KG, Mahar P, Frauwirth K, Chen Y, Wei M, Eng VM, Adelman DM, Simon MC, Ma A, Golden JA, Evan G, Korsmeyer SJ, MacGregor GR, Thompson CB. The combined

functions of proapoptotic Bcl-2 family members bak and bax are essential for normal development of multiple tissues. Mol Cell 2000;6(6):1389-1399.

Pettway GJ, Schneider A, Koh AJ, Widjaja E, Morris MD, Meganck JA, Goldstein SA, McCauley LK. Anabolic actions of PTH (1-34): use of a novel tissue engineering model to investigate temporal effects on bone. Bone 2005;36(6):959-970.

Pettway GJ, Meganck JA, Koh AJ, Keller ET, Goldstein SA, McCauley LK. Parathyroid hormone mediates bone growth though the regulation of osteoblast proliferation and differentiation. Bone 2008;42(4):806-818.

Poss KD. Advances in understanding tissue regenerative capacity and mechanisms in animals. Nat Rev Gen 2010;11:710-722.

Price JS, Allen S. Exploring the mechanisms regulating regeneration of deer antlers. Phil Tran Roy Soc London B 2004; 359(1445): 809-822.

Scutt A, Bertram P. Bone marrow cells are the targets for the anabolic actions of prostaglandin E2 on bone: induction of a transition from nonadherent to adherent osteoblast precursors. Jour Bone Min Res 1995;10(3):474-487.

Slate J, Van Stijn CT, Anderson RM, McEwan KM, Maqbool NJ, Mathias HC, Bixley MJ, Stevens DR, Molenaar AJ, Beever JE, Galloway SM, Tate ML. A deer (subfamily cervinae) genetic linkage map and the evolution of ruminant genomes. Genetics 2002;160:1587-1597.

Willis S, Day CL, Hinds MG, Huang DCS. The Bcl-2-regulated apoptotic pathway. Jour Cell Sci 2003;116:4058-4056.